

Non-linear finite-element modelling of newborn ear canal and middle ear

Li Qi

Department of BioMedical Engineering

McGill University, Montréal

January 2008

A thesis submitted to McGill University in
partial fulfillment of the requirements of the
degree of

Doctor of Philosophy

© Li Qi, 2008

Abstract

Early hearing screening and diagnosis in newborns are important in order to avoid problems with language acquisition and psychosocial development. Current newborn hearing screening tests cannot effectively distinguish conductive hearing loss from sensorineural hearing loss, which requires different medical approaches. Tympanometry is a fast and accurate hearing test routinely used for the examination of conductive hearing loss for older children and adults; however, the tympanograms are hard to interpret for newborns and infants younger than seven months old due to significant differences in the outer and middle ear. In this work, we used the finite-element method (FEM) to investigate the behaviour of the newborn canal wall and middle ear in response to high static pressures as used in tympanometry. The model results are compared with the analysis results of multi-frequency tympanometry measured in healthy newborns and with available tympanometry measurements in newborns with presumed middle-ear effusion.

Analysis results of multi-frequency tympanometry show that both susceptance and conductance increase with frequency. The equivalent volumes calculated from both tails of both the admittance and susceptance functions decreased as frequency increases. The volumes derived from susceptance decrease faster than do those derived from admittance. The 5th-to-95th percentile ranges of equivalent volume and energy reflectances are much lower than previous measurements in older children and adults.

Non-linear finite-element models of the newborn ear canal and middle ear were developed. The ear-canal model indicates that the Young's modulus of the canal wall has a significant effect on the ear-canal volume change, which ranges from approximately 27% to 75% over the static-pressure range of ± 3 kPa. The middle-ear model indicates that the middle-ear cavity and the Young's modulus of the tympanic membrane (TM) have significant effects on TM volume displacements. The TM volume displacement and its non-linearity and asymmetry increase as the middle-ear cavity volume increases. The simulated TM volume displacements, by themselves and also together with the canal model results, are compared with equivalent-volume differences derived from tympanometric

measurements in newborns. The results suggest that the canal-wall volume displacement makes a major contribution to the total canal volume change, and may be larger than the TM volume displacement.

Sommaire

Il est important d'effectuer un dépistage et un diagnostic précoce de l'audition du nouveau-né afin d'éviter qu'il éprouve plus tard des difficultés dans l'acquisition du langage et dans son développement psychosocial. Les épreuves actuelles de dépistage de l'audition des nouveau-nés ne permettent pas de distinguer efficacement entre une perte auditive due à une surdité de transmission et une perte sensorineurale, chacun de ces troubles exigeant un traitement médical différent. La tympanométrie est une épreuve rapide et exacte que l'on utilise habituellement pour déceler une perte auditive due à une surdité de transmission chez les enfants plus âgés et chez les adultes. Cependant, dans le cas des nouveau-nés et des enfants en bas âge, les tympanogrammes sont difficiles à interpréter en raison de différences importantes dans l'oreille moyenne et externe. Dans cette étude, nous avons utilisé l'analyse par éléments finis pour examiner les comportements que manifestent la paroi du conduit auditif et l'oreille moyenne des nouveau-nés en réaction aux pressions statiques élevées utilisées en tympanométrie. Les résultats du modèle sont ensuite comparés aux résultats d'analyses de tympanométrie multifréquence effectuées sur des nouveau-nés en santé, et aux mesures tympanométriques disponibles réalisées sur des nouveau-nés souffrant d'un épanchement présumé dans l'oreille moyenne.

Les résultats d'analyses de tympanométrie multifréquence indiquent que tant la susceptance que la conductance augmentent avec la fréquence. Les volumes équivalents calculés à partir de deux extrémités des fonctions d'admittance et de susceptance décroissent à mesure que la fréquence augmente. Les volumes issus de la susceptance diminuent plus rapidement que ceux issus de l'admittance. Les reflectances d'énergie et les volumes équivalents comprises dans une plage allant du 5^e au 95^e percentile sont beaucoup moins élevées que les mesures antérieures obtenues sur des enfants plus âgés et sur des adultes.

Deux modèles d'éléments finis non linéaires ont été développés; l'un pour le conduit auditif des nouveau-nés et l'autre, pour l'oreille moyenne. Le modèle du conduit auditif indique que le module de Young de la paroi du conduit auditif a un effet notable sur le changement de volume du conduit, lequel varie d'environ

27 % à 75 % pour une plage de pression statique de ± 3 kPa. Le modèle de l'oreille moyenne indique que la cavité de l'oreille moyenne et le module de Young de la membrane tympanique ont des effets notables sur les déplacements volumétriques du tympan. Les déplacements volumétriques du tympan, ainsi que sa non-linéarité et son asymétrie, augmentent au fur et à mesure que s'accroît le volume de la cavité de l'oreille moyenne. Les déplacements volumétriques simulés du tympan sont ensuite comparés, seuls et en conjonction avec les résultats obtenus pour le modèle du canal auditif, avec les écarts de volume équivalents issus des mesures tympanométriques réalisées sur des nouveau-nés. Les résultats suggèrent que le déplacement volumétrique de la paroi du conduit auditif contribue de façon substantielle à l'ensemble du déplacement du conduit auditif.

ACKNOWLEDGEMENTS

When I look back on my life as a PhD candidate, I have to say that without help, support and encouragement from several persons I would never have been able to finish this work.

I would like to express my deep and sincere gratitude to my supervisor, Professor W. R. J. Funnell. His broad knowledge and logical way of thinking have been of great value for me. His understanding, encouragement and patience are the basis of this work. His trust and honesty, and his efforts in understanding a student's personality and tailoring his approach accordingly, made AudiLab become another home for me.

I am very grateful to my families, my wife and my parents, for their love and everlasting support. During this work, we had our first baby, Vincent. He brings us so much happiness. I cannot image my life without him. I dedicate this work to my families, to honor their love, patience, and support.

I wish to thank Dr. Sam J. Daniel (Auditory Science Lab at the Montréal Children's Hospital). His support was essential for this study. He provided the X-ray CT scan for this work, and more importantly, his clinical perspective was extremely helpful for this work.

I would like to thank my Ph.D committee, Dr. Linda Polka, Dr. Gamal Baroud and Dr. Robert Kearney, for their constructive criticism and excellent advice. I am very grateful to Dr. Navid Shahnaz (University of British Columbia). I would like to give a special thank to Rindy Northrop (Temporal Bone Foundation, Boston) for providing histology images. Her warm welcome made my visit to Boston full of fun.

Thanks also to Yong, Shruti, Hengjin, Justyn and Nick for their kind help in the past few years. I would like to thank Daniel Fitzgerald for translating my abstract from English to French. A few lines are too short to make a complete account of my deep appreciation for the people who helped me. Thanks!

Financial support has been provided in part by the Canadian Institutes of Health Research and the Natural Sciences and Engineering Research Council (Canada).

Table of Contents

PREFACE: CONTRIBUTIONS OF AUTHORS.....	1
Paper: Analysis of multi-frequency tympanogram tails in three-week-old newborns (Chapter 3).....	1
Paper: A non-linear finite-element model of the newborn ear canal (Chapter 4).....	2
Paper: A non-linear finite-element model of the newborn middle ear (Chapter 5).....	3
CHAPTER 1: INTRODUCTION.....	4
1.1. MOTIVATION.....	4
1.2. OBJECTIVES.....	6
1.3. THESIS OUTLINE.....	6
CHAPTER 2. BACKGROUND AND LITERATURE REVIEW.....	8
2.1. ANATOMY OF OUTER AND MIDDLE EAR.....	8
2.1.1 Introduction.....	8
2.1.2. Anatomy of outer ear.....	10
2.1.3 Anatomy of middle ear.....	11
2.1.3.1. Tympanic membrane.....	11
2.1.3.2. Tympanic ring	12
2.1.3.3. Ossicles.....	12
2.1.3.4. Ligaments and muscles	13
2.1.3.5. Middle-ear cavity.....	14
2.2. INTRODUCTION OF TYMPANOMETRY.....	15
2.2.1 Principles of tympanometry.....	15

2.2.2. Clinical Application of tympanometry.....	19
2.2.3. Multi-frequency tympanometry	19
2.2.4. Tympanometry in newborns	20
2.3. FINITE-ELEMENT METHOD.....	21
2.3.1. Introduction of finite-element method.....	21
2.3.2. Non-linear hyperelastic material.....	22
2.3.3. Finite-element modelling of ear.....	26
CHAPTER 3: ANALYSIS OF MULTI-FREQUENCY TYMPANOGRAM TAILS IN THREE-WEEK-OLD NEWBORNS.....	28
PREFACE	28
ABSTRACT.....	28
3.1. INTRODUCTION.....	30
3.2. METHODS.....	34
A. Subjects.....	34
B. Procedure.....	34
C. Equivalent volume.....	35
D. Reflectance tympanometry.....	36
3.3. RESULTS.....	38
A. Variation of susceptance and conductance tails with frequency.....	38
B. Equivalent volume calculated from admittance and susceptance.....	42
C. Variation of equivalent volume with age.....	47
D. Reflectance tympanometry at both tails.....	48
3.4. DISCUSSION.....	51
3.5 ACKNOWLEDGEMENTS.....	56

CHAPTER 4: A NON-LINEAR FINITE-ELEMENT MODEL OF THE NEWBORN EAR CANAL.....	57
PREFACE.....	57
ABSTRACT.....	57
4.1. INTRODUCTION.....	58
4.2. MATERIALS AND METHODS.....	60
A. 3-D reconstruction.....	60
B. Material properties.....	63
C. Boundary conditions and load.....	63
D. Hyperelastic finite-element method.....	64
E. Volume calculation.....	65
4.3. RESULTS.....	65
A. Convergence tests.....	65
B. Sensitivity analysis.....	69
C. Model displacements and displacement patterns.....	70
D. Comparisons with experimental data.....	72
4.4. DISCUSSION AND CONCLUSIONS.....	82
ACKNOWLEDGEMENTS.....	84
CHAPTER 5: A NON-LINEAR FINITE-ELEMENT MODEL OF THE NEWBORN MIDDLE EAR.....	87
PREFACE.....	87
ABSTRACT.....	87
5.1. INTRODUCTION.....	88
5.2. MATERIALS AND METHODS.....	90
A. 3-D reconstruction.....	90

B. Material properties and hyperelastic models.....	92
C. Middle-ear cavity.....	96
D. Tympanometry measurements.....	98
5.3. RESULTS.....	99
A. Model displacements	99
B. Middle-ear cavity effects on TM volume displacement	101
C. Comparisons with tympanometric data	102
5.4. DISCUSSION AND CONCLUSIONS.....	108
ACKNOWLEDGEMENTS.....	112
APPENDIX:	113
1. Setting up equations.....	113
2. Numerical solutions.....	114
3. Results.....	114
CHAPTER 6: CONCLUSIONS AND FUTURE WORK.....	121
6.1. SUMMARY.....	116
6.2. MAJOR ORIGINAL CONTRIBUTIONS.....	116
6.3. CLINICAL IMPLICATIONS OF THIS WORK.....	118
6.4. FUTURE WORK.....	119
6.4.1. Experimental work.....	119
6.4.2. Three-dimensional reconstruction of newborn outer and middle ear	120
6.4.3. Finite-element modelling.....	120
REFERENCES.....	121

PREFACE: CONTRIBUTIONS OF AUTHORS

Paper: Analysis of multi-frequency tympanogram tails in three-week-old newborns (Chapter 3)

Journal: Ear and Hearing, submitted on 2008 Dec 19; revised and resubmitted on 2008 Jul 13.

First author: Qi L.

Proposed the idea of investigating newborn tympanogram tails; calculated and analyzed the data; wrote the manuscript.

Second author: Funnell W.R.J.

Proposed the idea of using tympanometry to evaluate simulation results; supervised the research and writing.

Third author: Shahnaz N.

Collected the data; reviewed the manuscript and provided comments and suggestions.

Fourth author: Polka L.

Supervised the data collection; reviewed the manuscript and provided comments and suggestions.

Fifth author: Daniel S.J.

Provided suggestions and comments, especially on clinical issues; reviewed the manuscript and provided comments and suggestions.

Paper: A non-linear finite-element model of the newborn ear canal
(Chapter 4)

Journal: *J Acoust Soc Am* (2006) 120: 3789-3798

First author: Qi L.

Proposed the hyperelastic method; created and tested the model; designed and ran simulations; analyzed and identified data for validation; wrote the manuscript.

Second author: Liu H.J.

Developed software for creating volume finite-element meshes from surface meshes, and assisted with its use for this application.

Third author: Lufty J.

Conducted initial segmentation of the CT scan.

Fourth author: Funnell W.R.J.

Proposed the idea of using a non-linear finite-element model to study the newborn ear canal; supervised the research and writing.

Fifth author: Daniel S.J.

Provided CT scans; provided suggestions and comments during the research; reviewed the manuscript.

**Paper: A non-linear finite-element model of the newborn middle ear
(Chapter 5)**

Journal: *J Acoust Soc Am* (2008) 124: 337-347

First author: Qi L.

Proposed the non-linear hyperelastic method; created, tested and evaluated the model; wrote the manuscript.

Second author: Funnell W.R.J.

Proposed the idea of using non-linear finite-element model to study the newborn middle ear; implemented solution of equations to calculate effects of air cavity; supervised the research and writing

Third author: Daniel S.J.

Provided CT scans; provided suggestions and comments, especially on clinical applications; reviewed the manuscript.

CHAPTER 1: INTRODUCTION

1.1. MOTIVATION

Hearing loss is one of the most common birth defects. It is reported that as many as 6 in 1000 newborns have hearing loss. Early identification of hearing loss in children is extremely important. Studies have shown that auditory stimuli in the first six months after birth are critical to the development of speech and language and children whose hearing loss is identified and corrected within six months of birth are likely to develop better speech and language skills than children whose hearing loss is detected later (Yoshinaga-Itano et al., 1998).

Universal newborn hearing screening (UNHS) is becoming the standard of healthcare in most places in Canada. The objective of UNHS is to identify newborns with sensorineural loss, a disorder of the inner ear and/or brain, as early as possible. An issue of great concern in UNHS is the high false-positive rates, which have been reported to be between 3% and 8% (Clemens et al., 2000). Such high false-positive rates may significantly increase the follow-up diagnostic costs, raise lasting anxiety in parents and may adversely affect the parent-child relationship. Conductive hearing loss (dysfunction of the outer and/or middle ear) is largely responsible for such high false-positive outcomes (e.g. Stuart et al., 1994; Keefe et al., 2002). As a result, it is important to differentiate sensorineural loss from conductive hearing loss.

Currently, evoked otoacoustic emissions (OAE) and auditory brain stem responses (ABR) are being used for UNHS. Both the OAE and ABR tests are objective and accurate examinations; however, neither test can effectively distinguish conductive hearing loss from sensorineural hearing loss. Tympanometry is a fast and accurate hearing test routinely used for the examination of conductive hearing loss for older children and adults; however, the tympanograms are hard to interpret for newborns and infants younger than seven months. For example, some newborns with confirmed middle-ear effusion show normal-appearing single-peak tympanograms (e.g., Paradise et al. 1976; Meyer et

al. 1997), while some normal-hearing newborns show ‘abnormal’ tympanograms with multiple peaks (e.g., Margolis and Popelka, 1975; Himelfarb et al., 1979; Marchant et al., 1986; Holte et al, 1991; Williams et al., 1995; Polka et al. 2002; Kei et al., 2003; Margolis et al., 2003; Shahnaz et al., 2008). More detailed descriptions of tympanometry in newborns can be found in Chapters 2 and 3.

In tympanometry measurements, in order to obtain the air volume between the probe tip and the tympanic membrane (TM), high static pressures are used. As a result, it is important to differentiate the volume displacements of the canal wall from the TM movement, because the latter is of clinical interest. In adults, the canal wall hardly moves in response to high static pressures, because the inner two-thirds of the canal are bone. The total ear-canal volume change is mainly contributed by the TM movements, assuming that the probe-tip movements are small. In newborns, the ear canal is surrounded almost entirely by soft tissue (McLellan and Webb, 1957). As a result, the canal-wall displacement may make a significant contribution to the total canal volume change. Although the importance of obtaining accurate ear-canal volume-change in newborns has been acknowledged (e.g., Holte et al, 1991; Keefe et al., 1993; Hsu et al, 1999), few studies have been conducted due to ethical issues and procedural problems. More detailed literature reviews can be found in Chapters 3, 4 and 5.

The purpose of this work is to investigate the behaviours of the newborn canal wall and middle ear in response to high static pressures as used in tympanometry. Our approach is to use the finite-element method (FEM) to model their behaviours, and the model results are compared with tympanometry measurements. The FEM is an invaluable research and design tool as it can be used to simulate the behaviour of structures in conditions that cannot be achieved experimentally. Therefore, it is an ideal tool to investigate the behaviours of biological tissues. Since the first TM finite-element model was developed (Funnell and Laszlo, 1978), the FEM has been widely used to investigate the behaviour of both human and animal ears (e.g., Wada et al., 1992; Funnell, 1996; Funnell and Decraemer 1996; Koike et al., 2002; Gan et al., 2002, 2004; Elkhouri et al., 2006). More detailed descriptions of the FEM and finite-element models of

the ear can be found in Chapter 2 and the non-linear finite-element models of the newborn ear canal and middle ear will be presented in Chapters 4 and 5.

1.2. OBJECTIVES

The overall objective is to obtain better techniques for diagnosis of conductive hearing loss in newborns. More specifically, the objectives of Chapters 3 to 5 are listed below:

- Chapter 3: Analysis of multi-frequency tympanogram tails in three-week-old newborns
 - To investigate the variations of both susceptance and conductance tails with frequency
 - To compare the equivalent volumes calculated from both positive and negative tails and from both admittance and susceptance
 - To investigate the variation of pressurized energy reflectance at the tails
- Chapter 4: A non-linear finite-element model of the newborn ear canal
 - To investigate newborn ear-canal wall volume displacements under tympanometric pressures
- Chapter 5: A non-linear finite-element model of the newborn middle ear
 - To investigate newborn TM volume displacements under tympanometric pressures

1.3. THESIS OUTLINE

This thesis is mainly based on three manuscripts, which are presented in Chapters 3, 4 and 5, respectively. Although background knowledge and a literature review have been given in each manuscript, in order for the audience to better understand this thesis an overall background and literature review is presented in Chapter 2, including introductions of the anatomy of the outer and middle ear; tympanometry; and the finite-element method. Chapter 3 presents the analysis of multi-frequency tympanometry tails (Qi et al., submitted). Chapters 4 and 5 present non-linear finite-element models of a newborn ear canal (Qi et al.,

2006) and a newborn middle ear (Qi et al., 2008), respectively. Chapter 6 contains the conclusions and suggestions for future work.

CHAPTER 2: BACKGROUND AND LITERATURE

REVIEW

The aim of this chapter is to provide an introduction to tympanometry, the anatomy of the outer and middle ear and the finite-element method. An extensive review of relevant past work is also presented in each section.

2.1 ANATOMY OF OUTER AND MIDDLE EAR

2.1.1 Introduction

In this section we first give a gross overview of the entire ear and then present a more detailed description of the outer and middle ear.

Human ears consist of three components: the external ear, the middle ear and the inner ear, as shown in Figure 1. The external ear includes the pinna and the external ear canal. The middle ear consists of the tympanic membrane, ossicles, ligaments, muscles and middle-ear cavity. The inner ear consists of two parts: the cochlea, and the labyrinth. The cochlea is snail-shaped and houses the outer and inner hair cells; it is designed to receive acoustic energy. The labyrinth is composed of the vestibule and semicircular canals, which are designed for the sense of motion and position. The anatomical description below focuses on the outer and middle ear. More details about the anatomy and function of the inner ear can be found elsewhere (e.g., Anson & Donaldson, 1981).

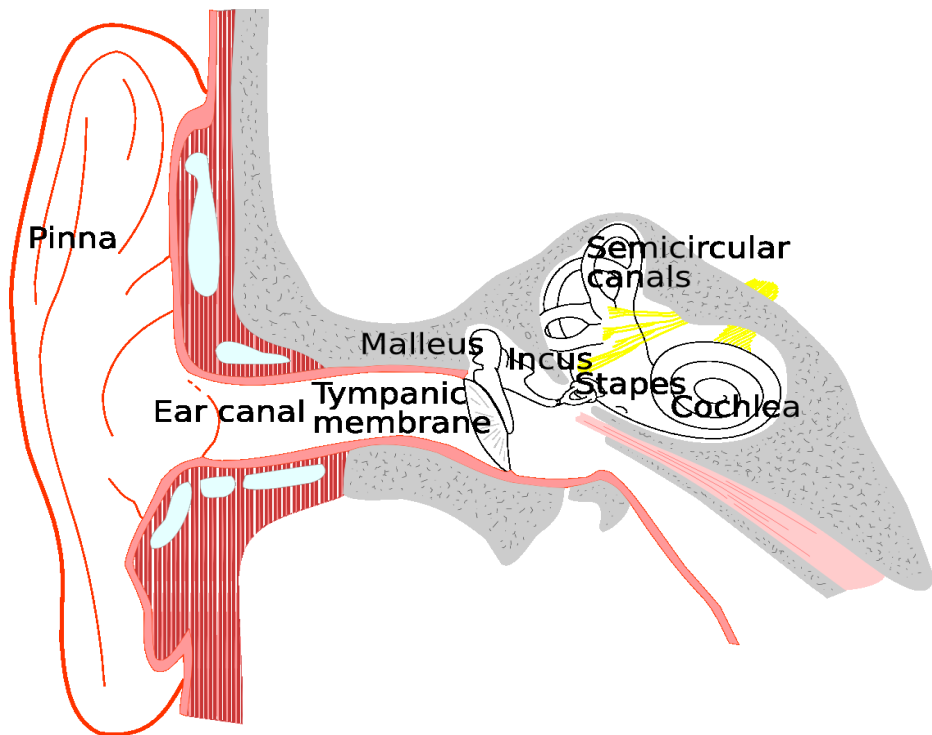
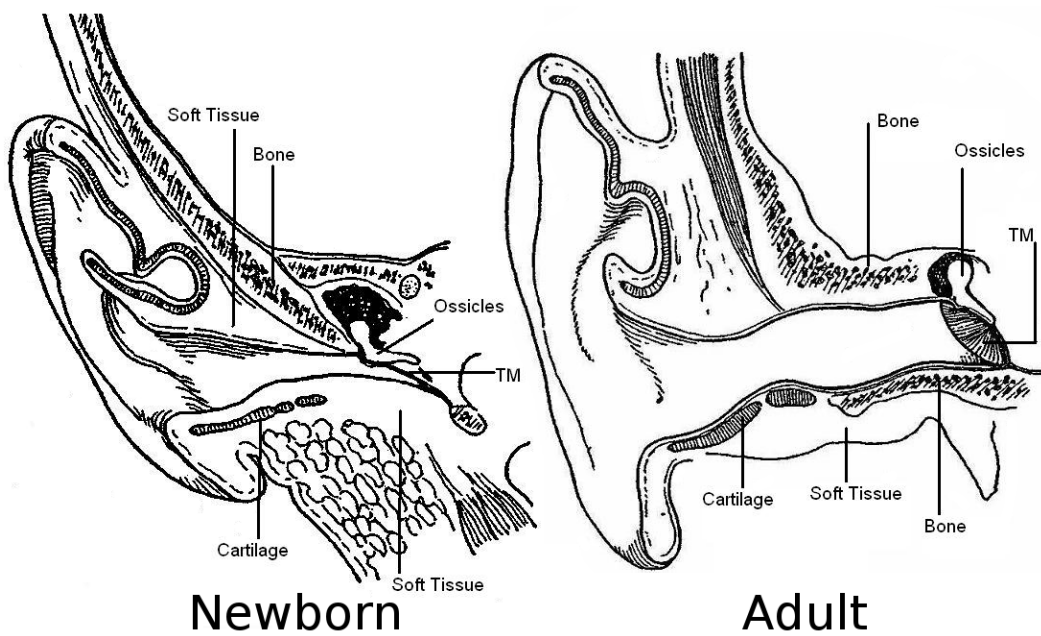


FIG. 1: Overview of ear anatomy (Modified from Cull, 1989)



*FIG. 2: Comparison of the EAC between newborns and adults
(Modified from Ballachanda, 1995)*

2.1.2. Anatomy of outer ear

The outer ear is composed of the pinna (or auricle) and the external auditory canal (EAC). The EAC is also known as the ear canal.

The anatomy of pinna is quite complex. It consists of the helix, antihelix, tragus, antitragus, concha and lobule. The helix is the most peripheral rim of the pinna. The concha is the central depression of the pinna and leads to the entrance of the EAC. At birth the pinna has not reached adult size. The growth of the pinna typically parallels that of the remainder of the head and neck until approximately 9 years of age, when the pinna reaches adult size (Anson and Donaldson, 1981).

The EAC extends from the bottom of the concha and advances medially into the deeper parts of the temporal bone, where it is terminated by the tympanic membrane (TM). In human adults, the ear canal generally has an *S*-shaped curve. The inner two thirds of the ear-canal wall are bony and the outer one third is composed of soft tissue. The average ear-canal length ranges from 20 to 34 mm and the average diameter is approximately 7 to 8 mm (e.g., Anson and Donaldson, 1981).

At birth, the ear canal in the human newborn is not completely mature. The ear canal undergoes further developmental changes until approximately the age of seven years (Northern and Downs, 1974). As shown in Figure 2, the EAC is much shorter and narrower in the newborn than in the adult. The length of the canal in neonates is difficult to measure directly because the TM is nearly parallel to the ear-canal wall and it may be considered to form part of the ear-canal wall. Crelin (1973) reported that the ear-canal length at birth is about 16.8 mm. McLellan and Webb (1957) reported that the ear-canal length is approximately 22.5 mm at birth. We reconstructed a 22-day-old newborn ear canal based on an X-ray CT scan, and found that the canal-roof length was approximately 19 mm, and the canal-floor length was approximately 25 mm. The reconstruction is discussed in more detail in Chapter 4. In newborns the EAC diameter is also much smaller than in adults. Keefe et al. (1993) estimated that the ear-canal diameter is 4.4 mm for 1-month-olds, 5.4 mm for 3-month-olds, and 6.3 mm for 6-month-olds. Based on our CT reconstruction, we found that the ear-canal diameter is between 1.6 and 4.8 mm

for a 22-day old newborn. More details about differences in the ear canal between newborns and adults can be found in Chapter 4.

2.1.3 Anatomy of middle ear

The middle ear is an air-filled cavity sealed off by the tympanic membrane laterally, and by the stapes footplate medially. The middle-ear cavity houses an ossicular chain consisting of the malleus, incus and stapes. These structures are held in place by ligaments, muscles and tendons. The Eustachian tube connects the middle ear to the throat; when opened it equalizes the pressure on both sides of the tympanic membrane.

2.1.3.1. Tympanic membrane

The tympanic membrane (TM) separates the ear canal from the middle ear. The TM is also called the eardrum. It has a conical shape with its apex pointing inwards. In adults, the average area of the TM is between 55 and 85 mm² (e.g., Anson and Donaldson, 1981), and the diameter of the TM is between 8 and 10 mm (Anson and Donaldson, 1981). The superior portion of the TM forms an angle of about 130° with the superior canal wall, while the inferior portion of the TM is tilted at about 50° with respect to the ear-canal floor (e.g., Anson and Donaldson, 1981).

At birth, the TM diameter has reached adult size (e.g., Anson and Donaldson, 1981); however, the TM has a very horizontal position at birth. Ikui et al. (1997) reconstructed the tympanic annulus from 15 subjects aged from 1 day old to 78 years old based on histological images. They used the tympanic annulus to represent the TM. They found that the plane of the tympanic annulus changes from a nearly horizontal orientation in neonates to a more vertical orientation by age two or three years.

The TM is comprised of two parts, pars flaccida and pars tensa. The pars flaccida is approximately one-tenth of the area of the entire TM surface. The pars flaccida is approximately 2 to 3 times thicker than the pars tensa (e.g., Lim, 1970). The thicknesses of the pars flaccida and pars tensa in human adults have been measured by several investigators; however, to the best of our knowledge, only

one study of newborn TM thicknesses has been conducted. Ruah et al. (1991) reported that the TMs in newborns are much thicker than adult TMs. More details about TM thicknesses in adults and in newborns can be found in Chapter 5 Section 2B.

The TM consists of three layers: the epidermis, the outer layer, whose ultrastructure is similar to the epidermis of skin; the lamina propria, the middle layer, which contains loose ground matrix and two layers of densely packed collagen fibres arranged in radial and circular patterns respectively; and the lamina mucosa, the thin inner layer, which contains a large number of columnar cells (e.g., Lim, 1970). The overall mechanical properties of the TM depend mainly on the lamina propria, which is characterized by the presence of type II collagen fibres (e.g., Lim, 1970). More details about the mechanical properties of the human adult and newborn TM can be found in Chapter 5 Section 2B.

2.1.3.2. Tympanic ring

At birth, the tympanic ring consists of an incomplete (U-shaped) circle of bone surrounding the TM; the ring gives rise to lateral processes that eventually become part of the ear-canal wall. The fusion of the tympanic ring continues throughout early postnatal life. Further growth and ossification of the tympanic ring continues until approximately the second year of the postnatal life and this partial ring becomes part of the temporal bone (e.g., Anson and Donaldson, 1981).

2.1.3.3. Ossicles

The ossicles are three bones, called the malleus, incus and stapes, as shown in Figure 1. The malleus, or hammer, is the most lateral bone of the ossicular chain. It includes a head, neck, lateral process, anterior process, and manubrium. The manubrium is attached along its length to the tympanic membrane. The anterior process extends from the neck and connects to the wall of the petrotympanic fissure. The malleus has a saddle-shaped articular surface that contacts the body of the incus.

The second bone in the ossicular chain is the incus, or anvil. The incus includes the body and the short, long, and lenticular processes. It connects the

malleus and stapes, with two synovial joints known as the incudomalleal and incudostapedial joints respectively. The anterior concave surface of the incus body articulates with the malleus head via the incudomalleal joint. The incus lenticular process articulates with the stapes head via the incudostapedial joint.

The stapes, or stirrup, is the smallest of the ossicles. It includes the head, two crura (the posterior and anterior crura) and the footplate. The head connects to the lenticular plate of the incus via the incudostapedial joint, and the footplate connects to the oval window via the annular ligament. The anterior crus is straighter than the posterior crus. Various shapes, thicknesses and curvatures have been observed for the footplate (Gulya and Schuknecht, 1995).

Studies have shown that development of the ossicles continues after birth. Ossicular weight and size are smaller in newborns (Olsewski, 1990). It has been reported that a long, narrow anterior malleal process exists in at least some newborns (Anson & Donaldson, 1981; Unur et al., 2002). Yokoyama et al. (1999) studied the postnatal development of the ossicles in 32 infants and children, aged from 1 day to 9 years. They found that the newborn malleus and incus contain much bone marrow, which is gradually replaced by bone. They concluded that ossification of the ossicles takes place after birth until about 25 months. More detailed descriptions of newborn ossicles can be found in Chapter 5 Section II.B.3.

2.1.3.4. Ligaments and muscles

The ossicular chain is suspended by a group of ligaments. There are four major ligaments. The malleus is suspended by superior, lateral and anterior ligaments. The incus is suspended by the posterior incudal ligament.

There are two striated skeletal muscles in the middle-ear cavity, holding the ossicles to the cavity wall. The tensor tympani is approximately two centimeters in length (Anson and Donaldson, 1981). It inserts onto the handle of the malleus, close to the neck of the malleus. The other end of the tensor tympani is embedded in the medial wall of the tympanic cavity. The stapedius muscle is the smallest skeletal muscle in the human body, and is approximately one centimeter in length (Anson and Donaldson, 1981). One end of the stapedius muscle is connected to

the stapes head and the other end is embedded in the mastoid wall of the tympanic cavity.

2.1.3.5. Middle-ear cavity

The middle-ear cavity is an irregular, air-filled space within the temporal bone, and is comprised of four parts: tympanic cavity, aditus ad antrum, mastoid antrum and mastoid air cells (e.g., Anson and Donaldson, 1981). The tympanic cavity contains the ossicular chain and lies between the TM and the inner ear. The tympanic cavity communicates with the outside by the Eustachian tube. The aditus ad antrum is situated at the posterior-superior portion of the tympanic cavity, and connects to the antrum. The antrum is a cavity at the base of the skull, directly behind the ears. The mastoid bones are full of air space, forming a system containing different sizes and numbers of mastoid air cells (Anson and Donaldson, 1981). The volume of the tympanic cavity in adults has large intersubject differences, ranging from 500 to 1000 mm³ (e.g., Gyo et al., 1986; Whittemore et al., 1998); the mastoid air cell system has a volume ranging from 1000 to 21000 mm³ (Molvaer et al., 1978; Koç et al., 2003).

The newborn middle-ear cavity is much smaller than that in adults. Ikui et al. (2000) reported that the tympanic cavity is about 1.5 times as large in adults as in infants. In addition, the mastoid grows in all three dimensions, length, width and depth, from birth to adulthood (Eby and Nadol, 1986); however, the volume of the mastoid in infants has not been quantitatively measured so far. More detailed descriptions of the middle-ear cavity can be found in Chapter 5 section II.C.

2.2. INTRODUCTION TO TYMPANOMETRY

2.2.1 Principles of immittance

Tympanometry is the measurement of the acoustic immittance of the ear as a function of ear-canal air pressure (e.g., Katz, 2002). Immittance is a collective term that refers to both impedance and admittance. Impedance is a measurement of the stiffness of a system.

Impedance (Z) is defined by the equation

$$Z = P/U \quad \text{Equation 2.1}$$

and admittance (Y) is defined by the equation

$$Y = U/P \quad \text{Equation 2.2}$$

where P is the sound pressure and U is the volume velocity. As shown in Equations 2.1 and 2.2, admittance (Y) is the reciprocal of impedance (Z). In current clinical measurements only admittance is reported, for two reasons: first, the air volume trapped between probe tip and TM simply shifts the admittance tympanograms higher or lower (e.g., Shanks and Lilly, 1981). Second, admittance tympanograms show greater changes than do impedance tympanograms. This makes visual analysis of admittance tympanograms easier (Shanks, 1984). In the rest of this chapter only admittance is discussed.

Both impedance and admittance are complex numbers, including both real and imaginary parts. Admittance can be expressed as

$$Y = G + jB \quad \text{Equation 2.3}$$

where G is the conductance and B is the susceptance. G is in phase with the delivered probe tone. B is an out-of-phase component which is comprised of two parts. One is the compliance component, the other is the mass component. Figure 3 is an illustration of the relationships among the admittance, susceptance and conductance. The unit of acoustical admittance is mho (the reciprocal of ohm). 1 mho is equal to $1 \text{ m}^3/10^5 \text{ Pa}\cdot\text{s}$. In tympanometry measurement, it is convenient to use millimho (mmho), which is 1/1000th of a mho.

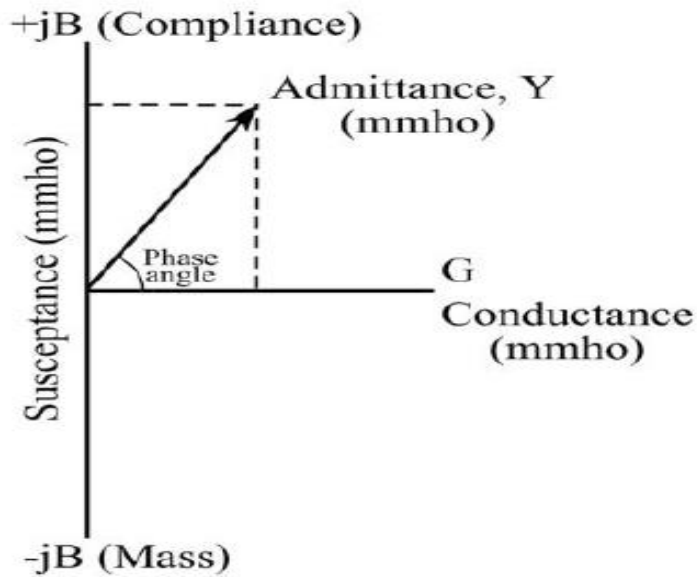


FIG.3: Illustration of admittance, susceptance and conductance (Katz, 2002)

The goal of tympanometry is to determine the immitance of the middle ear. In order to accurately estimate the middle-ear admittance, the admittance corresponding to the air trapped between the probe tip and TM must be subtracted from the total admittance measured at the probe tip. The ear canal and middle ear are acoustically configured as a parallel system because the sound pressure at probe tip and the sound pressure at the TM are nearly identical, due to the large wavelengths at the frequencies used in tympanometry. Terkildsen and Thomsen (1959) proposed the use of a high positive pressure (200 daPa) to estimate the impedance (or admittance) of the air volume trapped between probe tip and TM. Under such high pressure conditions, the admittance of the middle ear tends toward zero. As a result, the admittance measured at the probe tip could be attributed to the ear canal alone. Thus, the admittance at the positive tail would be the admittance of the air trapped between the probe tip and the TM (Y_{EAC}). Therefore, the middle-ear admittance (Y_{ME}) is equal to the difference between the measured admittance at the probe tip (Y) and the admittance at the positive tail, as shown in Figure 4. In order to easily calculate the trapped volume between probe tip and TM, the probe-tone frequency was chosen to be 226 Hz. In that case, the

admittance of a 1-cm³ air volume is 1 mmho. It should be noted that several studies have shown that +200 daPa is not sufficient to drive the TM admittance all the way to zero. More details about estimation of the volume between the probe tip and the TM can be found in Chapters 3 and 4.

Figure 5 is an illustration of a tympanometer. As shown in the Figure, a hand-held probe is inserted into the ear canal and forms a leak-free space from the probe tip to the TM. The probe is comprised of three components: a loudspeaker (A), a microphone (B) and a pump (C). A probe tone at a specific frequency generated by the loudspeaker is delivered to the ear canal through a tube, and static pressures generated by the pump are varied within the sealed canal. The microphone measures the sound pressure level at the probe-tip location. The voltage at the microphone output is continually monitored and used as a reference to maintain a constant probe-tone sound pressure in the ear canal. When the sound pressure level is too low, a greater voltage is applied to the loudspeaker to maintain a constant probe-tone sound pressure; if the sound pressure level is too high, the applied voltage is reduced. The voltage is then converted to an equivalent admittance value, which is typically shown as a function of static pressure for a specific probe-tone frequency. Figure 4 is a normal adult tympanogram obtained at 226 Hz (Wiley and Stoppenbach, 2002).

Tympanometry is widely used to examine middle-ear function. The middle ear is a mechano-acoustical system which is comprised of a combination of acoustical and mechanical masses, springs, and resistive elements. Admittance measurements of the middle ear are influenced by both mechanical and acoustical components. The trapped volume of air between the probe tip and the tympanic membrane and the air in the middle-ear cavity act as acoustical spring elements. The newborn ear-canal wall and tympanic membrane and the ligaments, tendons, and muscles of the middle ear act as mechanical springs. The newborn ear-canal wall, ligaments and muscles also act as mechanical resistive elements. The tympanic membrane and ossicles act as mechanical masses. Middle-ear disorders, such as ossicular chain disruption, change the mechano-acoustical characteristics of the middle-ear system and can be detected by measuring admittance. In the case

of ossicular chain disruption, for example, the admittance would be higher than usual.

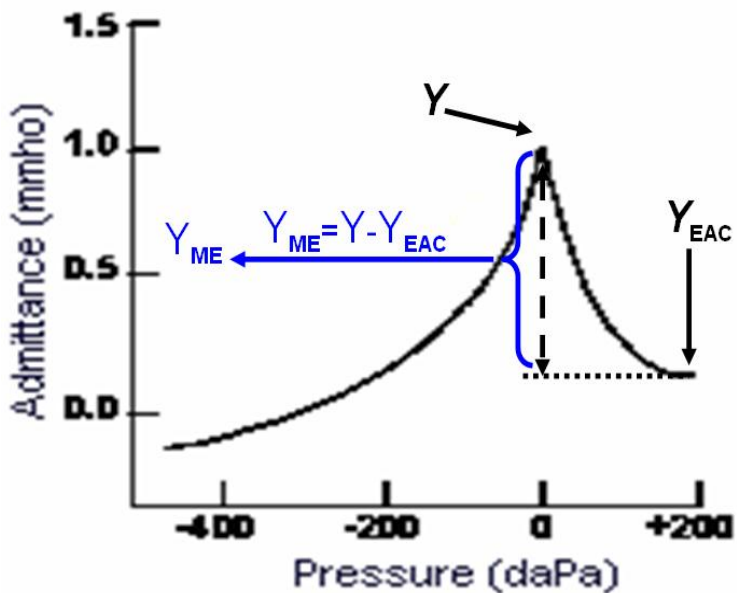


FIG. 4: Illustration of the relationship between the middle-ear admittance magnitude (Y_{ME}), and the measured admittance magnitudes at the probe tip (Y) and at the positive tail (Y_{EAC}).

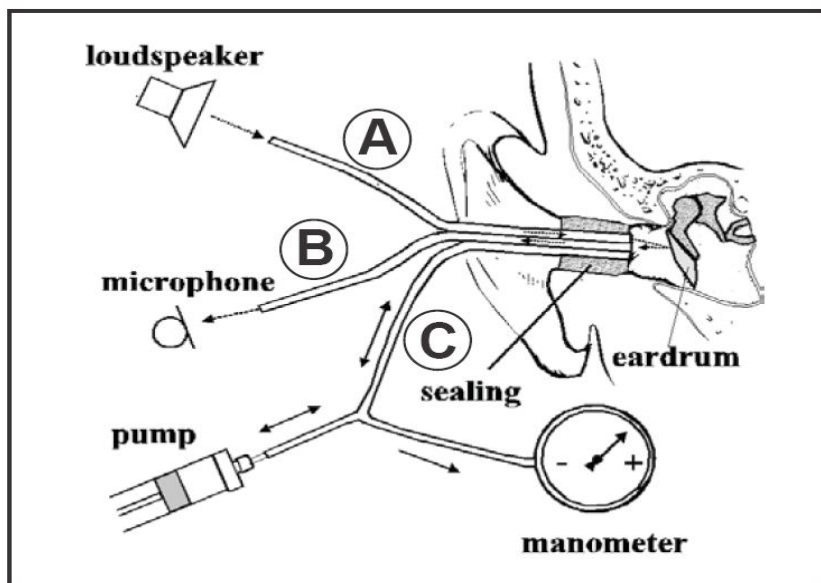


FIG. 5: Illustration of a tympanometer (Modified from Wiley and Stoppenbach, 2002)

2.2.2. Clinical application of tympanometry

Although the first clinical application of acoustic immittance measurement was conducted in the 1940s (Metz, 1946), clinical immittance measurements had not been widely used because early tympanometry devices only provided qualitative and semi-quantitative measurements of middle-ear impedance. Liden (1969) and Jerger (1970) proposed quantitative methods to measure tympanograms according to tympanometric features such as peak height and the width of the peak. After that, clinical immittance measurements became widely used. Tympanometry has now become a routine clinical procedure in audiology examinations for older children and adults. A more detailed description of clinical applications of tympanometry can be found elsewhere (e.g., Margolis and Hunter, 1999).

2.2.3. Multi-frequency tympanometry

Although tympanometry is most frequently performed at 226 Hz, the use of multiple frequencies has been shown to improve test sensitivity in some cases of conductive hearing loss. There are two methods to achieve multi-frequency tympanometry (MFT). One is called sweep frequency: admittance is measured when static pressures in the canal are varied from positive pressures to negative pressures in discrete steps. At each step, the probe-tone frequency is swept from low to high frequencies. The other method is called sweep pressure: static pressures in the ear canal are decreased continuously at a given pressure rate, e.g., 125 daPa/sec. During each sweep, the probe-tone frequency is held constant. These two methods are both used in commercial tympanometers.

MFT can measure the middle-ear admittance under static pressures from low frequencies up to 2 kHz. Colletti (1975, 1976, 1977) first recorded the impedance magnitude for patients with varied middle-ear pathologies for probe-tone frequencies of 200 to 2000 Hz. He found that tympanograms changed systematically with different middle-ear disorders. Vanhuyse et al. (1975) made a significant contribution to understanding tympanogram patterns at multiple frequencies, finding that the tympanometric pattern follows an orderly sequence. Beyond 2 kHz, the interaction between the impedance characteristics of the ear canal and the TM becomes complex, and the ear canal and the middle ear are no

longer configured as a parallel system.

The most common application of MFT is to measure the resonance frequency of the middle-ear system. The resonance frequency corresponds to the frequency at which compliance and mass components are equal. At the resonance frequency the susceptance is zero. Determining the resonance frequency has diagnostic implications because middle-ear disorders may alter the mass and stiffness components. For example, if the stiffness of a middle ear increases owing to a pathology such as otosclerosis, the middle-ear resonance frequency would increase. Conversely, if the stiffness of a middle-ear system decreases, as with an ossicular chain disruption, then the middle-ear resonance frequency would be lower than normal. In addition to the measurement of the resonance frequency, multi-frequency tympanometry can give the frequency at which the compensated phase angle is 45° ($F45^\circ$), where the compensated susceptance and the conductance have the same amplitude. It has been reported that $F45^\circ$ is the best single predictor for otosclerosis (e.g., Van Camp et al., 1986; Shahnaz and Polka, 1997, 2002). Although the advantages of multi-frequency tympanometry have been acknowledged, multi-frequency probe tones are not routinely used because the tympanograms are more complex than at 226 Hz.

2.2.4. Tympanometry in newborns

Currently there does not exist a clinically accepted body of normative tympanometric data for neonates or young infants (less than seven months old). Studies have shown that tympanograms are significantly different in young infants and adults. For example, tympanograms that in an adult would indicate a normal middle ear were frequently recorded from newborn ears with confirmed middle-ear effusion (e.g., Paradise et al., 1976; Marchant et al., 1986). This finding was attributed to the fact that significant differences in the outer and middle ear exist between newborns and adults (McLellan and Webb, 1957; Holte et al., 1991). For example, in adults, the inner two thirds of the ear-canal wall are bony and the outer one third is composed of soft tissue; in newborns, the ear canal is surrounded almost entirely by soft tissue. A more detailed description of anatomical and physiological differences in the outer and middle ear between

newborns and adults can be found in Section 2.2.

Holte et al. (1991) studied the admittance, susceptance and conductance for infants from birth up to four months of age. The tympanograms were recorded at five frequencies from 226 to 900 Hz. They concluded that 226-Hz tympanograms were easier to interpret than high-frequency tympanograms for newborns. Palmu et al. (1999) examined otitis media in infants from two to eleven months old using only 226-Hz tympanometry. They calculated the probability of the disease using Baye's theorem and concluded that using 226-Hz tympanometry is a good predictor for diagnosing otitis media in infants.

On the other hand, through the use of either MFT or a single high-frequency probe tone, many researchers have concluded that tympanometry with a high probe-tone frequency can accurately identify middle-ear effusion in newborns (e.g., Margolis and Popelka, 1975; Paradise et al., 1976; Himelfarb et al., 1979; Marchant et al., 1986). Most of them agreed that the best choice of a tympanometric probe frequency for newborns and young infants is 1000 Hz (Polka et al. 2002; Kei et al., 2003; Margolis et al., 2003; Calandruccio et al., 2006; Alaerts et al., 2007; Shahnaz et al., 2008). The 1000-Hz tympanograms were considered normal if there was any discernible peak. Flat tympanograms were considered abnormal.

A more detailed description of MFT and high-frequency tympanometry in newborns can be found in Chapter 3.

2.3. FINITE-ELEMENT METHOD

In this section, an introduction to the finite-element method (FEM) is presented in Section 2.3.1, and then the non-linear hyperelastic material model is introduced in Section 2.3.2. A review of previous finite-element models of the ear is given in Section 2.3.3.

2.3.1 Introduction to the finite-element method

The FEM is a numerical method for solving problems with complicated geometries and/or material properties and/or boundary conditions, where analytical solutions are hard to obtain. Since the FEM was introduced in the

1960s, it has been widely used in many engineering and physics areas such as mechanics, acoustics, thermal fields, electromagnetic fields etc.

In the FEM, a complicated system is divided into a large number of relatively simple, small but finite-size parts (elements), which are connected by nodes. As a result, although the entire system may have a complex structure and/or irregular boundary conditions, the individual element is easy to analyse. The element can be one-dimensional, two-dimensional or three-dimensional, and can be linear or higher order. Each finite element will have its own unique energy functional. The element potential energy can be calculated based on the principle of virtual work. Later, all of the individual parts are assembled to represent the entire system. The general procedure of the FEM includes several steps; for example, in the case of static mechanical analysis:

Step 1: Discretize the complex structure into a large number of finite elements connected at nodes

Step 2: Introduce an approximation of a variable over an element, e.g. displacement

Step 3: Express the behaviour of each element as a matrix equation:

$$[k]_e * \{u\}_e = \{f\}_e$$

where $[k]_e$ is the element stiffness matrix; $\{u\}_e$ is the node displacement vector; and $\{f\}_e$ is external load vector.

Step 4: Assemble the element equations into a set of global equations that model the behaviour of the entire system.

Step 5: Solve the system matrix equation to get the unknowns

$$\{u\} = [k]^{-1} * \{f\}$$

Step 6: Calculate the desired values, such as strain, stress etc.

This is a very brief introduction to some basic concepts involved in the FEM. More detailed descriptions can be found in many textbooks (e.g., Hartley, 1986).

2.3.2 Non-linear hyperelastic material

The FEM has been widely used to investigate the behaviour of biological soft tissue. Most biological soft tissue can be modelled as a linear and elastic material when deformations are small and slow; however, in nature, biological soft tissues

are characterized by very complex mechanical properties, such as hyperelastic, anisotropic, viscoelastic or viscoplastic. These complex properties are due to the fact that most soft tissue consist of different materials such as different cells or fibres, and these materials are inter-connected in a complicated way. In order to accurately describe the behaviour of soft tissues undergoing large deformation, non-linear properties should be taken into account. Although soft tissues have a variety of properties, in this section only hyperelastic properties are discussed. An extensive review of the material properties of soft tissue can be found elsewhere (e.g., Fung, 1993).

Large deformation is typically defined as strain greater than 3% or 5%. A typical stress-strain curve of hyperelastic materials is shown in Figure 6. As shown in the Figure, the overall behaviour is non-linear. When the strain becomes larger, the soft tissues become stiffer.

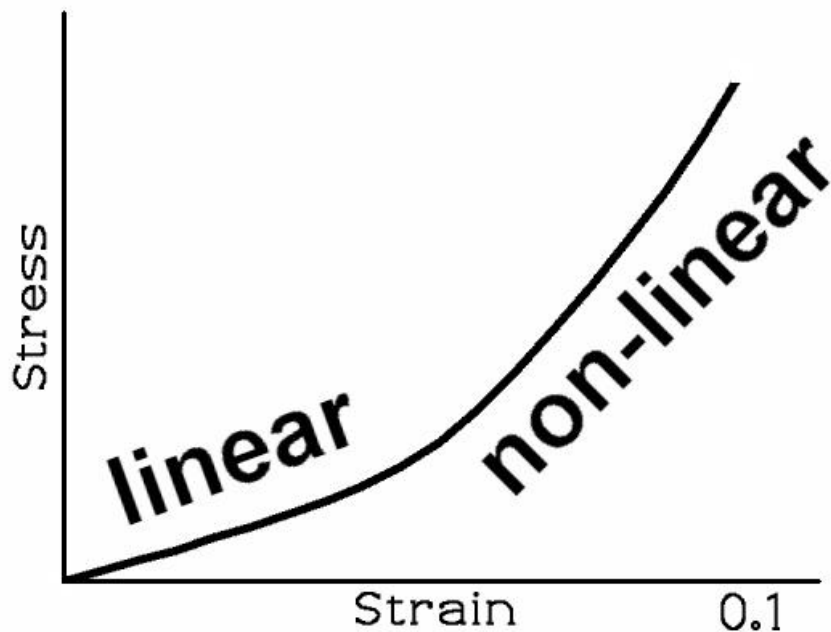


FIG. 6: A typical stress-strain curve of hyperelastic materials

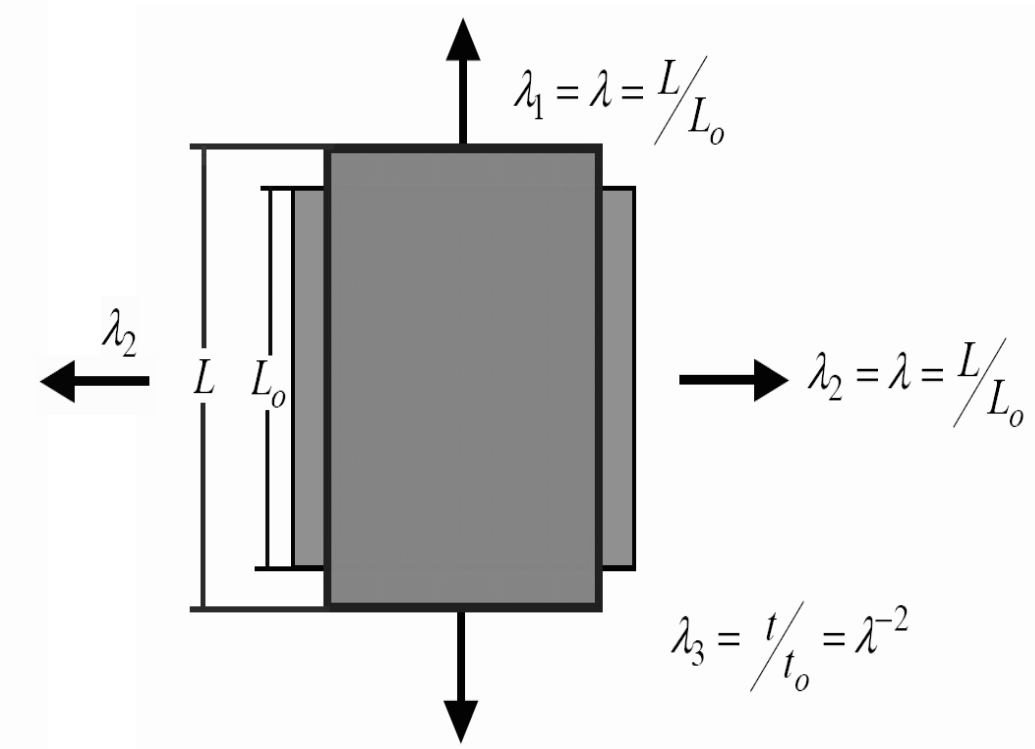


FIG. 7: Illustration of stretch ratio

A hyperelastic material is an elastic material that exhibits non-linear behaviour during large deformations. To model a hyperelastic material, a strain energy (W) is defined as a function of one of the strain or deformation tensors. Its derivative with respect to a strain component determines the corresponding stress component, as shown in Equation 2.4:

$$S_{ij} = \frac{(\partial W)}{(\partial E_{ij})} = 2 \frac{(\partial W)}{(\partial C_{ij})} \quad \text{Equation 2.4}$$

where S_{ij} is the second Piola-Kirchhoff stress tensor; E_{ij} is the Lagrangian strain tensor; C_{ij} is the right Cauchy-Green deformation tensor (Holzapfel, 2000).

Before proceeding to a detailed discussion of different forms of the strain energy, some important terms will be defined first. To better explain these concepts, a simple illustration of a rubber under biaxial tension is used, as shown in Figure 7. The stretch ratio (λ) is defined as

$$\lambda = \frac{L}{L_0} \quad \text{Equation 2.5}$$

where L_0 is the initial length; L is the length after deformation.

λ_1 , λ_2 , and λ_3 are called principle stretch ratios. λ_1 , λ_2 are in-plane deformations. λ_3 is the thickness variation (t/t_0). t_0 is the initial thickness; t is the thickness after deformation. Since we assume that the hyperelastic material is elastic, isotropic, and incompressible or nearly incompressible, we have $\lambda_1=\lambda_2=\lambda$ and $\lambda_3=\lambda^{-2}$.

Three strain invariants (I_1 , I_2 , I_3) and the volume ratio (J) can be calculated from the principle stretch ratios as shown in equation 2.6 and 2.7, respectively.

$$I_1 = \lambda_1^2 + \lambda_2^2 + \lambda_3^2 \quad \text{Equation 2.6.a}$$

$$I_2 = \lambda_1^2 \lambda_2^2 + \lambda_2^2 \lambda_3^2 + \lambda_1^2 \lambda_3^2 \quad \text{Equation 2.6.b}$$

$$I_3 = \lambda_1^2 \lambda_2^2 \lambda_3^2 \quad \text{Equation 2.6.c}$$

$$J = \lambda_1 \lambda_2 \lambda_3 = \frac{V}{V_0} \quad \text{Equation 2.7}$$

If a material is incompressible, $I_3=1$. V_0 is the initial volume and V is the volume after deformation. A strain energy function can be expressed as a function of either strain invariants (I_1 , I_2 , and I_3) or principle stretch ratios (λ_1 , λ_2 , and λ_3). Based on the strain energy (W), the stress tensor and the strain tensor can be calculated. Various strain-energy functions can be applied to soft tissue, such as neo-Hookean, Mooney-Rivlin, Arruda-Boyce, etc. In this work we use the polynomial method, which is a generalization of the Mooney-Rivlin method and which has been widely used to simulate large deformations in nearly incompressible soft tissues such as skin, brain tissue, breast tissue and liver (e.g., Samani and Plewes, 2004; Cheung et al., 2004).

A second-order polynomial strain-energy function can be written as

$$W = C_{10}(I_1 - 3) + C_{01}(I_2 - 3) + \frac{\kappa}{2}(J - 1)^2 \quad \text{Equation 2.8}$$

where W is the strain energy; C_{10} and C_{01} are material constants; κ is the bulk modulus; and J is the volume-change ratio, defined in equation 2.7. Under small strains the Young's modulus of the material (E) may be written as

$$E = 6 * (C_{10} + C_{01}) \quad \text{Equation 2.9}$$

Further details about the hyperelastic model can be found elsewhere (e.g., Holzapfel, 2000).

2.3.3 Finite-element modelling of the middle ear

Most mathematical models of the middle ear have been lumped circuit models (e.g., Zwislocki, 1963), two-port ‘black boxes’ (e.g., Shera & Zweig, 1991) or semi-analytical (e.g., Rabbitt & Holmes, 1986). The middle ear, however, is a complex 3-D mechano-acoustical system containing many interconnected, highly irregular, asymmetrical and nonuniform parts. In such a complex system, the only hope for a real quantitative understanding is the FEM.

Funnell and Laszlo (1978) introduced the use of the FEM for the study of the ear. They developed the first three-dimensional finite-element model of a cat eardrum based on an extensive review of the anatomical, histological and biomechanical nature of the eardrum. Since then, the FEM has been extensively used to investigate the static or dynamic behaviour of middle-ear subsets or the entire middle ear either in humans (e.g., Williams and Lesser, 1990; Wada et al., 1991; Williams et al., 1996; Beer et al., 1997, 1999; Prendergast et al., 1999; Ferris and Prendergast, 2000; Koike et al., 2002; Gan et al., 2002, 2004, 2006) or in animals (e.g., Funnell 1983; Funnell et al., 1987; Funnell et al., 1992; Ladak and Funnell, 1996; Siah and Funnell, 2001; Elkhouri et al., 2006).

Most previous finite-element models of the ear are linear models, which can only simulate the behaviour of the middle ear in response to low pressures. In recent years, a few non-linear finite-element models of the middle ear were presented. These models were designed to investigate the effects of large static pressures on the displacements of the tympanic membrane or ear-canal wall. These models are important for understanding tympanometry or otitis media, a common middle-ear disorder in which fluid is built up in the middle-ear cavity.

Ladak et al. (2006) developed the first non-linear middle-ear finite-element model. In their model, only a cat eardrum was considered, and the manubrium was assumed to be rigid along its length. The effects of large static pressures on the displacements of a cat eardrum were investigated. In their study, they only took the geometric non-linearity into account. They reported that the location of the maximum displacement moves when the pressures are changed and geometric non-linearity must be considered when simulating the eardrum response to high

pressures. At higher pressures, material non-linearity may become more important.

Qi et al. presented the first non-linear finite-element model of a human ear canal (Qi et al., 2006) and the first non-linear finite-element model of a human middle ear (Qi et al., 2008). These models are presented in Chapters 4 and 5.

Cheng et al. (2006) presented a non-linear hyperelastic finite-element model of a human adult TM to interpret their uniaxial tensile test results. Only the TM was taken into account in their model. The relationships of the stress and strain were expressed in the stress range from 0 to 1 MPa. Their results will be referred to in Chapter 5. Very recently, Wang et al. (2007) studied middle-ear pressure effects on the static and dynamic behaviour of the human ear using finite-element analysis. The static behaviour of the middle ear in response to pressure variations was investigated using a hyperelastic model. Then, based on the static deformation field, the nodal displacements of the TM and middle-ear ligaments were updated for dynamic analysis. They reported that the reductions of the TM and footplate vibration magnitudes under positive middle-ear pressure are mainly determined by non-linear material properties and the reduction of the TM and footplate vibrations under negative pressure was determined by both the non-linear geometry and material properties.

CHAPTER 3: ANALYSIS OF MULTI-FREQUENCY TYMPANOGRAM TAILS IN THREE-WEEK-OLD NEWBORNS

PREFACE

This paper is based on the data presented by Shahnaz et al. (2007). The analysis of results obtained in this chapter will be used to compare with the results from the ear-canal model (Chapter 4) and the middle-ear model (Chapter 5). The paper has been submitted to *Ear and Hearing*.

ABSTRACT

Objectives: The overall goal of this study is to analyze the behaviour of tympanogram tails in newborns. More specifically, the purpose of this study is threefold. The first goal is to investigate the variation of both susceptance and conductance tails with frequency. The second goal is to compare equivalent volumes calculated from both positive and negative tails and from both admittance and susceptance. The third goal is to investigate the variation of energy reflectance at the tails.

Design: Sixteen full-term healthy 3-week-olds participated in the study. All infants passed a hearing screening at birth and again at 3 weeks of age using automated auditory brainstem response. The admittance magnitude and phase were recorded at 9 frequencies (226, 355, 450, 560, 630, 710, 800, 900, 1000 Hz). The susceptance and conductance were derived from the recorded magnitude and phase. The equivalent volumes and energy reflectances were calculated from both positive and negative tails and from both admittance and susceptance.

Results: Results showed that both susceptance and conductance tails increase with frequency. The equivalent volumes calculated from both the positive and negative tails of both the admittance and susceptance functions decrease as

frequency increases. The volumes derived from susceptance decrease faster than do those derived from admittance. At low frequencies the differences between the equivalent volumes calculated from the susceptance and admittance are small because the conductance is small. At 1000 Hz the differences are larger: approximately 60% for positive tails and approximately 40% for negative tails. The 5th-to-95th percentile ranges of equivalent volume are much lower than previous measurements in older children and adults. The variability of estimates of the equivalent volume from both admittance and susceptance at low frequencies appear to be higher than those at high frequencies. Energy reflectances calculated from the admittance tails are lower than in older infants and adults.

Conclusions: Results suggest that the neonate ear canal is not a pure acoustic compliance, particularly at high frequencies. Positive and negative pressures appear to have different effects on the movement of the ear-canal wall and/or tympanic membrane, especially at high frequencies. If the equivalent volume is calculated from the admittance positive tail at 1000 Hz, as most tympanometers do for newborn hearing screening, the admittance of the middle ear will be significantly underestimated. The low energy reflectances obtained in this study may imply that there is a significant amount of sound energy absorbed by the newborn canal wall and that reflectance measurements are location-dependent.

3.1. INTRODUCTION

In tympanometry, the admittance of the middle ear is the main clinical interest but the admittance measured at the probe tip includes the effects of both the ear canal and the middle ear itself. The accuracy of the middle-ear admittance estimate therefore relies on obtaining an accurate estimate of the ear-canal admittance. Under certain conditions the effect of the ear canal can be represented as that of a pure acoustic compliance corresponding to its volume. The admittance corresponding to the canal volume can then be subtracted from the total admittance measured at the probe to yield the middle-ear admittance. The most commonly used method to estimate the canal volume is based on a procedure proposed by Terkildsen and Thomsen (1959). They suggested the use of a high positive pressure (200 daPa, or 2 kPa since $1 \text{ daPa} = 10 \text{ Pa}$) during the measurement, which would drive the admittance of the middle ear toward zero. Under such high-pressure conditions, the admittance measured at the probe tip can be attributed mainly to air trapped in the ear canal itself. The high-pressure extremes of the tympanogram are generally referred to as the ‘tails’. Shanks and Lilly (1981) reported that the canal volume (V_{ea}) is more accurately estimated from the negative tail at -400 daPa than from the positive tail at $+400 \text{ daPa}$, and more accurately from the susceptance tail than from the admittance tail. Despite the known errors, however, in clinical measurements V_{ea} is usually still taken from the admittance positive tail owing to better test-retest reliability (Margolis and Goycoolea, 1993) and a more consistent measure of tympanometric width (Margolis and Shanks, 1991).

The admittance is a complex number which includes an imaginary part, the susceptance, and a real part, the conductance. For adults, the conductance at the tail at 226 Hz is usually very small, so the susceptance and the admittance are nearly the same and the error introduced by using the admittance tail rather than the susceptance tail is negligible (Shanks & Lilly, 1981). This error increases at higher frequencies owing to an increase of the conductance but is usually still small in adults except in particular circumstances (e.g., Feldman, 1976, p. 145).

For newborns, the variations of the susceptance and conductance tails with frequency and the differences between equivalent volumes derived from the admittance magnitude and from the susceptance have not been investigated.

It has been reported that tympanograms are significantly different between infants and adults. The differences are due in part to differences in canal volume between infants and adults, both because the infant canal is smaller and because it often contains extraneous material at birth. Perhaps more important are deformations of the newborn ear-canal wall (e.g., Paradise, Smith & Bluestone, 1976; Margolis & Popelka, 1975; Holte, Margolis & Cavanaugh, 1991; Keefe, Bulen, Arehart & Burns, 1993). The human outer ear is not completely mature at birth. In adults, the inner two thirds of the ear-canal wall are composed of bone and the outer one third is composed of soft tissue; in newborns, the entire ear canal is surrounded by soft tissue (McLellan and Webb, 1957; Qi, Liu, Lutfy, Funnell & Daniel, 2006). Owing to the lack of ossification, newborn ear-canal walls exhibit significant deformations in response to the large quasi-static pressures used in tympanometry. To the best of our knowledge, only two studies have been conducted to investigate newborn ear-canal wall movement under high static pressures. Holte, Cavanaugh and Margolis (1990) experimentally measured canal wall displacements under high static pressures. They found that, with considerable variability, the diameter of the ear canal can change by up to 70% in response to high static pressures (± 2.5 to ± 3 kPa). More recently, Qi et al. (2006) presented a 3-D non-linear finite-element model of a 22-day-old newborn ear canal. The canal wall displacements and volume changes under high static pressures were investigated for various values of the material properties of the soft tissue surrounding the canal. The model predicted a ratio of ear-canal volume change to the original volume of from 27% (with a Young's modulus of 90 kPa) to 75% (with a Young's modulus of 30 kPa) in the static-pressure range of ± 3 kPa.

In newborn tympanometry, the conventional 226-Hz measurements cannot be interpreted in the same way as for adults. For example, some newborns with confirmed middle-ear effusion show normal-appearing single-peak tympanograms (e.g., Paradise et al., 1976; Meyer, Jardine & Deverson, 1997), while some

normal-hearing newborns show ‘abnormal’ tympanograms with multiple peaks (e.g., Margolis and Popelka, 1975; Holte et al., 1991; Shahnaz, Miranda & Polka, 2008). It has been reported that high-frequency tympanometry (1 kHz) is more easily interpreted and is more efficient than low-frequency tympanometry at detecting conductive hearing loss or dysfunction in very young infants (under 4 months of age) (e.g., Margolis and Popelka, 1975; Paradise et al. 1976; Himelfarb, Popelka & Shanon, 1979; Marchant, McMillan & Shurin, 1986; Kei, Allison-Levick & Dockray, 2003; Margolis, Bass-Ringdahl, Hanks, Holte & Zapala, 2003). Multi-frequency tympanometry provides more information than single-frequency tympanometry (e.g., Lilly 1984; Hunter and Margolis, 1992; Shahnaz and Polka, 1997, 2002) but to date there have been few measurements of multi-frequency tympanometry in newborns. Holte et al. (1991) studied the admittance, susceptance and conductance using multi-frequency tympanometry in infants less than 4 months old. They compared the measurement results at 6 frequencies (from 226 to 900 Hz) and concluded that the tympanograms were most easily interpreted at 226 Hz. McKinley, Grose and Roush (1997) measured both multi-frequency tympanograms (at 226, 678 and 1000 Hz) and evoked otoacoustic emissions (EOAE) in first-day neonates, and reported that no clear association emerged between admittance characteristics and EOAE results. Shahnaz et al. (2008) compared the admittance in adults and 3-week-old infants using multi-frequency tympanometry. They reported that at 1 kHz admittance tympanograms had a single peak for 74% of infant ears, while 78% of adult ears showed multiple-peak or irregular patterns. Calandruccio, Fitzgerald and Prieve (2006) studied middle-ear admittance at ambient pressure (Y_{TM}) and at +200 daPa (Y_{+200}) in 33 infants aged from 4 weeks old to 2 years old using multi-frequency tympanometry. They recorded tympanograms at 5 frequencies (from 226 to 1000 Hz) and found that both Y_{TM} and Y_{+200} generally increased with age. Finally, Shahnaz et al. (2008) investigated multi-frequency tympanometry in well babies and intensive-care-unit babies at 9 frequencies (from 226 to 1000 Hz). They found that the tympanograms obtained at 1 kHz are more sensitive and specific for presumably abnormal and normal middle-ear conditions, and that tympanometry at 1 kHz is a good predictor

of the presence or absence of transient EOAE's.

In addition to admittance, energy reflectance is an alternative way to study the mechano-acoustical characteristics of the middle ear. Energy reflectance is the ratio of incident to reflected energy in the ear canal, and has been measured from low frequencies up to 10 kHz. The energy reflectance is less dependent on the probe location than admittance is. Previous studies have suggested that energy reflectance may be clinically useful (e.g., Stinson, Shaw & Lawton, 1982; Voss and Allen 1994; Keefe et al. 1993; Keefe and Levi 1996; Margolis, Saly & Keefe, 1999; Allen, Jeng & Levitt, 2005). Most energy-reflectance measurements have been performed at ambient pressures. The concept of measuring energy reflectance as a function of ear-canal static pressure was proposed by Keefe and Levi (1996), who used the term 'reflectance tympanometry'. Later, Margolis et al. (1999) performed reflectance tympanometry in human adults and Margolis, Paul, Saly, Schachern and Keefe (2001) compared reflectance tympanometry patterns between chinchillas and human adults. Their studies suggested that reflectance tympanometry could be used for detecting conductive hearing loss. There have been very few reflectance tympanometry measurements in newborns or infants. To the best of our knowledge, the only such study was conducted by Sanford and Feeney (2008), with subjects ranging from 4-week-old infants to adults. The energy reflectance was measured at ambient, positive and negative pressures. They found significantly different patterns between infants and adults. Their findings suggested that energy-reflectance tympanometry may be useful in determining middle-ear pathology in very young infants.

This paper is based on the multi-frequency tympanometry data for well babies presented by Shahnaz et al. (2008). The overall goal of this study was to analyze the behaviour of tympanogram tails in newborns, in order to provide a basis for understanding tympanometry in newborns. More specifically, the purpose of this study was threefold. The first goal was to investigate the variation of both susceptance and conductance tails with frequency. The second goal was to compare V_{ea} calculated from both positive and negative tails and from both

admittance and susceptance. The third goal was to investigate the variation of pressurized energy reflectance at the tails.

We focus on 3-week-old newborns for three reasons. First, at birth both OAE and tympanometry measurements are affected by the residual mesenchyme and liquid that are often present in the ear canal and middle-ear cavity during the first few days after birth. For example, Roberts et al. (1995) reported that about 20% of full-term neonates still have liquid in the middle-ear cavity three days after birth. Thus, newborns may present a hearing loss immediately after birth, followed by an improvement in hearing as the debris and liquid are cleared. Consequently, hearing-screening tests conducted shortly after birth may lead to high false-positive rates. Second, it has been suggested that 1-kHz tympanometry measurements may not be effective in detecting middle-ear effusions in the newborn nursery but may be effective between 2 and 4 weeks of age (Margolis et al., 2003). Third, as part of its Early Hearing Detection and Intervention program (EHDI, 2003), the American Academy of Pediatrics (AAP) recommends that all infants be screened for hearing loss before the age of one month. For these reasons, 3-week-olds are appropriate study subjects.

3.2. METHODS

A. Subjects

Sixteen full-term healthy 3-week-old infants participated in the study. All infants passed a hearing screening at birth and again at 3 weeks of age using automated auditory brainstem responses (AABR). (See Shahnaz et al., 2008, for details on the screening protocol.) Fifteen out of sixteen subjects were measured with multi-frequency tympanometry in both left and right ears; one subject was measured only in the right ear.

B. Procedure

Tympanograms were recorded with a Model 310 computer-based immittance system with the extended high-frequency option (Virtual Corporation, no longer in production). The admittance magnitude and phase were recorded at 9 frequencies (226, 355, 450, 560, 630, 710, 800, 900 and 1000 Hz). The

susceptance and conductance were derived from the recorded magnitude and phase. The pressure was swept from +250 to -275 daPa with a pump rate of 125 daPa/sec. The system was calibrated in three different hard-walled cavities for admittance and phase angle, according to the procedure described in the manual; the phase angle was 90° in the calibration cavities. For a more detailed description of the recording method see Shahnaz et al. (2008).

C. Equivalent volume

Equivalent volumes are computed in mm³ from either the admittance tails (Equation 1) or the susceptance tails (Equation 2) (Shanks, Wilson & Cambron, 1993):

$$V_{ea}^{Y\pm} = Y^\pm * 1000 / (f / 226) \quad [\text{Equation 1}]$$

$$V_{ea}^{B\pm} = B^\pm * 1000 / (f / 226) \quad [\text{Equation 2}]$$

Here, Y^\pm and B^\pm are the admittance magnitude and the susceptance (mmho) at the positive tail (+) or negative tail (-); f is frequency (Hz); and $V_{ea}^{Y\pm}$ and $V_{ea}^{B\pm}$ represent the equivalent volumes (mm³) calculated from the positive or negative admittance and susceptance tails.

These equations assume that the frequency is low enough that the wavelength of sound is large compared with the dimensions of the canal, so that the sound pressure is approximately uniform; this assumption is generally held to be valid up to at least 1 kHz for the adult human ear canal. Given that the newborn ear canal is much shorter and smaller than the adult canal, the assumption can also be taken to be valid for newborns.

It should be noted that a small rigid-walled volume will have an admittance which is a pure susceptance (i.e., which has zero conductance), and its susceptance will be purely compliant (i.e., will include zero mass). If the conductance and mass are not zero, then the V_{ea} in Equations 1 and 2 cannot be interpreted as the physical volume of the acoustical system in question, but rather as a physical volume which would have the same admittance magnitude or susceptance, respectively, as the acoustical system in question. For newborns, for example, the equivalent volume calculated from the admittance magnitude (Equation 1) may differ

significantly from the volume of the canal owing to a non-zero conductance. One of the purposes of this study was to investigate the effects of non-zero conductance on the equivalent volumes calculated from the admittance magnitudes from 226 Hz to 1000 Hz.

All raw data were plotted, and outliers were identified for exclusion from subsequent analysis. Outliers may be due to any of several reasons, such as movement of probe or subject, probe tip blockage against the wall of the canal, ear-canal collapse, a leaky fit, or instrument error. Rather than simply excluding all points that were more than 3 standard deviations above or below the mean, we took into account the values of measurements at neighbouring frequencies for a given ear. As an example, Figure 1 shows all of the equivalent volumes calculated from the negative tail of admittance in left ears. Three points were excluded, annotated as 1, 2 and 3 in Figure 1. Points 1 and 2 were from the same ear. Point 1 indicates that the equivalent volume is 0 mm³ at 355 Hz, but the volumes at 226 and 450 Hz were approximately 350 and 450 mm³ respectively. The significant drop at point 1 may have been caused by a sudden canal collapse in response to high negative pressures. Similarly, points 2 and 3 may have been caused by movement of the probe tip during the measurement. In this way, a total of 45 points out of 1116 points were excluded, which is only about 4% of the total data. Removal of the outliers had relatively minor effects on the 5th and 95th percentiles and very little effect on the medians.

D. Reflectance tympanometry

We use equation 3 to calculate energy reflectance (Keefe and Levi, 1996):

$$R(f, P) = \frac{1 - Z_c Y(f, P)}{1 + Z_c Y(f, P)} \quad [\text{Equation 3}]$$

$R(f, P)$ is the reflectance coefficient, which is a function of frequency (f) and static pressure (P). Z_c is the ear-canal characteristic impedance. In this study, we assume the characteristic impedance of our subjects to be 480 g/s·cm⁴. Studies have indicated that the cross-section of the newborn ear canal is quite flattened in newborns (McLellan and Webb, 1957; Qi et al., 2006). In this study, the average ear-canal diameter was taken to be 3.2 mm based on a 3-week old CT scan (Qi et

al., 2006). As a result, we derived the characteristic impedance of $480 \text{ g/s}\cdot\text{cm}^4$, which is more or less consistent with the observations from Keefe et al. (1993), who reported that the canal diameter of one-month-old infants is 4.4 mm. $Y(f,P)$ is the admittance, a complex number, which we take from the positive and negative tails for each frequency. An energy-reflectance tympanogram is a plot of $|R(f,P)|^2$.

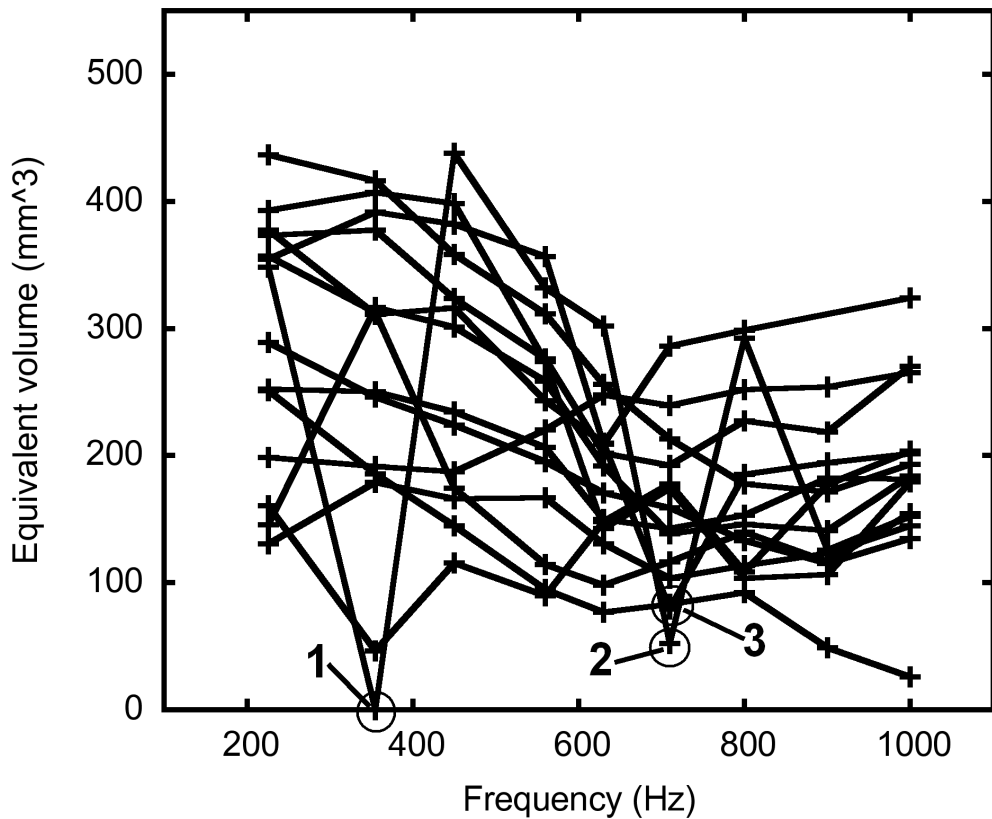


FIG. 1: Equivalent volumes calculated from susceptance at negative tails in the left ear from all subjects. Symbol + indicates individual subjects. 1, 2, and 3 indicate three points that were defined as outliers and excluded from the subsequent analysis.

3.3. RESULTS

Results (susceptance, conductance, equivalent volume and reflectance) obtained from the combined left and right ears are reported here, although previous studies have indicated that equivalent volumes show differences between the left and right ears (Keefe et al, 2000) below 1.4 kHz. More recently, Keefe, Gorga, Jesteadt & Smith (2008) reported that the equivalent volume cannot explain ear differences observed in otoacoustic emissions. In this study, we have not performed statistical comparisons of the left and right ears, mainly because our sample size is relatively small; in addition, the data at different frequencies are not independent and are not normally distributed. The qualitative descriptions that are given below apply equally to the left-ear, right-ear and combined data, and the quantitative values for left and right ears are very similar.

A. Variation of susceptance and conductance tails with frequency

Figures 2a and 2b show the frequency variations of susceptance at the positive tail (B_+) and at the negative tail (B_-), respectively, for the combined left and right ears. Curves are shown for the 5th, 25th, 50th, 75th and 95th percentiles. Generally, the susceptance at both the negative and positive tails increases as frequency increases. For the positive tail, the 5th-to-95th percentile range of susceptance is from 0.24 to 0.55 mmho at 226 Hz, and from 0.80 to 1.71 mmho at 1000 Hz. For the negative tail, the 5th-to-95th percentile range of susceptance is from 0.15 to 0.43 mmho at 226 Hz, and from 0.25 to 1.19 mmho at 1000 Hz.

The susceptances are generally about one third larger for the positive tails, but the susceptance changes by a factor of roughly 3 from 226 to 1000 Hz for both positive and negative tails. This is somewhat less than the factor of 4 that would be expected for a rigid-walled cavity acting as a pure compliance. There is some indication that the susceptance may tend to increase more sharply from 900 Hz to 1000 Hz.

Figures 3a and 3b show the frequency variations of conductance at both positive tails (G_+) and negative tails (G_-), respectively, again for the combined left and right ears. The curves for the positive and negative tails are very similar, with

similar values and both increasing from 226 Hz to 1000 Hz by a factor of about 6. For the positive tail, the 5th-to-95th percentile range of conductance is from 0.05 to 0.21 mmho at 226 Hz, and from 0.67 to 1.72 mmho at 1000 Hz. For the negative tail, the 5th-to-95th percentile range of conductance is from 0.04 to 0.20 mmho at 226 Hz, and from 0.54 to 1.17 mmho at 1000 Hz.

Comparing the susceptance results in Figure 2 with the conductance results in Figure 3, we see that at 226 Hz the conductances at both positive and negative tails are much smaller than the corresponding susceptances, approximating the behaviour of a rigid-walled cavity. At 1000 Hz, however, the conductances are comparable to the susceptances, which is certainly not consistent with a rigid-walled cavity acting as a pure compliance.

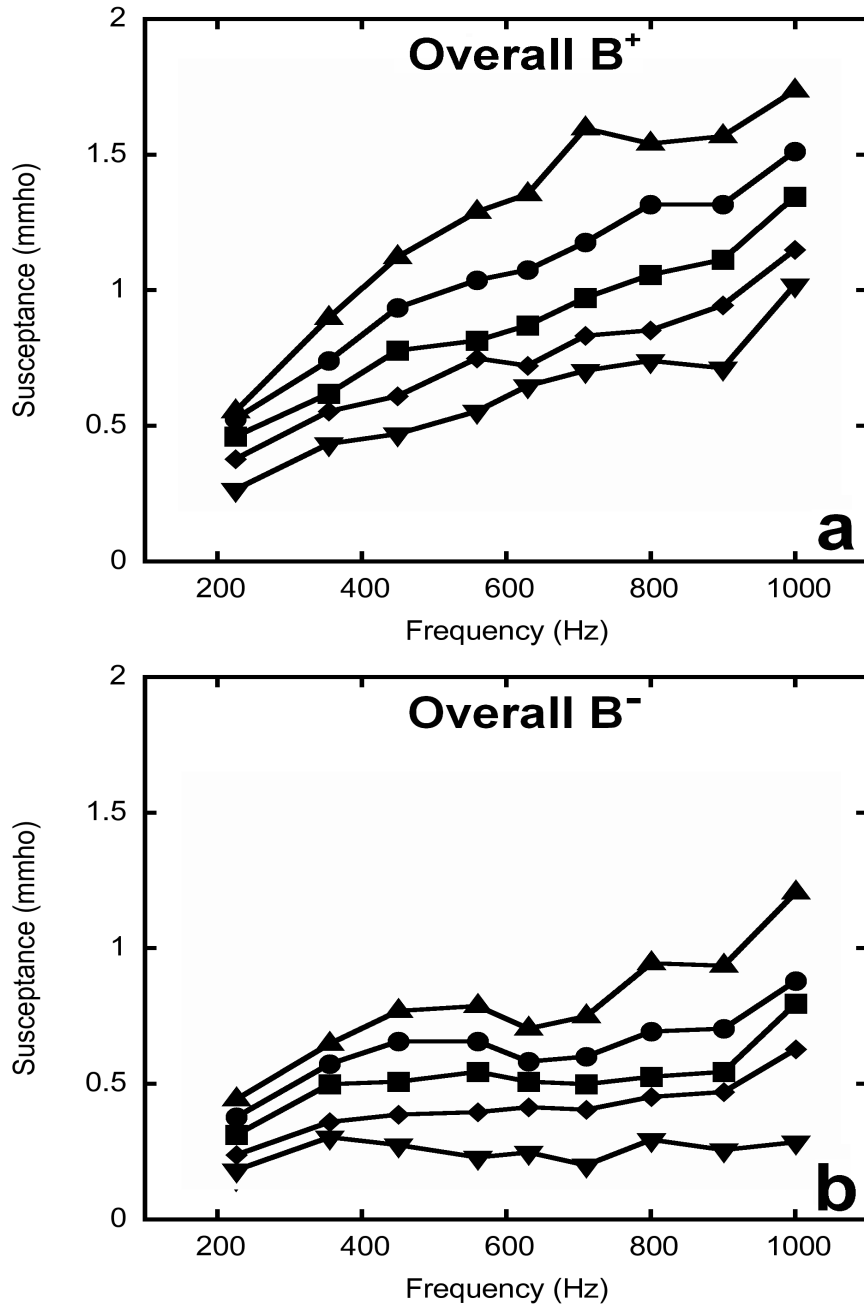


FIG. 2: 5th, 25th, 50th, 75th and 95th percentiles of the distributions of susceptances at each frequency. The susceptances were at (a) positive tails; (b) negative tails. Symbols: ▲ represents 95th percentile; ● represents 75th percentile; ■ represents 50th percentile; ▽ represents 25th percentile; ▼ represents 5th percentile.

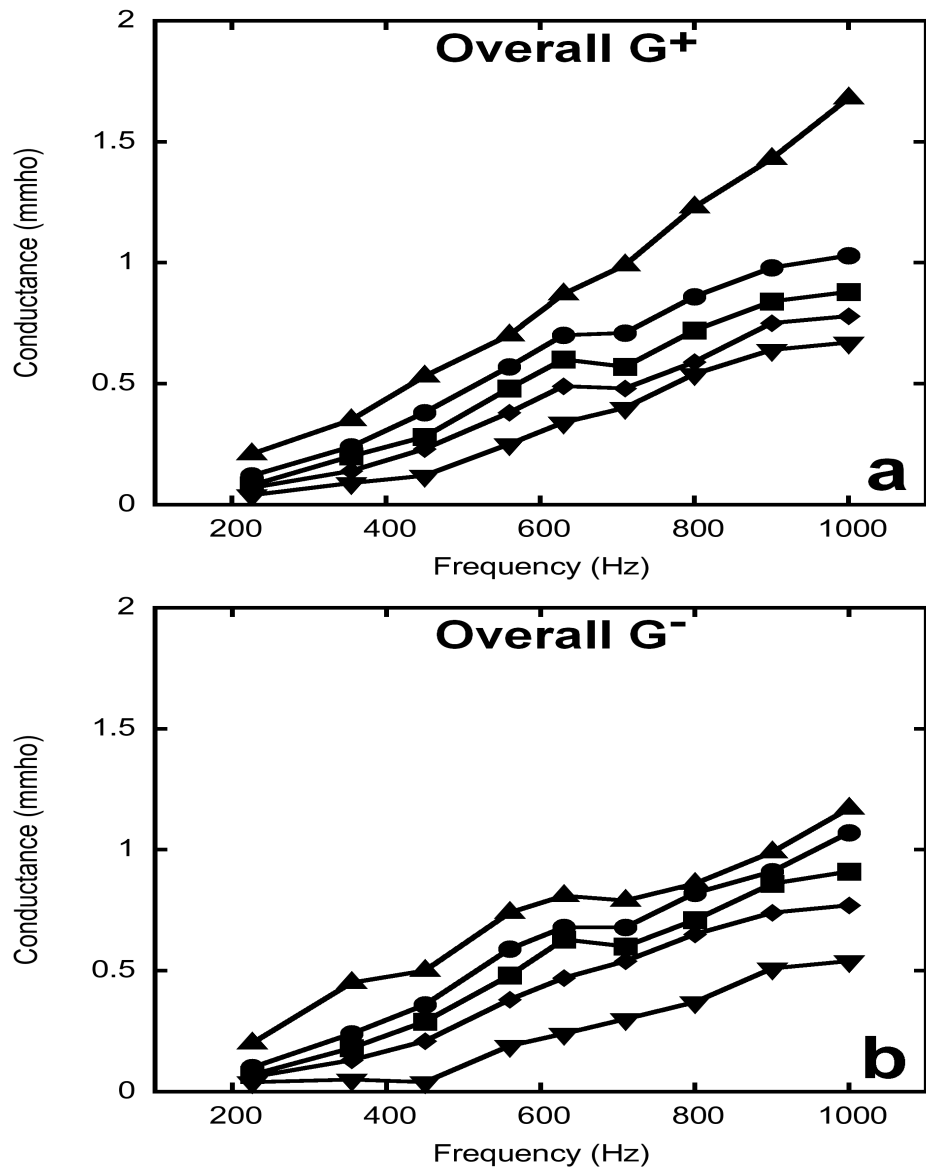


FIG.3: 5th, 25th, 50th, 75th and 95th percentiles of the distributions of conductances at each frequency. The conductances were at (a) positive tails; (b) negative tails. The symbols are the same as in Figure 2.

FIG.4: 5th, 25th, 50th, 75th and 95th percentiles of the distributions of equivalent volumes calculated from the admittance magnitude and susceptance at each frequency for positive tails: (a) from admittance magnitude; (b) from susceptance. The symbols are the same as in Figure 2.

B. Equivalent volume calculated from admittance and susceptance

Figure 4 shows the equivalent volumes calculated from the positive tails of the admittance magnitude (V_{ea}^{Y+}) and susceptance (V_{ea}^{B+}) for the combined left and right ears, computed using equations 1 and 2.

As shown in Figure 4a, both the 95th and 5th percentiles of V_{ea}^{Y+} stay almost constant over the entire frequency range, and the 75th, 50th and 25th percentiles gradually decrease as frequency increases. The 50th percentile of V_{ea}^{Y+} decreases from 450 mm³ at 226 Hz to 380 mm³ at 1000 Hz. The volumes derived from susceptance at the positive tail (V_{ea}^{B+}) also decrease as frequency increases, as shown in Figure 4b. The 50th percentile of V_{ea}^{B+} decreases from 430 mm³ at 226 Hz to 310 mm³ at 1000 Hz.

Figure 5 shows the equivalent volumes calculated from the negative tails of the admittance magnitude (V_{ea}^{Y-}) and susceptance (V_{ea}^{B-}), in the same format as used in Figure 4 for the positive tails. As shown in Figure 5a, the 95th, 75th and 50th percentiles of V_{ea}^{Y-} decrease as frequency increases. The 25th and 5th percentiles of V_{ea}^{Y-} stay almost constant over the entire frequency range, at approximately 190 mm³ and 240 mm³, respectively. Similar to those of V_{ea}^{Y-} , the 95th, 75th, 50th and 25th percentiles of V_{ea}^{B-} also decrease as frequency increases, as shown in Figure 5b. The 50th percentile of V_{ea}^{B-} decreases from 290 mm³ at 226 Hz to 180 mm³ at 1000 Hz. The 5th percentile of V_{ea}^{B-} stays almost constant over the entire frequency range, at approximately 106 mm³.

In summary, the equivalent volumes calculated from admittance magnitude and susceptance show similar trends, generally decreasing as frequency increases. The volumes derived from susceptance show a stronger frequency-dependent characteristic, decreasing faster than those derived from admittance magnitude.

Figure 6 shows comparisons of volumes derived from susceptances with those derived from admittance magnitudes. Figure 6a compares the 5th-to-95th percentile range of equivalent volumes derived from the positive tails of the admittance and the susceptance, for left and right ears combined. Figure 6b compares the same range for the volumes derived from the negative tails. Three

relationships can be observed in Figure 6. First, the equivalent volumes calculated from the admittance tails are larger than those calculated from the susceptance tails, and quite markedly so at some frequencies. (The volumes calculated from admittance magnitude cannot be *less* than those calculated from susceptance, since $|Y|$ must be greater than or equal to B .) Second, the variabilities of equivalent volumes derived from both admittance and susceptance are noticeably less at the higher frequencies. For example, the 5th-to-95th percentile range of equivalent volumes derived from the positive and negative tails of the susceptance are about 310 mm³ and 280 mm³ for 226 Hz, respectively, but only about 190 mm³ and 210 mm³ for 1000 Hz. Third, the differences between the admittance-derived volumes and susceptance-derived volumes are small at low frequencies but increase as frequency increases. At 226 Hz the differences between the admittance-derived volumes and the susceptance-derived volumes are approximately 10% for both positive and negative tails. At 1000 Hz, the difference is approximately 60% for positive tails and approximately 35% for negative tails.

Shanks et al. (1993) calculated the mean equivalent volume in 26 adults using susceptance at both the positive tails (V_{ea}^{B+}) and the negative tails (V_{ea}^{B-}) from 226 Hz to 1120 Hz. Figure 7 compares their mean adult V_{ea}^{B+} and V_{ea}^{B-} with the 5th, 25th, 50th, 75th and 95th percentiles of V_{ea}^{B+} and V_{ea}^{B-} (for both ears combined) obtained in this study. Two relationships can be observed. First, V_{ea}^{B+} and V_{ea}^{B-} in the 3-week-old infants recorded in this study show trends similar to those in adults. Generally, the equivalent volumes decrease as frequency increases and are smaller for negative tails than for positive tails. Second, the mean adult equivalent volumes, for both tails, are much larger than those of 3-week-olds. The mean equivalent volume calculated from the positive tails of the admittance in adults is larger than our median in 3-week-olds by a factor of approximately three. The mean adult equivalent volume calculated from the negative tails is larger than our median by a factor of approximately four.

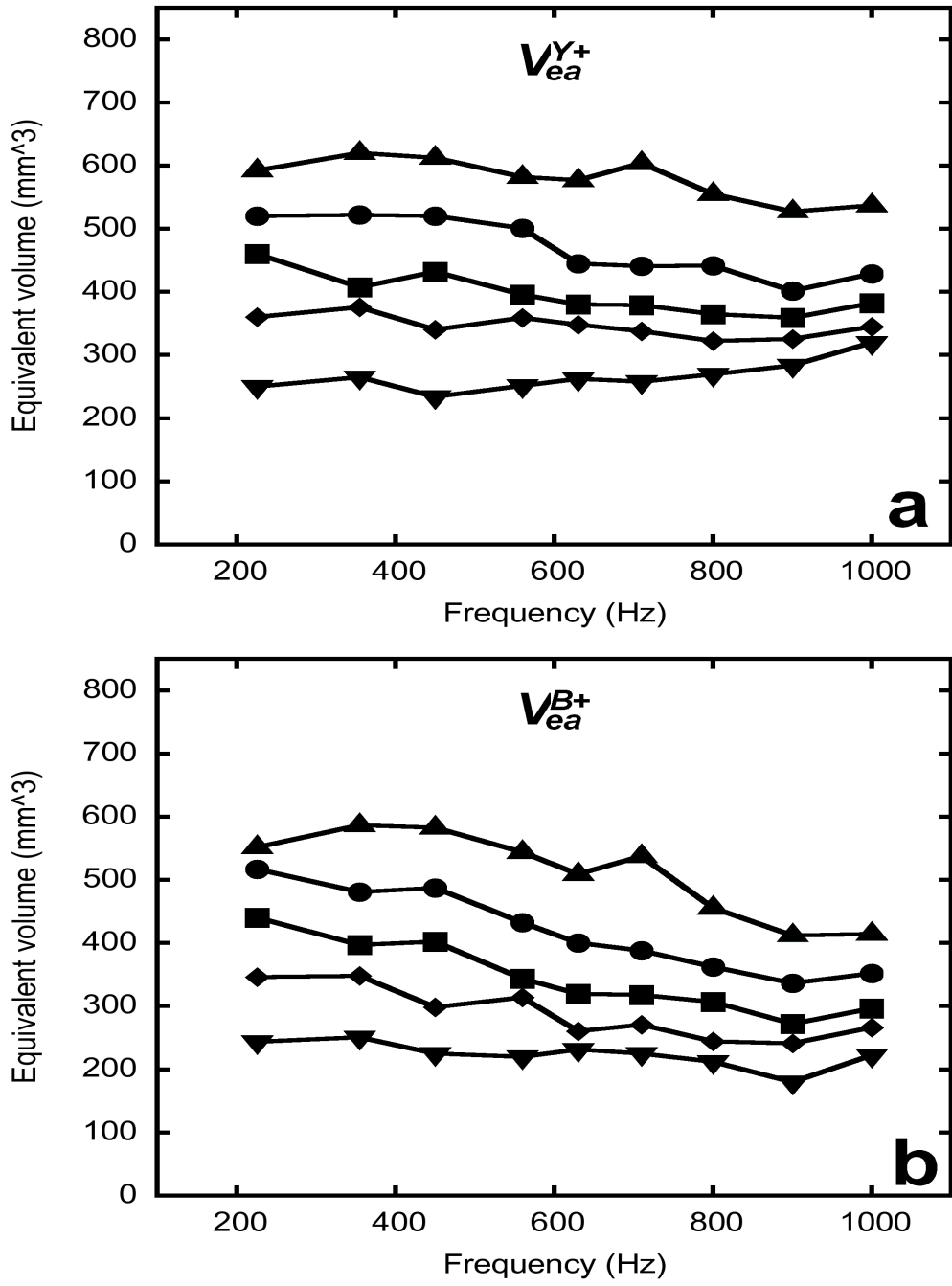
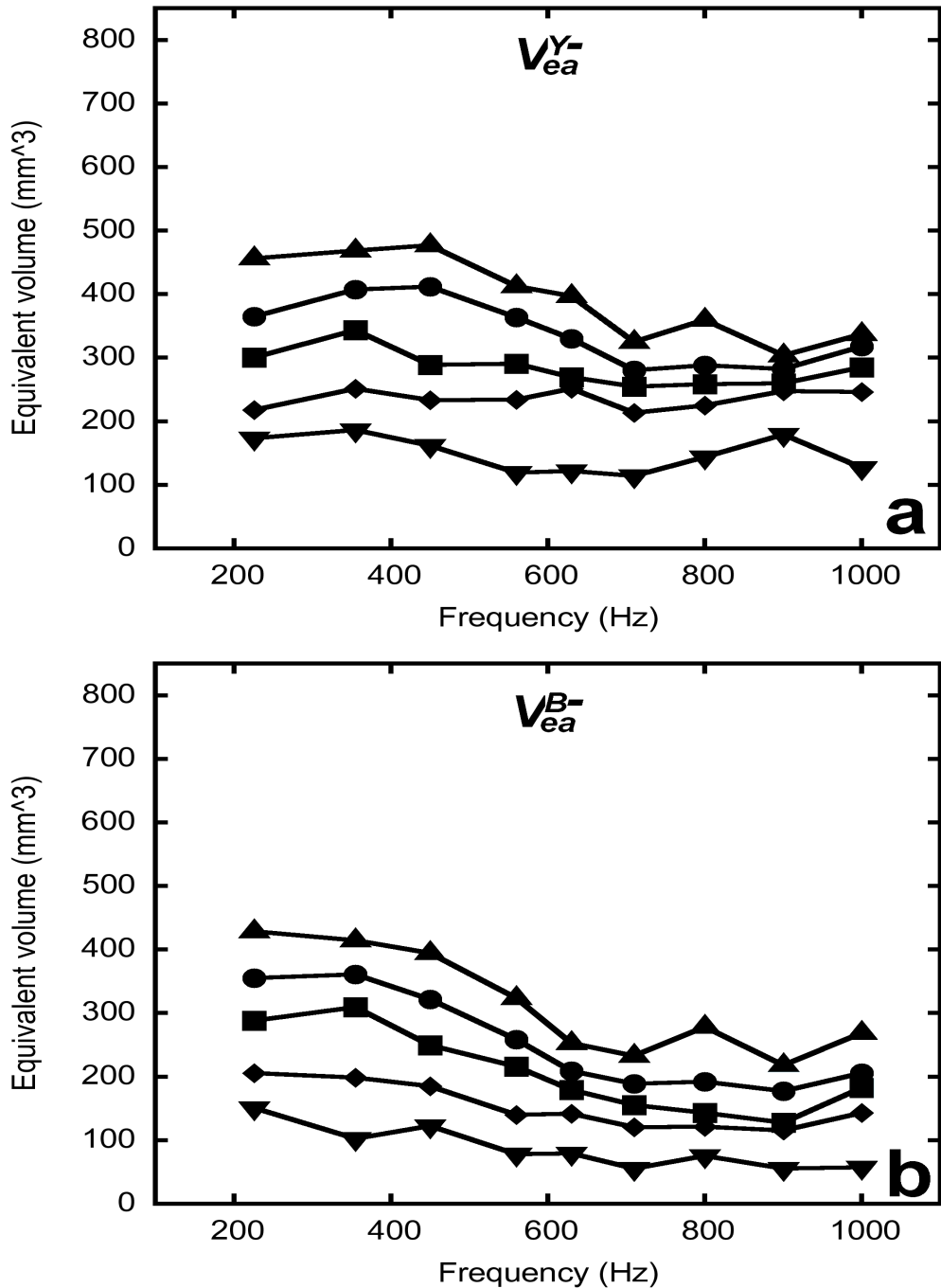


FIG. 4: 5th, 25th, 50th, 75th and 95th percentiles of the distributions of equivalent volumes calculated from the admittance magnitude and susceptance at each frequency for positive tails: (a) from admittance magnitude; (b) from susceptance. The symbols are the same as in Figure 2.



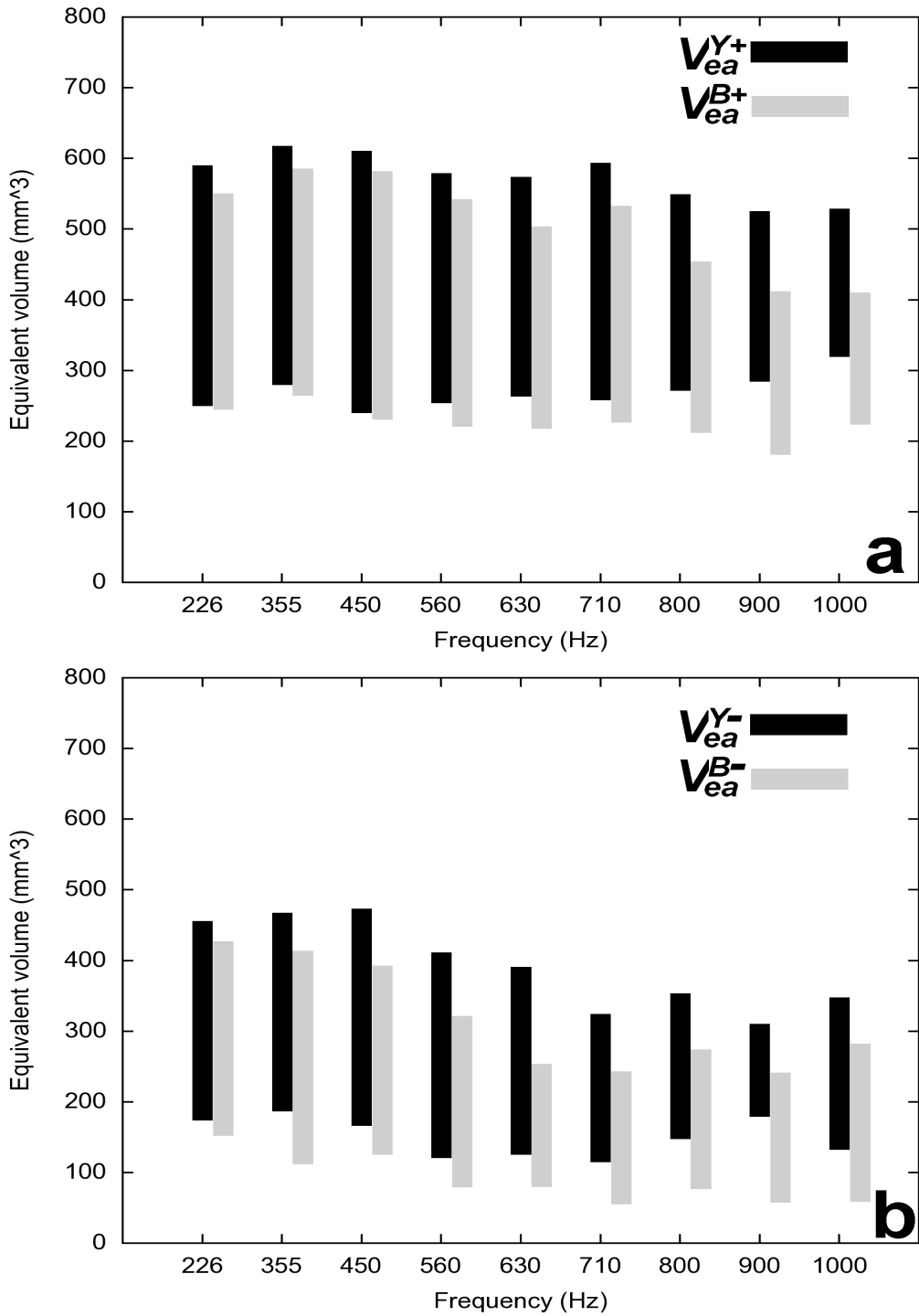


FIG. 6: Comparison of 5th-to-95th percentile ranges of equivalent volumes calculated from the admittance magnitude and susceptance at each frequency for both positive and negative tails: (a) from positive tails; (b) from negative tails.

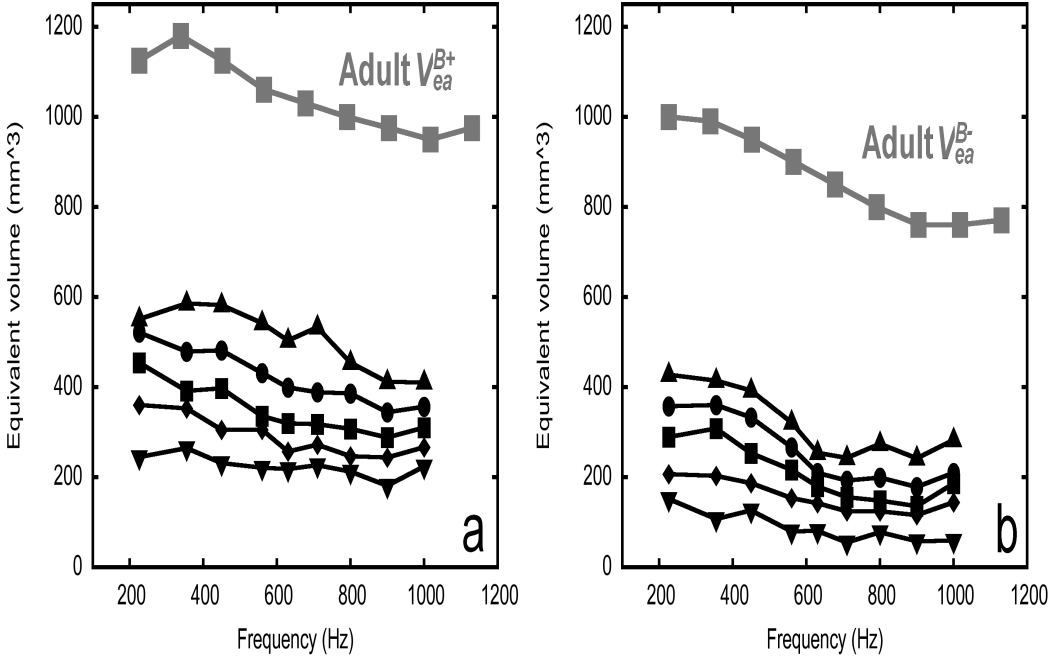


FIG. 7: Comparison of 5th, 25th, 50th, 75th and 95th percentiles of the distributions of equivalent volumes calculated from the susceptance in newborns (obtained in this study) with the mean equivalent volumes calculated from the susceptance in adults (grey symbols with grey lines, Shanks et al. 1993): (a) from positive tails; (b) from negative tails. The symbols are the same as in Figure 2.

C. Variation of equivalent volume with age

Figure 8 compares the 5th-to-95th percentile ranges of equivalent volumes for both adults (Margolis & Heller 1987) and children (Margolis & Heller, 1987; Shanks, Stelmachowicz, Beauchaine & Schulte, 1992) with the newborn values obtained in this study. Margolis and Heller (1987) reported that for adults the 90% range of V_{ea} is approximately 650 to 1500 mm³, and for 3-year-old to 6-year-old children the 90% range is approximately 400 to 900 mm³. Shanks et al. (1992) calculated the equivalent volume based on admittance tails in 334 children, aged from 6 weeks old to about 7 years old. They reported that the 90% range of V_{ea} is approximately 300 to 900 mm³. All of these previous equivalent volumes were

calculated at 226 Hz from positive admittance tails. For adults and older children, the equivalent volumes calculated from admittance magnitude and susceptance at 226 Hz are similar (Shanks and Lilly, 1981), justifying the comparison here of previous admittance-based values with our susceptance-based values for newborns. As shown in Figure 8, V_{ea} increases as age increases. In this study, we found the 5th-to-95th percentile range for the 3-week-old infant V_{ea} to be, at 226 Hz, from 245 to 550 mm³ using the susceptance positive tail, and from 152 to 427 mm³ using the susceptance negative tail. At 1000 Hz, the 5th-to-95th percentile ranges of V_{ea} are from 223 to 410 mm³ using the susceptance positive tail, and from 60 to 280 mm³ using the susceptance negative tail. By comparison, the adult range of 650 to 1500 mm³ is much higher, and the ranges found for older infants and children are intermediate in value.

D. Reflectance tympanometry at both tails

Figure 9 shows the energy reflectance calculated at both positive (ER+) and negative (ER-) tails in this study, and also the energy reflectance previously measured in adults and 4-week-old infants. Margolis et al. (1999) measured the energy reflectance in 20 adults. The energy reflectance was measured at ambient pressure, positive pressure (+3 kPa) and negative pressure (-3 kPa) from 226 to 11310 Hz. We show only their data for +3 and -3 kPa from 226 to 1000 Hz. Sanford and Feeney (2008) measured the energy reflectance at ambient pressure, at ±2 kPa and at ±1 kPa, from 250 Hz to 8000 Hz, in 4-week-old infants. We show only their data for ±2 kPa from 250 to 1000 Hz.

As seen in the Figure, the ER+ and ER- obtained in this study have almost the same magnitude, and both decrease from 226 to 630 Hz and then vary little across the rest of the frequency range. The 50th percentiles of ER+ and ER- are approximately 0.85 at 226 Hz, and then decrease to 0.4 and 0.3 respectively at 630 Hz. From 630 to 1000 Hz, the ER+ gradually decreases from about 0.4 to 0.3, and the ER- gradually decreases from about 0.3 to 0.2. The trend of the 50th percentiles of ER+ and ER- obtained in this study is similar to that of the mean energy reflectance measured by Sanford and Feeney, which decreases to 630 Hz and then stays almost constant from 630 Hz to 1000 Hz. At 226 Hz, the mean

energy reflectances in 4-week-old infants are comparable to the 50th percentiles of the ER+ and ER- obtained in this study. At frequencies above 630 Hz the energy reflectances at +2 kPa and -2 kPa in 4-week-old infants are larger than the ER+ and ER- obtained in this study by a factor of approximately two.

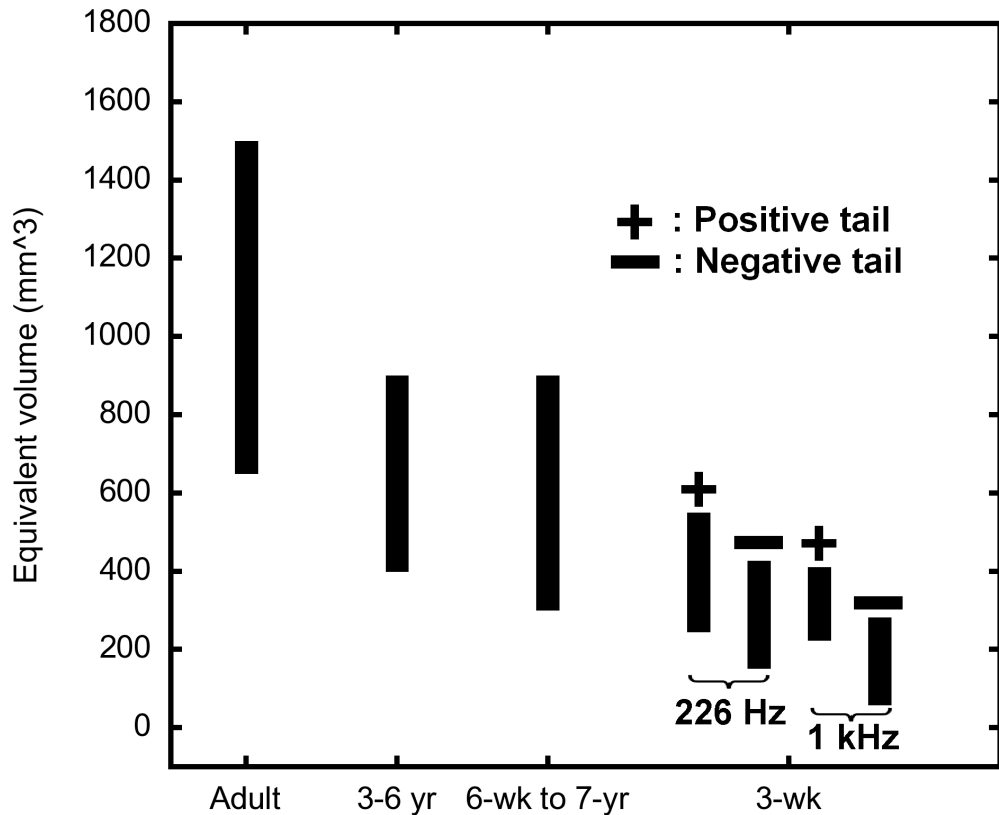


FIG. 8: Comparison of 5th-to-95th percentile ranges of the equivalent volumes for adults (Margolis and Heller, 1987), 3-to-6-year-old children (Margolis and Heller, 1987), 6-week-old to 7-year-old children (Shanks et al. 1992), and 3-week-old infants (this study). The equivalent volumes for adults and older children were calculated from admittance at positive tails at 226 Hz. The newborn equivalent volumes were calculated from susceptance at positive (+) and negative (-) tails at 226 Hz and 1000 Hz.

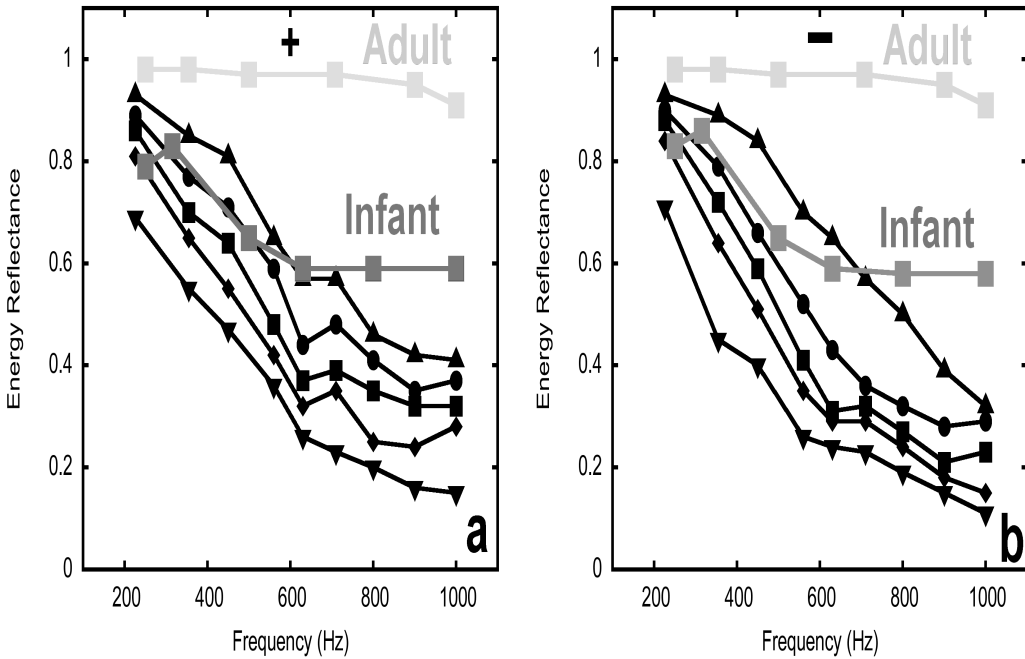


FIG. 9: 5th, 25th, 50th, 75th and 95th percentiles of the distributions of energy reflectances at each frequency. The energy reflectances were calculated from (a) positive tails (+); (b) negative tails (-). The symbols are the same as in Figure 2. Light-grey symbols and lines represent measurements from adults (Margolis et al., 1999); the reflectances for positive and negative tails are almost identical. Dark-grey symbols and lines represent the measurements from 4-week-old infants (Sanford and Feeney, 2008); the reflectances for positive and negative tails are very similar.

3.4. DISCUSSION

At a given frequency, the admittance which best characterizes the mechanics of the middle ear is the input admittance of the middle ear itself. To estimate this admittance from the admittance that is actually measured at the probe tip, one must estimate the effects of the ear canal and then compensate for those effects. It is generally assumed that the effects are those of a rigid-walled volume that can be estimated from the measurements at the high-pressure tails of the tympanogram, but the values obtained at the tails depend on frequency, on whether the positive or negative tail is used, and on whether admittance or susceptance is used.

Our study indicates that equivalent volumes calculated from both the admittance magnitude and the susceptance show a similar tendency: they decrease as frequency increases. This is presumably because the mass component of the susceptance increases as frequency increases, which results in a decrease of the total susceptance and therefore also of the admittance magnitude (at least in the absence of a conductance increase). The admittance-magnitude-derived equivalent volume decreases more slowly with frequency because its conductance component is increasing with frequency. Similar trends are seen in adults, as shown in Figure 7.

The fact that the equivalent volumes vary with frequency indicates that the extreme positive and negative pressures have not driven the canal wall and tympanic membrane to the point of being rigid. This agrees with our model simulation results (Qi et al., 2006; Qi, Funnell & Daniel, 2008). The models showed that the canal-wall and tympanic-membrane volume displacements did not reach plateaus when the pressure was varied between -3 kPa and $+3$ kPa for the canal wall and between -4 kPa and $+2$ kPa for the tympanic membrane. Shanks and Lilly (1981) also reported that even at ± 4 kPa the adult ear canal is not rigid if the probe tip is placed on the cartilaginous part of the ear canal.

Our study shows that at low frequencies the differences between estimates of V_{ea} from admittance magnitude and from susceptance are small but that at high frequencies the difference is larger. The reason for this is that at low frequencies

the conductance is usually quite small compared with the susceptance, so the admittance magnitude and susceptance are almost the same, but at high frequencies the conductance becomes quite large. At 226 Hz, the 5th and 95th percentiles of susceptance are 0.24 and 0.55 mmho at the positive tail (Figure 2a), and 0.15 and 0.43 mmho at the negative tail (Figure 2b). At the same frequency, the 5th and 95th percentiles of conductance are only 0.05 and 0.21 mmho at the positive tail (Figure 3a), and 0.04 and 0.2 mmho at the negative tail (Figure 3b). At 1000 Hz the conductances at both positive and negative tails are comparable to the susceptances. The 5th and 95th percentiles of susceptance are 0.80 and 1.71 mmho at the positive tail (Figure 2a), and 0.25 and 1.19 mmho at the negative tail (Figure 2b). The 5th and 95th percentiles of conductance are 0.67 and 1.72 mmho at the positive tail (Figure 3a), and 0.54 and 1.17 mmho at the negative tail (Figure 3b). These large conductances are presumably associated with vibration of the newborn canal wall and middle ear. Shanks and Lilly (1981) reported that in adults the difference between V_{ea} estimated from admittance and that estimated from susceptance is small at 226 Hz, but that the difference increases to approximately 9% at 660 Hz. In the present study, the difference at 660 Hz is larger: approximately 20% and 30% for the positive and negative tails, respectively. The difference increases to approximately 50% at 1 kHz. The discrepancies between estimates from admittance magnitude and those from susceptance are therefore more pronounced in newborns than in adults. Most current commercial tympanometers calculate V_{ea} using the admittance magnitude at the positive tail. According to our study, this protocol is acceptable for newborns at 226 Hz because the difference in V_{ea} calculated from admittance magnitude and from susceptance is small there. At 1000 Hz, however, an overestimation of the equivalent volume by 50% would lead to a serious underestimation of middle-ear admittance and might lead to higher false-positive rates in newborn hearing screening.

Our results also indicate that the variability of estimates of V_{ea} appear to be smaller at high frequencies than at low frequencies (Figures 4 to 6). The reason for this is unclear. It may suggest that the high-frequency volume estimates are

better suited to compensating for the ear canal. However, the high-frequency estimates are presumably more contaminated by mass and resistive effects, which may make the volume estimates less accurate. In any case, measurements from a larger number of newborns are required to pursue this issue.

Our study provides preliminary normative data for equivalent volumes in 3-week-old infants. Figure 8 compares the 90% range (5th-to-95th percentile range) of equivalent volumes for both adults and children with the 3-week-old values obtained in this study. All of these previous equivalent volumes were calculated at 226 Hz from positive tails. Our equivalent volumes, calculated from both positive and negative tails and for both 226 Hz and 1000 Hz, are smaller than those for adults, which is consistent with the fact that the newborn ear-canal is much smaller than the adult canal. The equivalent volumes calculated for 3-week-old infants from the positive tail for both 226 and 1000 Hz, and the equivalent volume calculated for 226 Hz from the negative tail, are comparable to the smallest equivalent volumes for 3-to-6-year-old and 6-week-to-7-year-old children. The equivalent volumes calculated for 3-week-old infants from negative tails for 1000 Hz are lower than even the smallest equivalent volumes for the other age groups.

Our results (susceptance, conductance and reflectance) suggest that positive and negative static pressures may have different effects on the vibration of the canal wall and/or the tympanic membrane, especially at high frequencies. This may be because the mass distribution changes in response to the high static pressures. For example, it has been reported that newborn ossicles are not completely ossified at birth (Yokoyama, Iino, Kakizaki & Murakami, 1999), and that the joints in the newborn middle ear are not as tight as those in adult ears (Anson & Donaldson, 1981). It is possible that positive and negative pressures change the orientations of the ossicles. This might lead to a different mass distribution, which could contribute to the high-frequency differences in admittance phase at the tails. The flexible canal wall and incomplete tympanic ring may also cause the tympanic-membrane position to change in response to high positive or negative pressures, possibly leading to an additional change in the mass distribution. Related pressure effects have been reported by Sanford and Feeney (2008), who performed

reflectance tympanometry in 4-week-old infants. They reported that high positive (+2 kPa) and negative (-2 kPa) static pressures have significantly different effects on energy reflectance at high frequencies (above 2 kHz). The energy reflectance at positive pressures was much lower than that at negative pressures. They hypothesized that differential effects of canal static pressure above 2 kHz are related to increased flexibility of immature ossicular joints, with negative pressures resulting in a functional decoupling of the ossicular chain and positive pressures resulting in improved coupling. Further experiment and modelling should help to clarify the mechanisms behind the response of the middle ear to large pressures.

Our study shows that, up to at least 1000 Hz, the pressurized energy reflectance increases as age increases (Figure 9). Compared with our results, higher energy reflectances were obtained in the study of Sanford and Feeney (2008), perhaps because the infants in their study were older than those in our study: 4.5 ± 0.4 weeks old (mean \pm SD) vs. 3 weeks old. Holte et al. (1991) measured ear-canal wall displacements in response to static pressures in infants from 1 day old to a few months old. They reported that the canal-wall displacements decreased significantly as age increased. The ratio of the canal-wall displacement to the resting canal diameter was about $10\% \pm 12\%$ in 14–21-day-old infants (for combined positive and negative pressures) but only about $0\% \pm 3\%$ for 30–37-day-old infants. The smaller movement of the canal wall in response to static pressures suggests a correspondingly smaller vibration amplitude in response to probe tones, possibly explaining the higher energy reflectances in the study of Sanford and Feeney. As seen in Figure 9, in adults the mean energy reflectances at ± 3 kPa are close to 1 from 226 to 1000 Hz, which is much higher than the values in newborns. This is probably because the canal wall in adults is bony and because the stiffness of the tympanic membrane in adults is much larger than that of the newborn tympanic membrane (Ruah, Schachern, Zelterman, Paparella & Yoon, 1993). The lower pressurized energy reflectance obtained in this study and in that of Sanford and Feeney (2008) may imply that there is a significant amount of sound energy absorbed by the canal wall. In that case, the reflectance

measurement results would be location-dependent and might be significantly affected by the location of the probe tip.

Our results suggest that the newborn ear canal is not a pure acoustic compliance, particularly at high frequencies. Significant differences exist between equivalent volumes calculated from the admittance-magnitude tails and from the susceptance tails. If the equivalent volume is calculated from the admittance-magnitude positive tail at 1000 Hz, as most tympanometers do for newborn hearing screening and diagnosis, the admittance of the middle ear will be significantly underestimated, especially for high frequencies. This suggests that susceptance should be used to estimate the equivalent volumes in newborns. Moreover, the volume estimated from negative tails is smaller than that estimated from positive tails in newborns. This is presumably due to changes in the physical volume in response to the static pressures, implying that the true ambient-pressure canal volume should not be estimated from either tail alone but should be taken to have some intermediate value. As a first step in investigating multi-frequency tympanometry in newborns, we have analyzed only 3-week-old infants with normal hearing. The number of subjects (16) is not large but gives a good sample size for this particular age. Further work is required with a large number of infants over a range of ages and with abnormal hearing. The present study shows how much ear-canal volume estimates vary across different tympanometric indices and probe frequencies. It brings us a step closer to understanding the acoustical and mechanical properties of the newborn outer and middle ear, which will ultimately allow us to refine the application of tympanometry in infants. In order to improve the quality of newborn hearing screening and diagnosis, further work needs to include both experimental and modelling work. Such work will be important in attempts to understand phenomena such as the frequency dependence of the conductance. This will be useful in determining which combination of frequencies and pressures gives an equivalent volume that is closest to the actual ear-canal volume. More generally, it will help in developing reliable methods for estimating the admittance of the ear canal across a range of frequencies, correcting for the

effects of the ear canal, and extracting more information about middle-ear status from tympanometry.

ACKNOWLEDGEMENTS

This work was supported by the Canadian Institutes of Health Research, the Natural Sciences and Engineering Research Council (Canada), the Fonds de recherche en santé du Québec, the Montréal Children's Hospital Research Institute, the McGill University Health Centre Research Institute, and the Hearing Foundation of Canada. We thank C. Sanford and P. Feeney for providing the energy reflectance data used here.

CHAPTER 4: A NON-LINEAR FINITE-ELEMENT MODEL OF THE NEWBORN EAR CANAL

PREFACE

This chapter is based on the paper *A non-linear finite-element model of a newborn ear canal*, which was published in the *Journal of the Acoustical Society of America*. The purpose of this paper is to investigate the behaviour of the newborn canal wall in response to high static pressures as used in tympanometry.

ABSTRACT

We present a three-dimensional non-linear finite-element model of a 22-day-old newborn ear canal. The geometry is based on a clinical X-ray CT scan. A non-linear hyperelastic constitutive law is applied to model large deformations. The Young's modulus of the soft tissue is found to have a significant effect on the ear-canal volume change, which ranges from approximately 27% to 75% over the static-pressure range of ± 3 kPa. The effects of Poisson's ratio and of the ratio $C_{10}:C_{01}$ in the hyperelastic model are found to be small. The volume changes do not reach a plateau at high pressures, which implies that the newborn ear-canal wall would not be rigid in tympanometric measurements. The displacements and volume changes calculated from the model are compared with available experimental data.

PACS numbers: 43.64.Bt, 43.64.Ha

4.1. INTRODUCTION

Children whose hearing loss is identified and corrected within six months of birth are likely to develop better language skills than children whose hearing loss is detected later (Yoshinaga-Itano et al., 1998). It is recommended that all infants be screened for hearing loss before the age of three months (NIDCD, 1993; Joint Committee on Infant Hearing, 2000).

Although hearing loss is one of the most frequently occurring disorders in newborns, early diagnosis is difficult. Auditory brain-stem response (ABR) screening tests and otoacoustic emissions (OAE) tests can provide objective hearing-loss assessments. Neither test, however, can distinguish conductive hearing loss, which in newborns is often transient, from sensorineural hearing loss. The two types of hearing loss require different medical approaches.

Tympanometry is a fast and simple hearing test routinely used in clinics for the evaluation of conductive hearing loss. Tympanometry involves the measurement of the acoustic admittance of the middle ear in the presence of a range of static pressures. In order to obtain an accurate result for the middle-ear admittance as seen from the tympanic membrane, the complex admittance measured at the probe tip must be adjusted to compensate for the complex admittance due to the ear-canal volume between the probe tip and the tympanic membrane. The accuracy of the middle-ear admittance estimate therefore relies on obtaining an accurate estimate of the admittance of the enclosed air volume.

Studies have shown that middle-ear admittance measurements differ significantly between newborns and adults, in both low-frequency (226 Hz) and higher-frequency (e.g., 1 kHz) tympanometry (Paradise et al., 1976; Holte et al., 1990, 1991; Keefe et al., 1993; Keefe and Levi, 1996; Shahnaz, 2002; Polka et al., 2002; Margolis et al., 2003). Holte et al. (1990) measured ear-canal wall movement in newborns of different ages and found that the diameter of the ear canal can change by up to 70% in response to high static pressures. Keefe et al. (1993) measured ear-canal reflectance over a wide frequency range. They concluded that significant differences between newborn and adult tympanograms

are presumably due in part to the incomplete development of the newborn ear-canal wall and tympanic ring.

The outer ear and the middle ear in human newborns are not completely mature at birth, and various anatomical and physiological changes occur between birth and adulthood (Saunders et al., 1983). The tympanic membrane and the ossicles have reached adult size at birth but the external auditory canal is much smaller than its adult size. In adults the tympanic membrane lies at about a 45-degree angle from the horizontal, while in newborns it is nearly horizontal. The tympanic ring is not completely developed until the age of two years (Saunders et al., 1983). Furthermore, in adults, the inner two thirds of the ear-canal wall are bony and the outer one third is composed of soft tissue; in newborns, the ear canal is surrounded almost entirely by soft tissue (McLellan and Webb, 1957). This lack of ossification presumably allows the external ear canal to change volume significantly in response to large static pressures.

Although the importance of obtaining accurate ear-canal volume-change measurements has been acknowledged, few studies have been conducted to date. Owing to ethical issues and procedural problems it is difficult to measure newborn ear-canal volume change experimentally. The finite-element method is an invaluable research and design tool as it can be used to simulate the behaviour of structures in conditions that cannot be achieved experimentally. Since the first finite-element model of the tympanic membrane was developed (Funnell and Laszlo, 1978), this method has been widely used to investigate the behaviour of both human and animal ears (e.g., Wada et al., 1992; Funnell, 1996; Funnell and Decraemer 1996; Koike et al., 2002; Gan et al., 2002, 2004; Elkhouri et al., 2006). To the best of our knowledge, no finite-element model of the newborn ear canal has been produced until now.

The purpose of this study is to use modelling to investigate newborn ear-canal volume changes under high static pressures. We present here a non-linear three-dimensional model of a healthy newborn ear canal. The geometry of the model is based on a clinical X-ray computed tomography (CT) scan of the ear of a 22-day-old newborn.

We chose a 22-day-old newborn ear canal for two reasons. First, during the first few days of a newborn's life, the outer ear may contain debris and the middle-ear cavity may be filled with amniotic fluid (Eavey, 1993). Newborns are therefore likely to present with conductive hearing loss during the immediate postnatal period, followed by an improvement in hearing as the debris and fluid are cleared. Consequently, hearing-screening tests conducted shortly after birth may lead to high false-positive rates. Second, as part of its Early Hearing Detection and Intervention program (EHDI, 2003), the American Academy of Pediatrics (AAP) recommends that all infants be screened for hearing loss before the age of one month. For these reasons, a 22-day-old newborn is an appropriate study subject.

A hyperelastic constitutive law is applied to model soft tissue undergoing large deformations. Plausible ranges for material-property values are based on data from the literature. Model results are then compared with available experimental measurements.

4.2. MATERIALS AND METHODS

A. 3-D reconstruction

The geometry of the model is based on a clinical X-ray CT scan (GE LightSpeed16, Montreal Children's Hospital) of the right ear of a 22-day-old newborn (study number A07-M69-02A, McGill University Institutional Review Board). The infant had a unilateral congenital atresia (absent external ear canal) on the left side. The external and middle ear on the right side was found to be entirely normal anatomically and exhibited normal hearing. The CT scan contained 47 horizontal slices, numbered from superior to inferior. The scan had 0.187-mm pixels and a slice spacing of 0.625 mm. The ear canal is present in slices 34 to 42. Figure 1 shows slices 11, 34, 37, 40, 42 and 47. The region surrounding the right ear canal in Figure 1 (slice 37) has been enlarged, segmented and labelled in Figure 2. Figure 2 includes the ear canal itself, the soft tissue surrounding the ear canal, the tympanic membrane, the ossicles, the temporal bones, and the simulated probe tip. Rather than including the entire head

in the model, the anterior, posterior and medial surfaces were positioned so as to include the temporal bone and a generous amount of soft tissue. More details are given in section III A.

In this study we used 37 slices, from slice 11 to slice 47. From slice 11 to slice 33, every second slice was used; from 34 to 47, every slice was used. A locally developed program, *Fie*, was used to segment the cross-sections of the temporal bone and soft tissue, as shown in Figure 2. The contours were imported into a 3-D surface-triangulation program, *Tr3*, and the surface was generated by optimally connecting contours in adjacent slices. The surface model is shown in Figure 3. Both *Fie* and *Tr3* are available at <http://audilab.bmed.mcgill.ca/sw/>. Figure 3a is a posterior view of the ear canal and the temporal bone surface. Figure 3b is an antero-lateral view. In order to better display the relationships between the ear canal and the temporal bone, the soft tissue is not shown in Figure 3. It can be seen that there is more temporal bone superior to the ear canal. Figure 4 shows the enclosed ear canal surface. The ear-canal superior wall is much shorter than the inferior wall, as seen in Figure 4a. The tympanic membrane terminates the canal wall in a very horizontal position. It may be considered to form part of the ear canal wall for the innermost 8 mm or so of canal length. As shown in Figure 4b, the superior and inferior walls (D1) are wider than the anterior and posterior walls (D3), which agrees with the observations of McLellan and Webb (1957). Table I provides a summary of ear-canal and tympanic-membrane data from the literature for the adult ear and the newborn ear, and the corresponding data for the finite-element model.

A solid-element model with tetrahedral elements was then generated from the triangulated surface using Gmsh (<http://www.geuz.org/gmsh/>) and imported into COMSOL™ version 3.2 (www.comsol.com) for finite-element analysis.

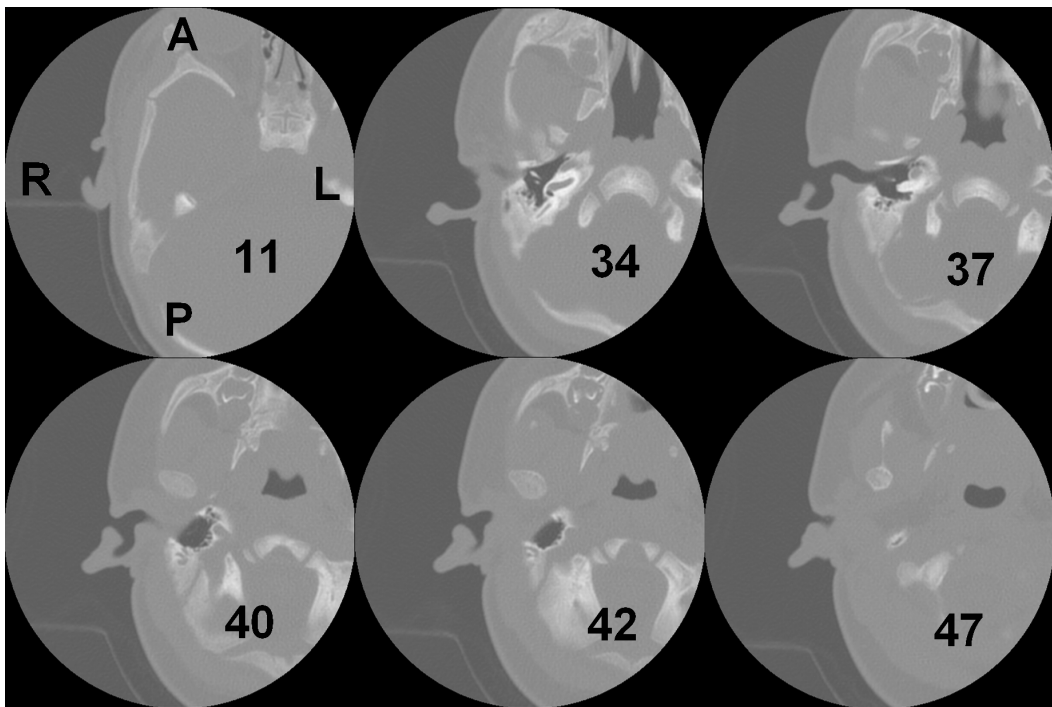


FIG. 1: X-ray CT data for 22-day newborn. Slices 11, 34, 37, 40, 42 and 47 are shown. Slices 34 to 42 include the ear canal. A is anterior; P is posterior; R is right; L is left.

B. Material properties

There are three types of cartilage in the human body: articular cartilage, elastic cartilage and fibrocartilage (Fung, 1993). Elastic cartilage is found in the wall of the external auditory canal (McLellan and Webb, 1957). Articular and elastic cartilage have a similar structure, both containing type II collagen, but elastic cartilage contains more elastic fibres and is therefore more flexible than articular cartilage (Fung, 1993). The Young's modulus of elastic cartilage in adult is between 100 kPa and 1 MPa (Zhang et al., 1997; Liu et. al., 2004). The mechanical properties of cartilage are age-dependent. Williamson et al. (2001) found that the tensile Young's modulus of bovine articular cartilage increased by an average of 275% from newborn to adult.

To the best of our knowledge, the stiffness of human newborn elastic cartilage has never been measured. In this study, we used three Young's moduli: 30 kPa, 60 kPa and 90 kPa. The lowest value is close to the lowest stiffness of soft tissue such as fat (4.8 kPa, Wellman et al., 1999) and gland (17.5 kPa, Wellman et al., 1999) and 90 kPa is close to the lowest stiffness of cartilage in adult humans.

The ear-canal soft tissue is assumed to be homogeneous, isotropic and nearly incompressible. The Poisson's ratio of elastic cartilage in newborns is taken to be 0.475. This value has been widely used in soft-tissue modelling (Torres-Moreno et al., 1999; Cheung et al., 2004; Chui et al., 2004). The soft tissue is also assumed to be hyperelastic, as discussed in Section II D.

C. Boundary conditions and load

In newborn tympanometric measurement, the volume change caused by high static pressures has two sources. The first is tympanic-membrane movement; the second is ear-canal wall movement. The ear canal and the middle ear are configured as a parallel acoustic system. The same uniform static pressure is applied to the ear-canal wall and to the tympanic membrane. The total volume change is equal to the sum of the contributions of these two components. In this study, we focus only on the contribution of ear-canal-wall movement to volume change. We thus assume that the tympanic membrane is rigid and the ossicles, ligaments, etc. are not taken into account. Given that the bones are also assumed

to be rigid in this model, only their surface representation is needed. The probe tip is also assumed to be rigid and its position is taken to be 5 mm inside the ear canal (Keefe et al., 1993), as shown in Figure 2. All other parts of the model are free to move. Static pressure is applied to the ear-canal wall from the inside of the canal.

D. Hyperelastic finite-element method

While undergoing tympanometry procedures, the newborn ear-canal wall deforms significantly under the high static pressures. Accordingly, linear elasticity with the infinitesimal-deformation formulation is not appropriate to formulate the finite-element model. As a result, we used a hyperelastic finite-deformation formulation.

In finite-deformation theory, the deformation gradient $\mathbf{F} = \partial\mathbf{x}/\partial\mathbf{X}$ is defined where \mathbf{X} denotes a point in the reference configuration. The current position of the point is denoted by $\mathbf{x} = \mathbf{X} + \mathbf{u}$ where \mathbf{u} is the displacement from the reference position to the current position. Using $\mathbf{C} = \mathbf{F}^T \mathbf{F}$, the ‘strain invariants’ are defined as

$$I_1 = \text{tr}(\mathbf{C}) \quad [\text{Equation } 1]$$

$$I_2 = \frac{1}{2}(I_1^2 - \text{tr}(\mathbf{C} \cdot \mathbf{C})) \quad [\text{Equation } 2]$$

where tr is the trace operator.

Various strain-energy functions can be applied to soft tissue, such as neo-Hooke, Mooney-Rivlin, Arruda-Boyce, etc. In this study we focus on the polynomial method, which is a generalization of the neo-Hooke and Mooney-Rivlin methods and which has been widely used to simulate large deformations in almost incompressible soft tissues such as skin, brain tissue, breast tissue and liver (e.g., Samani and Plewes, 2004; Cheung et al., 2004). A second-order polynomial strain-energy function can be written as

$$W = C_{10}(I_1 - 3) + C_{01}(I_2 - 3) + \frac{\kappa}{2}(J - 1)^2 \quad [\text{Equation } 3]$$

where W is the strain energy; C_{10} and C_{01} are material constants; κ is the bulk modulus; and J is the volume-change ratio. J is defined as

$$J = \det \mathbf{F} \quad [\text{Equation 4}]$$

where \det is the determinant operator.

Under small strains the Young's modulus of the material, E , may be written as

$$E = 6(C_{10} + C_{01}) \quad [\text{Equation 5}]$$

Further details about the hyperelastic model can be found elsewhere (e.g., Holzapfel, 2000).

The ratio $C_{10}:C_{01}$ is here taken to be 1:1, which has been widely used for biological soft tissue (e.g., Mendis et al., 1995; Samani and Plewes, 2004).

E. Volume calculation

The air volume between the probe tip and the tympanic membrane can be calculated using the three-dimensional divergence theorem:

$$\iiint_M \operatorname{div} \mathbf{F} dV = \iint_S \mathbf{F} \cdot \mathbf{n} dS \quad [\text{Equation 6}]$$

where M is a solid volume with a closed boundary surface, S , whose unit normal vector is denoted by \mathbf{n} . The divergence of \mathbf{F} is defined as

$$\operatorname{div} \mathbf{F} = \frac{\partial \mathbf{F}}{\partial x} + \frac{\partial \mathbf{F}}{\partial y} + \frac{\partial \mathbf{F}}{\partial z} \quad [\text{Equation 7}]$$

By choosing \mathbf{F} such that $\operatorname{div} \mathbf{F}=1$, we can easily obtain the ear-canal volume as

$$V = \iiint_M \operatorname{div} \mathbf{F} dV = \iint_S \mathbf{F} \cdot \mathbf{n} dA \quad [\text{Equation 8}]$$

There is an infinite number of choices for \mathbf{F} that have $\operatorname{div} \mathbf{F}=1$. In our study, we simply choose $\mathbf{F}=(x,0,0)$. The air volume can therefore be computed by integration over the deformed surface of the corresponding closed volume. Further details can be found elsewhere (e.g., Matthews, 2000, p. 97).

4.3. RESULTS

A. Convergence tests

Convergence tests are used to investigate how many elements should be used in the model. The results of a finite-element simulation depend in part on the resolution of the finite-element mesh, that is, on the numbers and sizes of the elements used. In general, the greater the number of elements the more accurate

the results, but also the longer the time required for the computations. Nonlinear simulations in particular can be very time-consuming.

In our convergence tests, the first step was to decide how much of the scan to incorporate in the x direction (from lateral to medial) and y direction (from posterior to anterior). The second step was to decide how many slices should be used in the model. For both step 1 and step 2, the surface models have a nominal mesh resolution of 18 elements per diameter. The last step was to decide what mesh resolution to use for the model. In the convergence tests the Young's modulus is 60 kPa and the Poisson's ratio is 0.475.

As shown in Figure 2, three different models are compared. The first one (small model) has a lateral-medial size of about 32 mm and an anterior-posterior size of about 28 mm. The second model (middle model) is about 36 mm by 39 mm. The third one (large model) is about 41 mm by 50 mm. All three models were generated based on slices 11 to 47.

The three models were compared based on the absolute values of the maximum displacements for both negative and positive pressures of 3 kPa, and on the ear-canal volume change for the same pressure. All three models have almost the same maximum displacements. The volume changes for model 1 were 6.7% larger than those of model 2 because model 1 contains less bone to constrain the wall motion, but models 2 and 3 differed by only about 1%. This implies that the middle model provides enough accuracy and it is the one used for the remaining simulations.

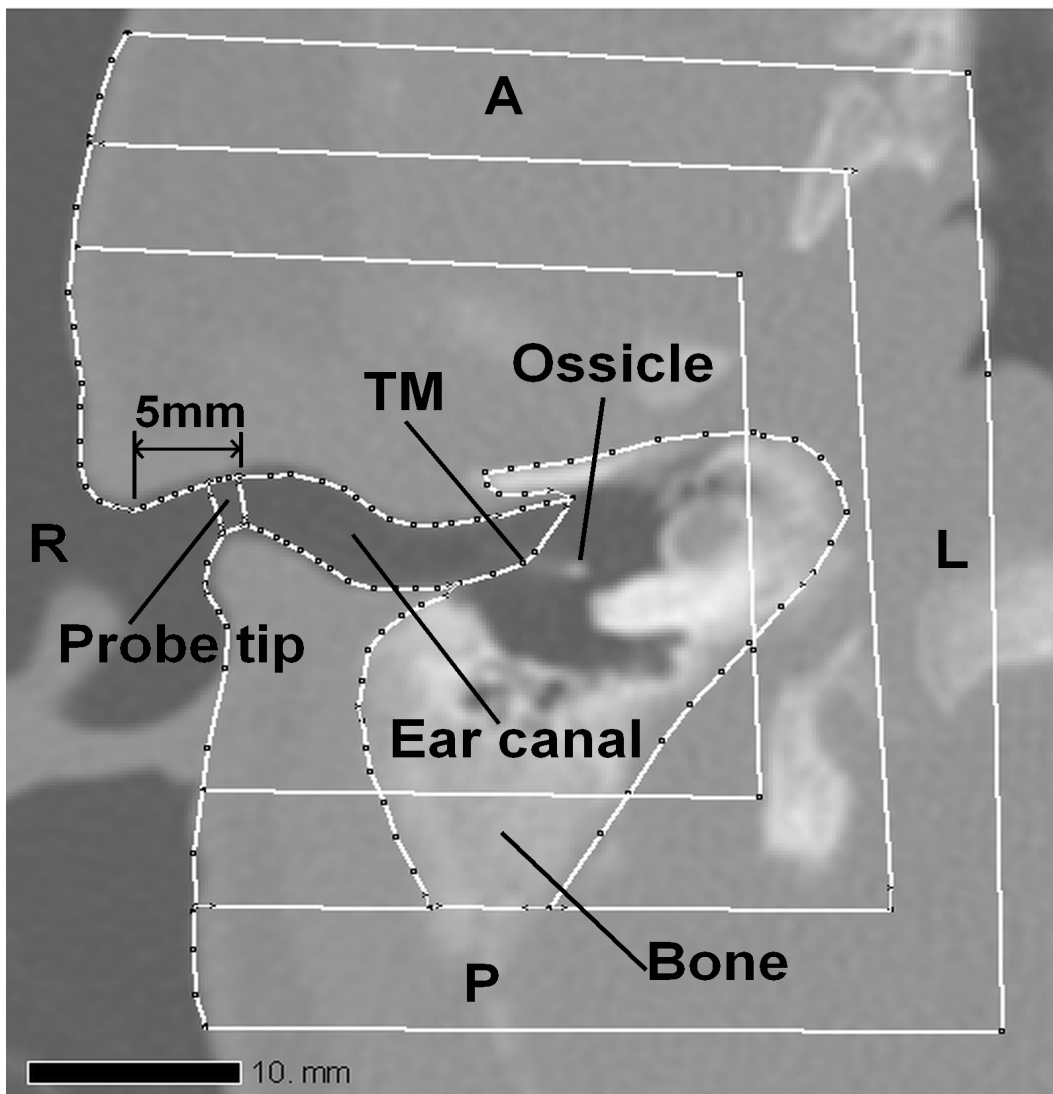


FIG. 2: Slice 37, showing segmented structures. TM is tympanic membrane. The probe tip is positioned at 5 mm from the entrance of the ear canal. A is anterior; P is posterior; R is right; L is left. Three different sizes of models are shown; more details are given in Section III A.

As mentioned earlier, the ear canal is present in slices 34 to 42. In order to investigate how many slices above and below the canal should be incorporated into the model, five different models were studied. Figure 5 illustrates the different configurations. Model 1 was composed of 20 slices, from slice 28 to slice 47. Model 2 included 5 more slices superiorly; it contains 25 slices, from 23 to 47. Model 3 included 5 more slices inferiorly. Since our CT scan did not include any slices inferior to slice 47, we created five artificial slices (numbered 48 to 52) by extrapolation and comparison with CT scans for newborns of about 3 months of age. The artificial slices included only soft tissue, the boundary conditions of which were made the same as those of the other soft tissue in the model. Model 3 was thus composed of 30 slices, from 23 to 52, slices 48 to 52 being artificial. Model 4 was based on model 3, the only difference being the incorporation of another 5 artificial slices inferiorly; the model thus contained 35 slices, from 23 to 57. Finally, model 5 was composed of 37 slices, from 11 to 47; no artificial slices were included in model 5.

As before, the different models were compared based on the absolute values of the maximum displacements and on the ear-canal volume changes for both negative and positive pressures of 3 kPa. The maximum displacements were almost same; the differences were less than 2%. The volume changes for model 1 are up to 8.9% larger than those for the other models, presumably because it has fewer constraints due to the temporal bone superior to the canal, but the volume changes for models 2 to 5 are all within 1.3%. These results imply that our 37-slice dataset is sufficient even though there are not very many slices inferior to the ear canal. For the remainder of this paper we use model 5.

In order to decide what mesh resolution should be used, four different resolutions were compared. The initial surface models have nominal numbers of elements per diameter of 12, 15, 18 and 22 respectively. The resulting solid models have 9076, 12786, 19233 and 23674 tetrahedral elements respectively. As the mesh resolution increases, the maximum displacement of the entire model increases monotonically. The difference in maximum displacement between the 9076-element model and the 12786-element model was about 4%, and the

difference between the 12786-element model and the 19233-element one was about 5%. The difference between the 19233-element model and the 23674-element one, however, was less than 1%, and the location of the maximum displacement changed by less than 1mm. The model with 19233 elements was selected for further simulations.

B. Sensitivity analysis

Sensitivity analysis is used to investigate the relative importance of model parameters. In this study we focus on the ear-canal volume change under high static pressures, and therefore the effects of parameters on ear-canal volume changes were investigated. Sensitivity was analyzed for Young's modulus, Poisson's ratio and the $C_{10}:C_{01}$ ratio. The Young's modulus was found to have the greatest impact on the volume change. Figure 6 shows ear-canal volumes corresponding to different Young's moduli for static pressures from -3 to $+3$ kPa. As Young's modulus increases, the model canal-wall volume changes decrease significantly.

Values from 0.45 to 0.499 have been used in the literature for Poisson's ratio for soft tissue (Li et al., 2001; Samani and Plewes, 2004). A value of 0.5 corresponds to incompressibility. Increasing Poisson's ratio from 0.45 to 0.499, with a Young's modulus of 60 kPa, resulted in a 1.5% reduction in volume change at $+3$ kPa, and a change of only 1.1% at -3 kPa. The model is thus insensitive to Poisson's ratio, which is consistent with previous modelling (Funnell et al., 1978; Qi et al., 2004).

Three different ratios of C_{10} to C_{01} were studied, namely, 1:0, 1:1 and 0:1. The sum of C_{10} and C_{01} is kept constant at 10 kPa, corresponding to a small-strain Young's modulus of 60 kPa as given by Equation 5. The volume changes occurring with the three combinations of C_{10} and C_{01} differ by less than 3% at $+3$ kPa and by even less at -3 kPa. The model is thus insensitive to the $C_{10}:C_{01}$ ratio when the sum of C_{10} and C_{01} remains constant. This is consistent with the results of Mendis (1995), who used a three-dimensional Mooney-Rivlin model for brain tissue and found that, when the deformation is under 30%, the different combinations of C_{10} and C_{01} had little effect on model displacements.

C. Model displacements and displacement patterns

The ear-canal wall of the model displays non-linear elastic behaviour leading to an *S*-shaped pressure-displacement relation under high static pressures, as shown in Figure 7. The displacement curves are very similar in shape to the volume curves shown in Figure 6. As the Young's modulus increases, the maximum displacement decreases in approximately inverse proportion.

The smaller the Young's modulus is and the larger the displacements are, the stronger the non-linearity is. When Young's modulus is 90 kPa, the pressure-displacement relation becomes almost linear. When Young's modulus is 30 kPa, the slopes of the curves decrease significantly as the pressure becomes either more negative or more positive, but the displacement curve does not reach a plateau by either -3 kPa or +3 kPa.

The maximum displacement of the entire model occurs on the medial inferior surface of the ear canal. The maximum is quite localized. Figure 8 shows the displacement patterns on the superior and inferior surfaces of the canal for a pressure of +3 kPa, when Young's modulus is 60 kPa. The displacements of the inferior surface are bigger than those of the superior surface. This is because there is temporal bone around the top of the newborn ear-canal but the bone around the bottom has not completely developed, as shown in Figure 3.

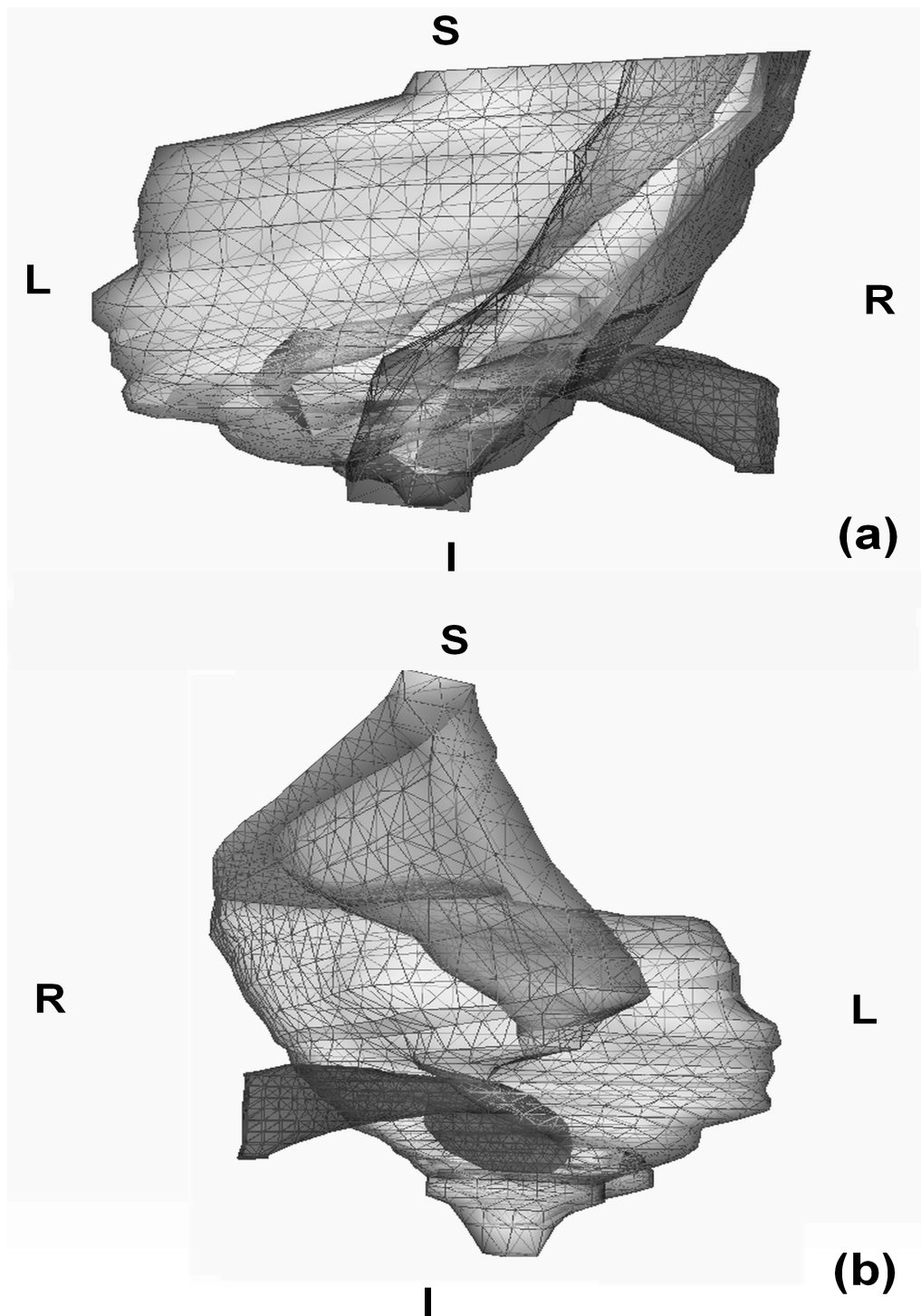


FIG. 3: Surface mesh of finite-element model. The ear canal and temporal bone surface are displayed; the soft tissue is not shown. (a) Posterior view. (b) Antero-lateral view. S is superior; I is inferior; R is right; L is left.

D. Comparisons with experimental data

In this section we shall compare our simulation results with two sets of experimental data, maximum canal-wall displacement measurements (Holte et al., 1990) and tympanometry (Shahnaz, 2002; Polka et al., 2002).

1. Displacement measurements

Holte et al. (1990) measured the maximum displacements of ear-canal walls in newborns of different ages. Positive and negative pressures of 2.5 to 3 kPa were introduced by a syringe system. Displacements of the ear-canal wall and tympanic membrane were recorded by an otoscope with a videocassette recorder. The videotapes were reviewed, and ear-canal wall diameters at ambient pressure and at maximum static pressures were measured with a transparent ruler. The relative change in ear-canal wall diameter under maximum static pressure was expressed as a percentage of the resting diameter. For newborns aged from 11 to 22 days, the diameter change was $7.9\% \pm 11.1\%$ for the positive pressure, and $-15.0\% \pm 22.1\%$ for the negative pressure.

The maximum displacement in our model takes place on the medial inferior surface of the ear canal, which probably corresponds to a location beyond that which Holte et al. were able to observe. McLellan and Webb (1957) used an otoscope to examine 20 cleansed ear canals from 10 healthy full-term newborns. They concluded that the inferior wall ascends from the tympanic membrane, and from the external orifice of the canal, to a transverse ridge which divides the inferior wall into inner and outer portions. Unlike the outer portion, the inner portion of the inferior wall can hardly be seen with an otoscope. Since Holte et al. also used an otoscope in their experiments, it would have been difficult for them to observe the inner part of the inferior wall. We conclude, therefore, that their diameter-change measurements were taken lateral to the ridge. As shown in Figure 8, in our model the displacements of the canal wall are larger at the ridge than they are lateral to the ridge; we therefore assume that Holte et al. measured the diameter changes at the ridge. In our model the ridge is located 11 mm from the probe tip. We use the model displacements at this point for comparison with the measurements of Holte et al.

McLellan and Webb (1957) observed a sagittal cross section at the ridge which appeared oval in shape in 16 ears, with the longer diameter being anterior-posterior. In our model, the resting diameters at the transverse ridge are shown in Figure 4. The narrowest diameter (D2) at 11 mm is about 1.6 mm, and the widest diameter (D3) is about 4.4 mm. Since the resting diameters were not mentioned by Holte et al., we do not know if the narrowest or the widest diameter was applied when the ratios of ear-canal wall displacements to resting diameters were calculated. Thus, for our model, the ratios of displacement (at the 11-mm position) to diameter was calculated for both resting diameters (1.6 and 4.4 mm), and for both ± 2.5 kPa and ± 3 kPa. The results are shown in Figure 9 together with the experimental results of Holte et al. For positive pressures, when the narrowest resting diameter (1.6mm) is applied the results for the model with a Young's modulus of 30 kPa is beyond the experimental range; when Young's modulus is 60 kPa, part of the simulation results are within the experimental range; when Young's modulus is 90 kPa, they are totally within the experimental range. For negative pressures, the simulation results with a Young's modulus of 30 kPa are partly within the experimental range; for 60 and 90 kPa they are all within the experimental range. When the widest resting diameter (4.4mm) is applied, all of the simulation results are within the experimental range for both positive and negative pressures.

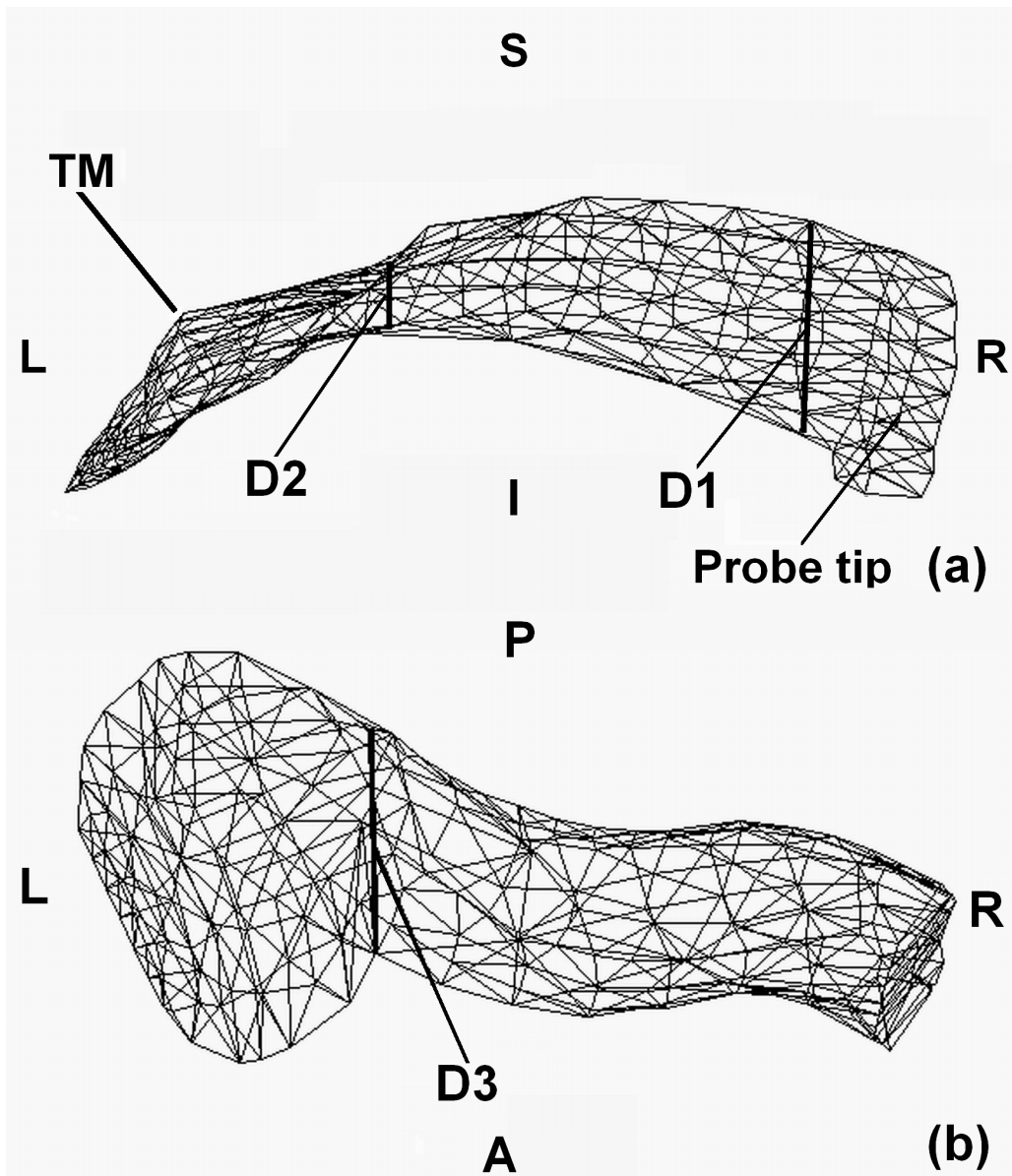


FIG.4: Ear canal model. (a) Posterior view. (b) Inferior view. D1 (4.8mm) is the maximum diameter, in the superior-inferior direction; D2 (1.6mm) is the minimum diameter, in the superior-inferior direction; D3 (4.4mm) is the maximum diameter in the anterior-posterior direction. S is superior; I is inferior; P is posterior; A is anterior; R is right; L is left.

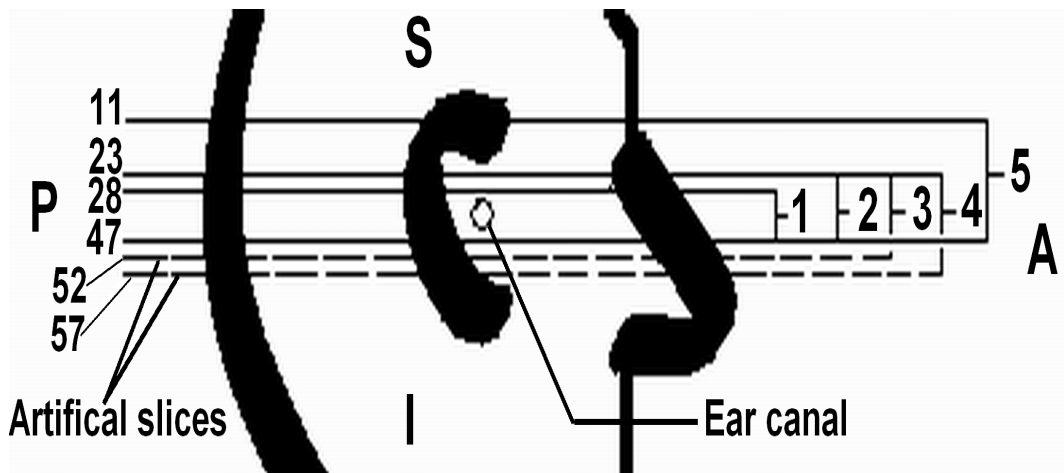


FIG. 5: Slices used in test models 1 to 5. Slices 48 to 57 are artificial slices, as discussed in the text. A is anterior; P is posterior; S is superior; I is inferior.

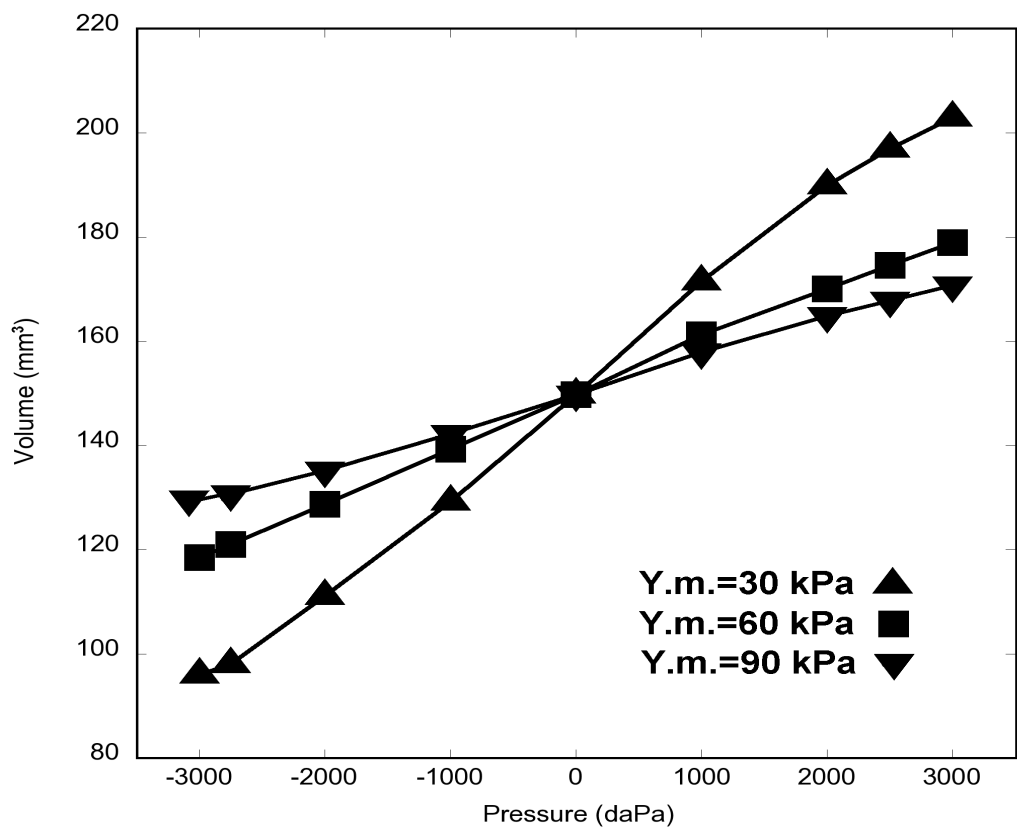


FIG. 6: Calculated ear-canal volume for three different Young's moduli (Y.m.). When pressure is 0, ear-canal volume is 150 mm³.

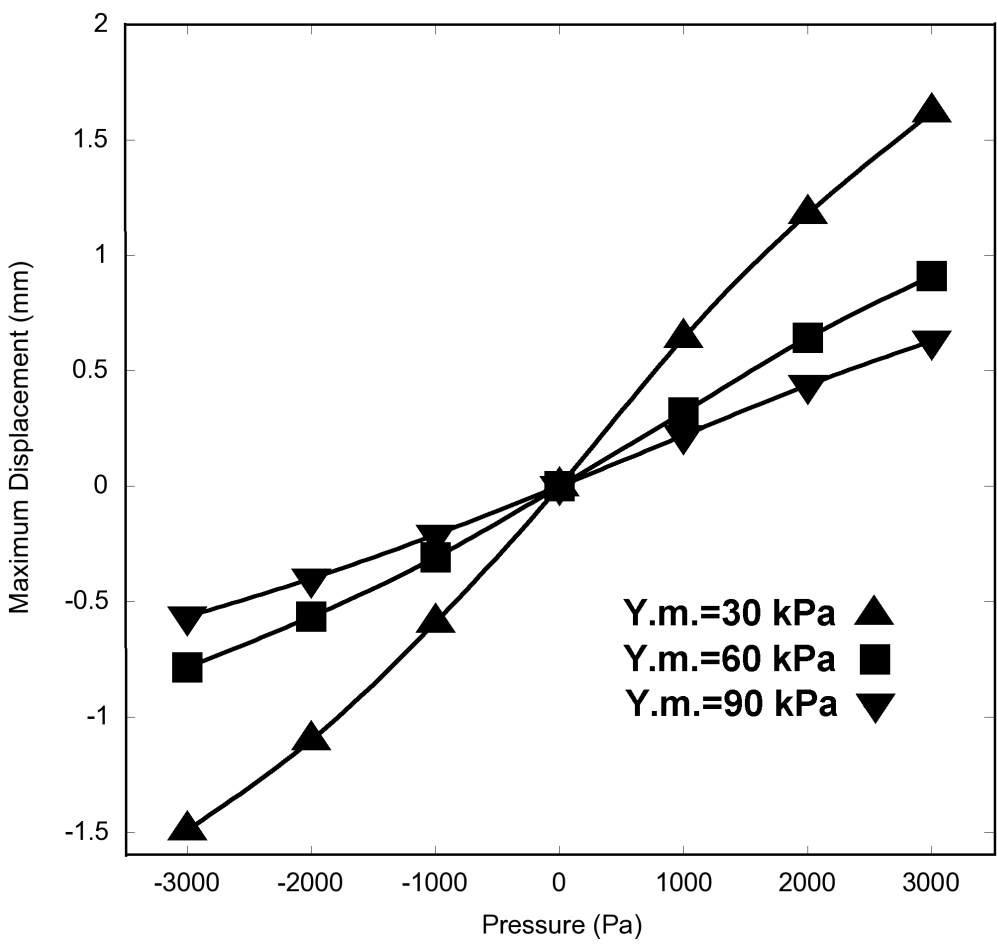


FIG. 7: Maximum displacement of the entire model for three different Young's moduli.

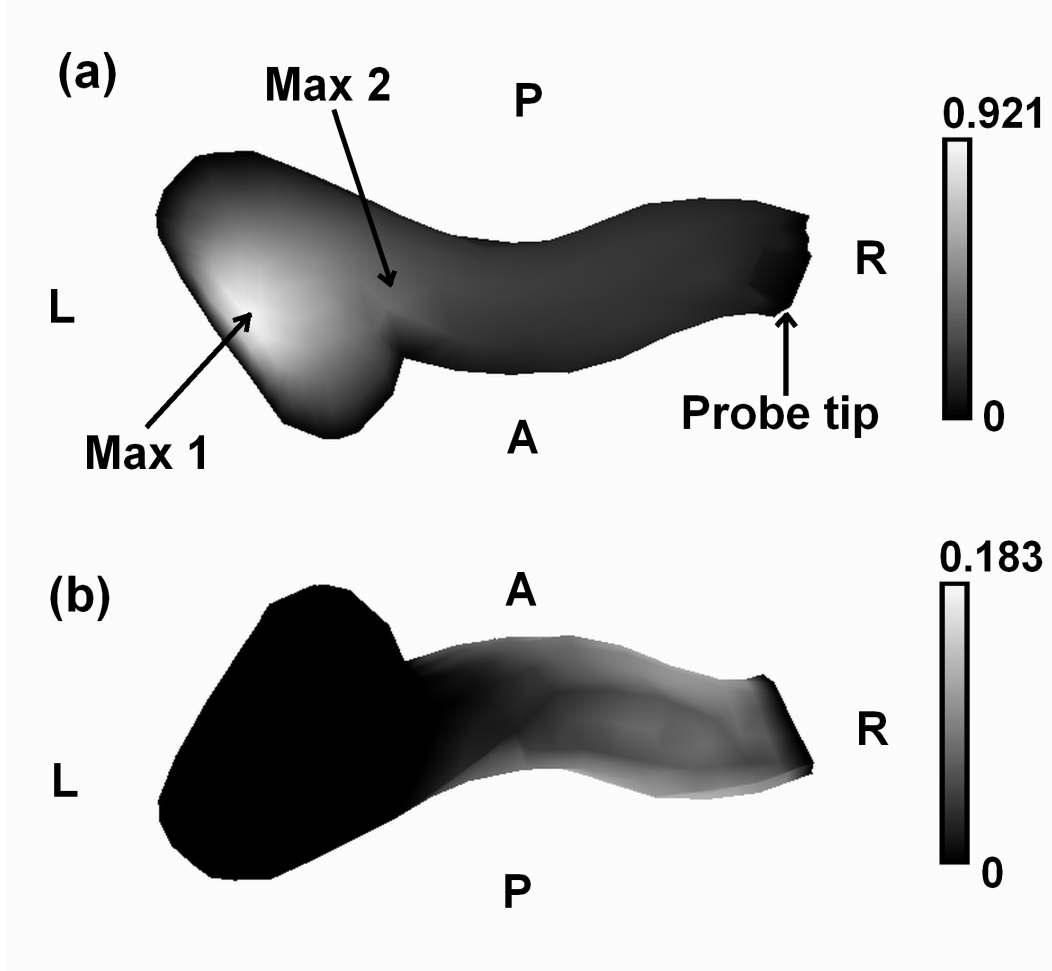


FIG. 8: Displacement pattern of ear-canal wall for static pressure of +3 kPa. (a) Ear-canal floor. Grey-scale is from 0 to 0.921 mm (b) Ear-canal roof. Grey-scale is from 0 to 0.183 mm. Max 1, the maximum displacement of the entire model, is 0.921 mm. Max 2, the maximum displacement observable from the probe tip, is 0.452 mm. Since the tympanic membrane (TM) and the probe tip are assumed to be fixed, the corresponding displacements are zero. A is anterior; P is posterior; R is right; L is left.

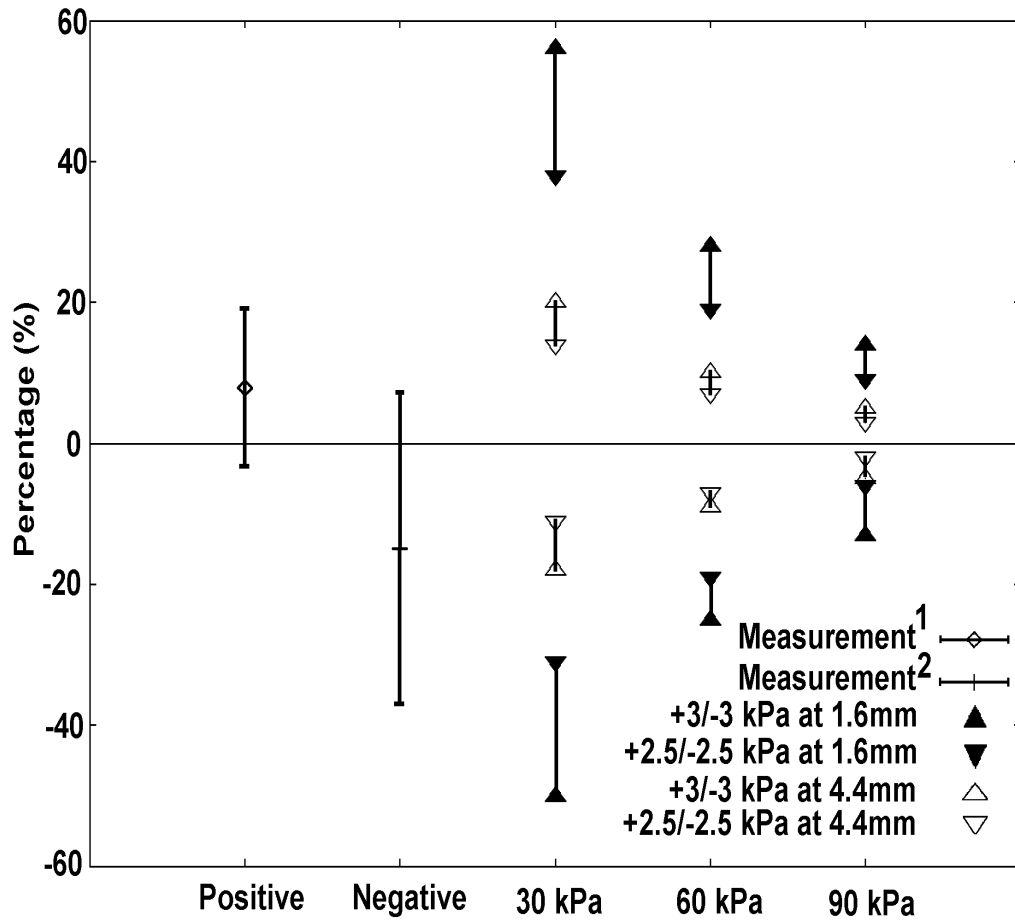


FIG. 9: Comparison of experimental data (Holte et al., 1990) with simulation results. Positive = experimental data for pressures of +2.5 to +3 kPa; Negative = experimental data for pressures of -2.5 to -3 kPa. Triangles represent simulation results for Young's moduli of 30, 60 and 90 kPa, respectively. Filled and open triangles indicate the use of 1.6 and 4.4 mm, respectively, as the denominator when computing percentage changes. Upward-pointing and downward pointing triangles indicate the use of ± 3 kPa and ± 2.5 kPa, respectively, as the pressure for the simulation results.

2. Tympanometry

Polka et al. (2002) showed complete susceptance and conductance tympanograms for two 3-week-old infants measured at 226, 600, 800 and 1000 Hz. Both infants had normal hearing as measured by automated auditory brainstem response (ABR) screening. Figure 10 shows one of the 226-Hz measurements.

For frequencies up to about 1 kHz, the adult ear canal can be modelled as a lumped acoustical element (e.g., Shanks and Lilly, 1981). This assumption is valid up to higher frequencies in the newborn canal because it is smaller than the adult canal. The susceptance measured at the probe tip includes the susceptance of the enclosed air volume (B_V), and the susceptances due to the vibration of the ear-canal wall (B_W) and tympanic membrane (B_{TM}) in response to the probe tone. Thus, the susceptances at the extreme positive pressure and negative pressure are given by

$$B^+ = B_V^+ + B_W^+ + B_{TM}^+ \quad [\text{Equation 9}]$$

and

$$B^- = B_V^- + B_W^- + B_{TM}^- \quad [\text{Equation 10}]$$

The difference between the two is given by

$$\Delta B = B^+ - B^- = [B_V^+ - B_V^-] + [B_W^+ - B_W^-] + [B_{TM}^+ - B_{TM}^-] \quad [\text{Equation 11}]$$

Given the near symmetry of the non-linear response predicted by the model, as shown in Figure 7, it may be reasonable to assume that the vibrations at the extreme positive and negative pressures are similar. In that case their effects cancel and the susceptance change is mainly determined by the actual volume change due to the static displacement of the canal wall and tympanic membrane.

Table II shows the susceptance and conductance values at the extreme static pressures (-275 and +250 daPa, i.e., -2.75 and +2.5 kPa), and their differences, from the measurements of Polka et al. (2002). The fact that the conductance changes are very small for seven out of the eight measurements supports the assumption that the vibrations are similar at the extreme positive and negative pressures.

The table also includes the equivalent-volume changes corresponding to the susceptance changes, computed using

$$\Delta V_{eq} = \Delta B \rho c^2 / 2\pi f \quad [\text{Equation 12}]$$

where ρ is the air density (1.2 kg/m^3), c is the sound speed (343 m/s), and f is the frequency (cf. Shanks and Lilly, 1981).

Figure 11 shows model volume changes obtained for different Young's moduli, compared with the experimentally measured equivalent-volume changes from Table II. The volume changes obtained for the model are lower than those observed experimentally, which is consistent with the fact that the experimental equivalent-volume changes include contributions not only from ear-canal wall movement but also from tympanic-membrane movement.

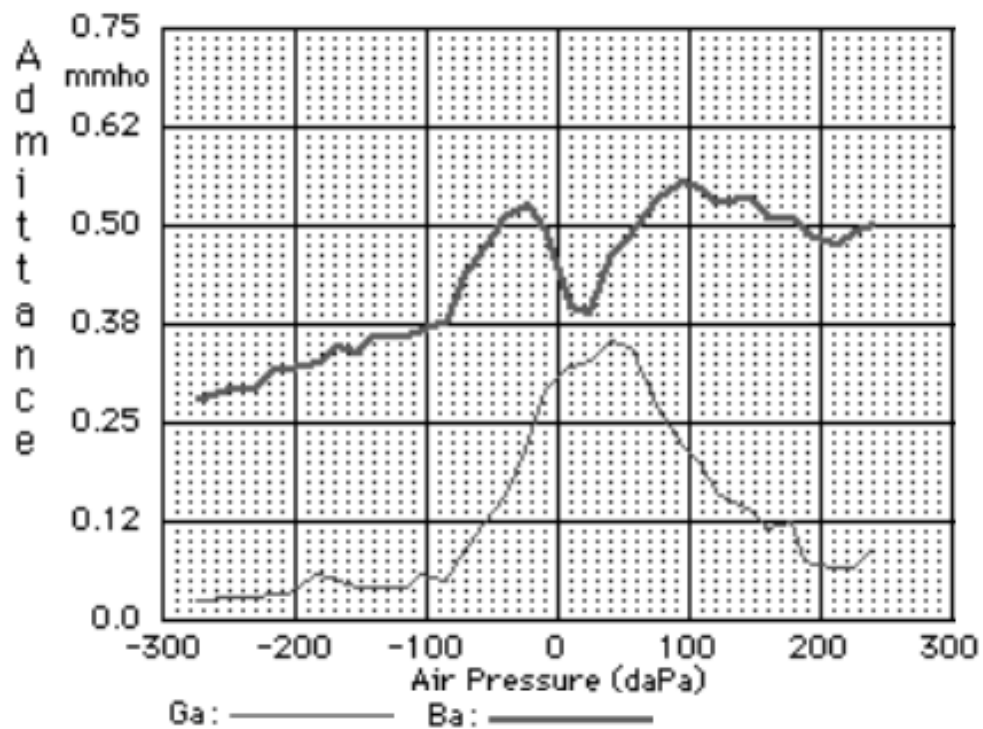


FIG. 10: Susceptance and conductance tympanogram at 226 Hz for 3-week-old newborn (based on Polka et al., 2002).

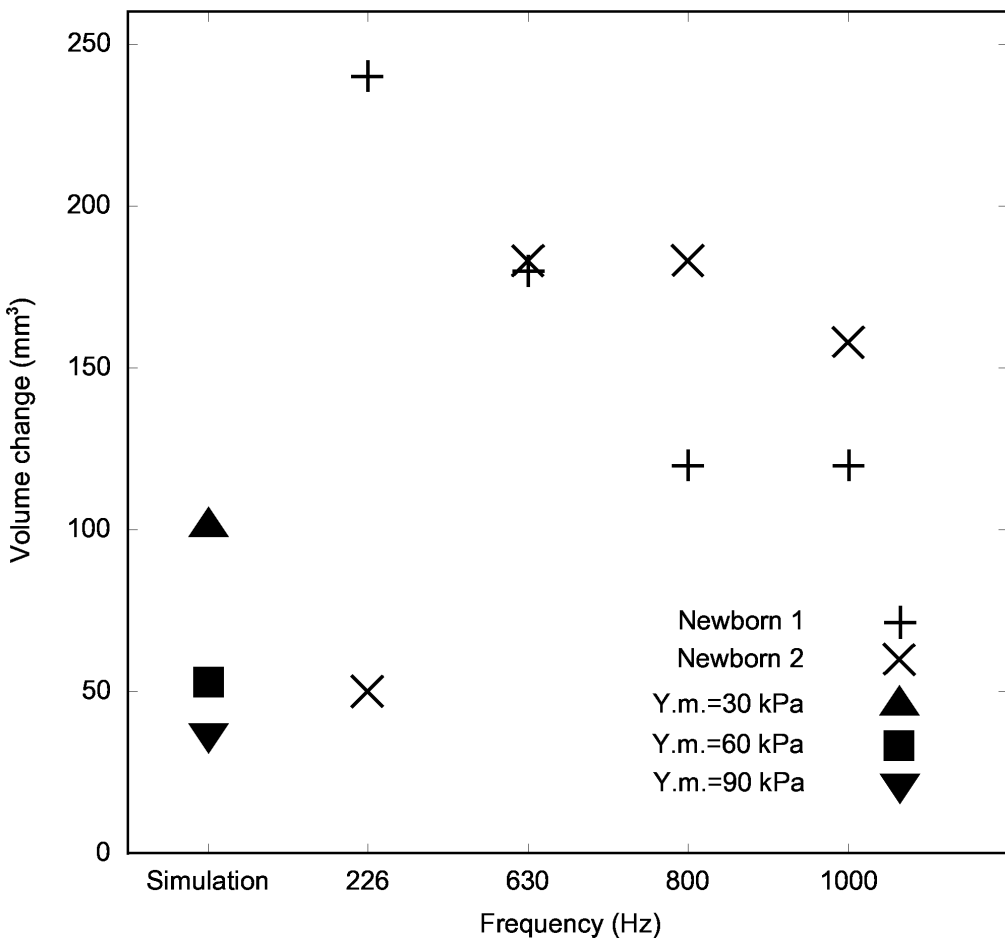


FIG. 11: Comparison of simulation results with equivalent-volume changes taken from tympanograms for two newborns. ▲, ■ and ▼ represent the volume changes from the simulation results for three different Young's moduli. + and × represent the tympanogram-based equivalent-volume changes for 226, 630, 800 and 1000 Hz.

4.4. DISCUSSION AND CONCLUSIONS

A non-linear hyperelastic model of the newborn ear canal is presented and compared with available experimental data.

For static pressures from -3 kPa to $+3$ kPa, the canal-wall displacements and volume changes are non-linear, with the degree of non-linearity increasing as the Young's modulus decreases and the displacements increase. Our sensitivity analysis indicates that the Young's modulus of the tissue in the ear-canal wall plays the most important role in determining volume changes. The effects of varying the Poisson's ratio and the $C_{10}:C_{01}$ ratio are found to be small.

In our simulations, the displacements of the ear-canal wall are slightly larger under positive pressures than under negative pressures. In the measurements of Holte et al., however, the mean diameter changes were much bigger for negative pressures than for positive pressures. In the measurements, a large overlap exists between the percentage displacement changes for the positive pressures and those for the negative pressures, as shown in Figure 9. Possible reasons for the variability include individual differences between ears, age-related changes from 11 days to 22 days, and uncertainty in the applied pressures. It is not clear whether the displacements under the positive pressures and the negative pressures are significantly different or not.

The cross-section of the newborn ear canal is quite flattened; in our model, for example, the horizontal and vertical diameters are 1.6 mm and 4.4 mm, respectively, just lateral to the tympanic membrane. We do not know which diameter was used by Holte et al. in computing percentage changes. When the narrowest diameter was applied to our model results, the model with a Young's modulus of 30 kPa produces diameter changes far above the experimental range under positive pressures. In Holte's measurements, in a younger age group (1 to 11 days) the diameter changes may be up to 70%. This may indicate that Young's modulus of the newborn ear-canal is 30 kPa for younger newborns, and between 60 and 90 kPa for older newborns. However, for a better comparison with the model, it would be desirable to be able to know where their measurements were made in the canal, and to know which diameter was used in the calculations.

In tympanometry a change of equivalent volume consists of two components. One component is the actual air-volume change caused by static pressures, which should be independent of frequency. The actual volume change is caused by the static displacement of both the ear-canal wall and the tympanic membrane. The other component is due to the vibration of the ear-canal wall and tympanic membrane in response to the probe tone. Assuming that the vibrations caused by the probe tone at the positive and negative extreme pressures cancel each other out, as discussed above, the difference between the experimental value and the simulation value may be taken to be the volume change caused by the static displacement of the newborn tympanic membrane. The average equivalent-volume change across all four frequencies in Table II and Figure 11 is 154 mm³. The equivalent-volume changes at 630, 800 and 1000 Hz seem to fit the pattern of frequency independence quite well, but the values at 226 Hz do not – one is too high and the other is too low. It is not clear why this is so. Dropping these two values and taking the average over the three higher frequencies yields an equivalent-volume change of 157 mm³, very close to the value obtained using all four frequencies. According to the simulation results, when the Young's modulus of the ear-canal wall is 30, 60 and 90 kPa, the ear-canal volume change is 101, 53 and 37 mm³, respectively, from -2.75 kPa to 2.5 kPa. Subtracting these values from the average equivalent-volume change of 157 mm³ yields predicted volume changes caused by tympanic-membrane displacement of about 56, 104 and 120 mm³ respectively.

Shanks and Lilly (1981) measured adult ear-canal volume change over a static pressure range of ± 4 kPa. They found a mean ear-canal volume change of 113 mm³ caused by the movement of the cartilaginous part of the wall of the ear canal and the movement of the probe tip. Our simulated volume changes for the newborn are mostly less than those measured by Shanks and Lilly for adult ears. This is reasonable because the diameter and length of the newborn ear canal are much less than those of the adult ear canal. We also do not take probe-tip and tympanic-membrane movements into account and our pressure range is ± 3 kPa rather than ± 4 kPa. If we compare the ratio of volume change to the original

volume, the results of Shanks and Lilly (1981) correspond to an average ratio of about 16% in the range ± 4 kPa in adult, while the ratio in newborn is from 27% (for a Young's modulus of 90 kPa) to 75% (for a Young's modulus of 30 kPa) in the range of ± 3 kPa based on our model results.

The simulated ear-canal volume changes do not reach a plateau when the pressure is varied between -3 kPa and $+3$ kPa, which is consistent with the report by Shanks and Lilly (1981) that even at ± 4 kPa the adult ear canal is not rigid if the probe tip is placed on the cartilaginous part of the ear canal. The failure of the model to reach a plateau is also consistent with the non-flat tails often found in susceptance tympanograms in newborns (Paradise et al., 1976; Holte et al., 1990).

As a first step in modelling the newborn ear-canal wall, we have taken into account only the hyperelastic properties of the ear canal. Further work is required to incorporate in the model the tympanic membrane and the middle ear, and the probe tone itself. Modelling of the response to the probe tone will require inclusion of inertial and damping effects which are not in the current model. The addition of viscoelastic effects would permit simulation of the effects of the timing and direction of the large quasi-static pressure changes used in tympanometry (Osguthorpe and Lam, 1981). It will also be important to obtain a better idea of the types of tissue present: X-ray data will need to be supplemented by data obtained from sources such as MRI and histology.

ACKNOWLEDGEMENTS

This work was supported by the Canadian Institutes of Health Research and the Natural Sciences and Engineering Research Council (Canada). We thank N. Shahnaz and L. Polka for providing the tympanometry data used here, as it appeared in their 2002 poster presented to the Acoustical Society of America.

TABLE I. Summary of adult and newborn ear canal and TM data

	Adult	Newborn (Published)	Data in the model
Ear Canal			
Shape	S shape	Straight	Straight
Roof length (mm)	25-30 ^{1,2}	13-22.5 ³	16
Floor length (mm)	25-30 ^{1,2}	17-22.5 ³	22.5
Diameter (mm)	10 ¹	4.4 ⁴	1.6-4.8
Bone	Inner	None	None
Soft tissue	Outer 1/3 ¹	Entire EAC	Entire EAC
TM			
Diameter along the manubrium (mm)	8-10 ¹	Adult size ¹	8.7
Diameter perpendicular the	7-9 ¹	Adult size ¹	8.3
Surface area (mm ²)	55-85 ¹	Adult size ¹	67

¹ Saunders et al., 1983² Stinson MR and Lawton BW, 1989³ 2-month old newborn measurement (McLellan and Webb, 1957)⁴ Average ear-canal diameter for 1-month-old newborn (Keefe et al., 1993)

Table II Tympanometry results for two 22-day-old infants

Newborn 1				
Frequency (Hz)	226	630	800	1000
B ⁺ (mmho)	0.5	1	0.875	1
B ⁻ (mmho)	0.26	0.5	0.45	0.47
ΔB (mmho)	0.24	0.5	0.425	0.53
ΔV (mm ³)	240	180	120	120
G ⁺ (mmho)	0.05	0.5	0.8	1.1
G ⁻ (mmho)	0	0.6	0.7	0.6
ΔG (mmho)	0.05	-0.1	0.1	0.5
Newborn 2				
Frequency (Hz)	226	630	800	1000
B ⁺ (mmho)	0.3	1.01	1.45	1.8
B ⁻ (mmho)	0.25	0.5	0.8	1.1
ΔB (mmho)	0.05	0.51	0.65	0.7
ΔV (mm ³)	50	183	183	158
G ⁺ (mmho)	0.05	0.5	0.8	0.9
G ⁻ (mmho)	0.05	0.65	0.8	0.9
ΔG (mmho)	0	-0.15	0	0

Tympanometry data are from Polka et al. (2002). B⁺, B⁻, G⁺ and G⁻ are susceptance and conductance measurements at extreme positive and negative pressures. ΔB is the susceptance difference between extreme positive and negative pressures. ΔV is the equivalent-volume difference corresponding to ΔB. ΔG is the conductance difference between extreme positive and negative pressures.

CHAPTER 5: A NON-LINEAR FINITE-ELEMENT MODEL OF THE NEWBORN MIDDLE EAR

PREFACE

This chapter is based on the paper *A non-linear finite-element model of a newborn middle ear*, which was published in the *Journal of the Acoustical Society of America*. The purpose of this chapter is investigate the behaviour of the newborn middle ear in response to high static pressures.

ABSTRACT

A three-dimensional static non-linear finite-element model of a 22-day-old newborn middle ear is presented. The model includes the tympanic membrane (TM), malleus, incus and two ligaments. The effects of the middle-ear cavity are taken into account indirectly. The geometry is based on a computed-tomography scan and on the published literature, supplemented by histology. A non-linear hyperelastic constitutive law is applied to model large deformations. The middle-ear cavity and the Young's modulus of the TM have significant effects on TM volume displacements. The TM volume displacement and its non-linearity and asymmetry increase as the middle-ear cavity volume increases. The effects of the Young's moduli of the ligaments and ossicles are found to be small. The simulated TM volume changes do not reach a plateau when the pressure is varied to either -3 kPa or $+3$ kPa, which is consistent with the non-flat tails often found in tympanograms in newborns. The simulated TM volume displacements, by themselves and also together with previous ear-canal model results, are compared with equivalent-volume differences derived from tympanometric measurements in newborns. The results suggest that the canal-wall volume displacement makes a major contribution to the total canal volume change, and may be larger than the TM volume displacement.

5.1. INTRODUCTION

High static pressures are used in several types of hearing examination, including admittance tympanometry (e.g., Shanks and Lilly, 1981; Margolis and Shanks, 1991; Keefe et al., 1993), reflectance tympanometry (e.g., Keefe and Levi, 1996; Margolis et al., 2001; Sanford and Feeney, 2007), pressure-volume measurement (e.g., Elner et al., 1971; Gaihede, 1999) and pressurized acoustical transfer function measurement (Keefe and Simmons, 2003). Understanding the mechanical response of the middle ear to high static pressures is important for understanding the results of such measurements.

The mechanical deformations of the tympanic membrane (TM) in response to high static pressures have been experimentally studied in human adult (Elner et al., 1971; Dirckx and Decraemer 1991; Dirckx and Decraemer 1992; Vorwerk et al., 1999; Gaihede, 1999) and in animals (von Unge et al., 1993; Dirckx et al., 1997; Dirckx et al., 1998; Dirckx and Decraemer, 2001; Larsson et al., 2001; Lee and Rosowski, 2001; Rosowski and Lee, 2002; Ladak et al., 2004; Larsson et al., 2005; Dirckx et al., 2006). The TM in response to high static pressures has also been studied by the non-linear finite-element method (Ladak et al., 2006; Cheng et al., 2007). To date, neither mechanical measurements nor modelling studies have been reported for the newborn middle ear.

Understanding the volume displacement of the newborn TM in response to high static pressures is important for interpreting pressurized measurements in newborn hearing screening and diagnosis. As we have discussed in more detail in a previous paper (Qi et al., 2006), it is important to be able to distinguish conductive hearing loss from sensorineural hearing loss soon after birth but the usual clinical test, tympanometry, gives quite different results in newborns than it does in adults. For example, some newborns with confirmed middle-ear effusion exhibit normal-appearing single-peak tympanograms (e.g., Paradise et al., 1976; Meyer et al., 1997). This is because the external ear and middle ear in newborns differ significantly from those in adults. For one thing, unlike the adult ear canal, of which the inner two thirds are bone, the entire newborn ear canal is composed

of soft tissue. It is thus difficult to differentiate the clinically interesting TM volume displacement from the associated canal-wall volume displacement in response to high static pressures (as used in tympanometry). Holte et al. (1990) first measured newborn canal-wall displacement in response to static tympanometric pressures (± 2.5 to ± 3 kPa) using video otoscopy. They found, with considerable variability, that the diameter of the ear canal can change by up to 70% in newborns at birth. We recently presented a non-linear newborn ear-canal model, which for the first time simulated the newborn canal-wall displacement (Qi et al., 2006). Our results indicated that the volume changed by between approximately between 27 and 75% in response to static pressures of ± 3 kPa. The purpose of the present study is to extend our earlier work by including the middle ear, in order to investigate newborn TM volume displacements under tympanometric pressures.

In this study, we present a three-dimensional non-linear finite-element model of a 22-day-old newborn middle ear. The geometry is based on a clinical X-ray computed tomography (CT) scan and the published literature. A polynomial hyperelastic constitutive law is applied to model large deformations of the TM. Plausible ranges of material properties of the newborn middle ear are explored. The volume displacement of the TM under high static pressures is estimated in both open-cavity and closed-cavity conditions. The simulated TM volume displacement is compared with equivalent-volume differences calculated from measurements in both healthy full-term newborns (Margolis et al., 2003; Shahnaz et al., 2007) and neonatal intensive care unit (NICU) newborns (Margolis et al., 2003).

5.2. MATERIALS AND METHODS

A. 3-D reconstruction

The geometry of the model is based on the same data as our ear-canal model (Qi et al., 2006), namely, a clinical CT scan of a 22-day-old newborn. The CT scan contained 47 horizontal slices. Two local programs, Fie and Tr3 (<http://audilab.bmed.mcgill.ca/sw/>), were used to generate a surface model. A solid model with tetrahedral elements was then generated using Gmsh (<http://www.geuz.org/gmsh/>) and imported into COMSOL version 3.3 (<http://www.comsol.com>) for finite-element analysis. Figure 1 shows a medial view of the TM, ossicles and ligaments.

The TM, malleus, incus, anterior mallear ligament and posterior incudal ligament were modelled using second-order ten-node tetrahedral elements. Second-order tetrahedral element can model complex structures more accurately with fewer elements. This leads to more accurate simulation results and save computation time.

The pars flaccida is not included in this study for two reasons. First, the area of the pars flaccida is much smaller than that of the pars tensa (e.g., Anson & Donaldson, 1981). Second, even in the gerbil, with a much larger pars flaccida, the volume displacement of the TM is caused mainly by the deformation of the pars tensa when the static pressures are varied from 0.4 to 2 kPa. The volume displacements of the pars flaccida remain nearly unchanged for pressures above 0.4 kPa (Dirckx et al., 1998).

Dirckx and Decraemer (2001) studied gerbil eardrum deformations under quasi-static pressures of ± 2 kPa. They found that the cochlea, tensor tympani and stapes had little influence on eardrum deformations. Thus, in this model, we do not take into account the tensor tympani, the stapes or the cochlear load.

There are two synovial joints linking the ossicles together. The incustapedial joint was not included here because the stapes was not included. Studies have shown that the incudomallear joint is somewhat flexible (e.g.,

Decraemer and Khanna, 1995; Nakajima et al. 2005) but it has for simplicity been assumed to be rigid in this study The effect on TM volume displacement is probably small.

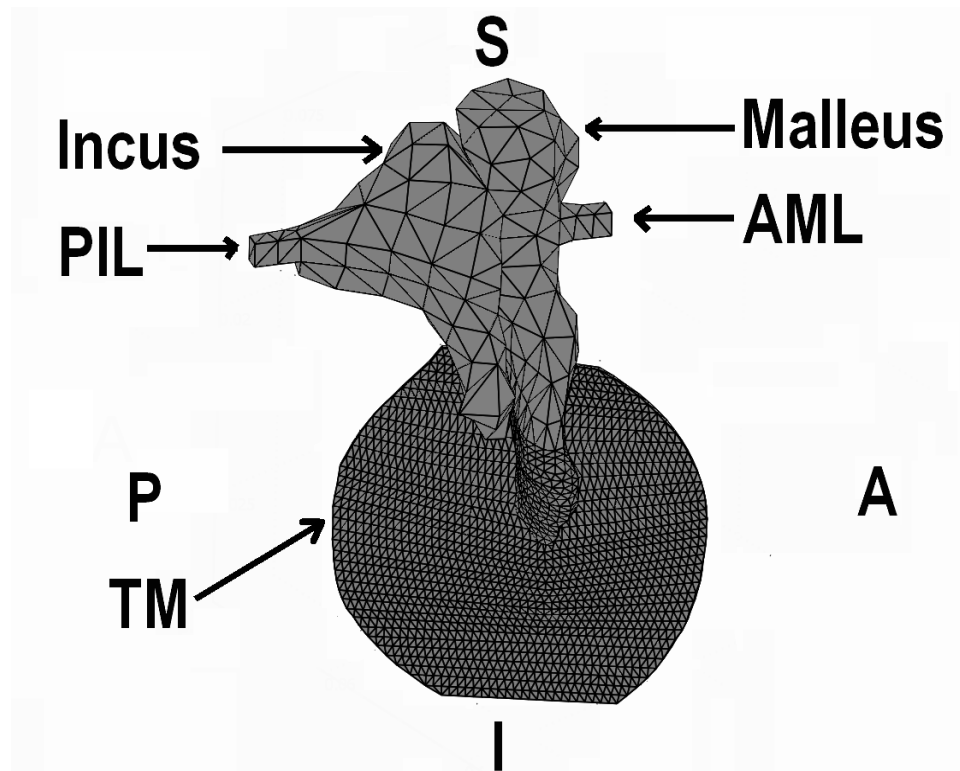


FIG. 1. Medial view of the middle-ear model. S is superior, I is inferior, P is posterior, A is anterior. AML is the anterior malleolar ligament, PIL is the posterior incudal ligament.

B. Material properties and hyperelastic models

1. Thickness of TM

The thickness distribution of the human adult TM has been measured by several investigators (e.g., Lim, 1970; Schmidt and Hellstrom, 1991). It has been found that there is significant variation in the thickness across the surface of the TM and large intersubject differences. Recently, Kuypers et al. (2006) measured three human adult TM thicknesses using confocal microscopy. They found that the pars tensa has a rather constant thickness in a central region, ranging from 0.040 to 0.12 mm across three subjects. The study of newborn TM thickness is sparse. To the best of our knowledge, the only study was conducted by Ruah et al. (1991). They investigated the thickness distribution for different ages of human TMs using histological images with the help of both light and electron microscopy. They measured the thicknesses of TMs from 54 temporal bones, aged from newborn to adult. They found that from newborn to adult the thickness of the TM decreases significantly. Thicknesses of the pars tensa were measured in 4 different quadrants. They found in newborns that the thickness of the posterior-superior region ranged from 0.4 to 0.7 mm; the thicknesses of the posterior-inferior, anterior-superior and anterior-inferior regions were similar, ranging from 0.1 to 0.25 mm; and the thickness of the umbo area ranged from 0.7 to 1.5 mm.

In this study, a non-uniform thickness for the TM model was developed based on the measurements of Ruah et al., (1991), supplemented by thickness measurements on histological images from two one-month-old ears. The thicknesses of the posterior-inferior, anterior-superior and anterior-inferior quadrants are all 0.1 mm in our model. The thickness of the posterior-superior quadrant is 0.5 mm. In the vicinity of the umbo the TM thickness (excluding the manubrium) is 0.75 mm.

2. Young's modulus of TM

The TM consists of three layers: the epidermis, the outer layer, whose ultrastructure is similar to the epidermis of skin; the lamina propria, the middle layer, which contains loose ground matrix and two layers of densely packed collagen fibres arranged in radial and circular patterns, respectively; and the lamina mucosa, the thin inner layer, which contains a large number of columnar cells (Lim, 1970). The overall mechanical properties of the TM depend mainly on the lamina propria, which is characterized by the presence of type II collagen fibres.

The Young's modulus of the human adult TM has been investigated by both experimental and modelling studies. Békésy (1960) firstly measured Young's modulus of TM using a beam-bending test on a strip of cadaver TM. He reported a Young's modulus of 20 MPa. Kirikae (1960) measured the Young's modulus of a strip of TM using a longitudinal vibration. He reported a Young's modulus of about 40 MPa. Decraemer et al. (1980) used a quasi-static uniaxial tensile test on strips of TM. They found that the incremental Young's modulus was shown to vary with the stress level, from almost zero up to a value of approximately 23 MPa. Cheng et al. (2007) also used uniaxial tensile tests and combined the experimental results with an Ogden hyperelastic model. They estimated that the Y.m of the TM is between 0.4 MPa and 22 MPa, again depending on the stress level. Fay et al. (2005) proposed three approaches to estimate the Young's modulus of the TM in adult human and cats. They concluded that the Young's modulus of the adult human TM is between 30 and 90 MPa for an isotropic model and 100 to 400 MPa for an orthotropic TM model. Their values are much higher than those of other investigators at least in part because they are calculated based on the thicknesses of the dense fibrous layers of the TM rather than on the overall thickness.

To date, the Young's modulus of the newborn TM has not been investigated. Ruah et al. (1991) examined the ultrastructure of the TM from newborns to adults using electron microscopy. They observed that with age the TM becomes less vascular and less cellular, and has more collagen fibres and elastins. They

concluded that age-related changes occurring in the lamina propria of the TM are very similar to changes observed in the human skin. Although no direct measurements of the mechanical properties of the TM in newborns are available, the age-related mechanical properties of various other collagenous tissues have been studied. The mechanical properties of collagen are mainly decided by its density, length and cross-linking, and by the diameters and orientations of the collagen fibrils and fibres. The lengths of collagen fibres also increase with age. It has been reported that fibres in rat tail tendon increased from 20–100 nm at 4 weeks old to 30–200 nm by 1 year old (e.g., Schwarz, 1957). It has also been found that collagen density and cross-links increase with age and that collagen becomes more aligned with age (e.g., Hall, 1976; Stoltz, 2006). Age-related Young's modulus changes of human skin have also been reported. Rollhauser (1950) studied the age-related Young's modulus of skin from 3-month-old infants to adults. He found that the Young's modulus of skin in adults is approximately 7 to 8 times as large as that in infants. Similar results were reported by Yamada (1970). They found that the Young's modulus of skin in adults is about 6 times as large as the Young's modulus of infant skin. Grahame and Holt (1969) found that the Young's modulus of skin increased by a factor of 2 from 19 years old to 80 years old. Histological examination of the skin also shows that as the age of the skin increases the collagen density becomes higher and the collagen fibres become less extensible (Agache et al., 1980).

In this study, three Young's moduli are used for the TM: 0.6, 1.2 and 2.4 MPa. Consistent with the adult/infant ratios of 6 to 8 found by Rollhauser (1950) and Yamada (1970), the 0.6 MPa value is several times smaller than a typical small-strain Young's modulus from Decraemer et al. (1980); and 2.4 MPa is approximately 8-10 times smaller than the measurement of Békésy (1960) and the large-strain value of Decraemer et al. (1980).

3. Young's moduli of ossicles and ligaments

Studies have shown that development of the ossicles continues after birth. Ossicular weight and size are smaller in newborns (Olsewski, 1990). It has been

reported that a long, narrow anterior malleolar process exists in at least some newborns (Anson & Donaldson, 1981; Unur et al., 2002). We observed a long process in our 1-month-old histological images. We do not see a long process in our 22-day-old newborn CT scan, probably due to the limited resolution of the scan.

Yokoyama et al., (1999) studied the postnatal development of the ossicles in 32 infants and children, aged from 1 day to 9 years. They found that the newborn malleus and incus contain much bone marrow, which is gradually replaced by bone. They concluded that ossification of the ossicles takes place after birth until about 25 months.

In this study, the Young's modulus of the ossicles is assumed to be 1, 3 or 5 GPa. The value of 5 GPa is at the low end of the range of the Young's modulus of bone given by Nigg and Herzog (1999), and it is approximately 2.5 times smaller than the values used in adult middle-ear models (e.g., Koike et al., 2002). Similarly, the Young's modulus of the ligaments is assumed to be 1, 3 or 5 MPa, which is approximately 2 to 10 times smaller than typical values used in human adult middle-ear models (e.g., Koike et al., 2002). Ligaments were assumed to be hyperelastic. Ossicles were assumed to have linear material properties due to the high Young's modulus.

4. Hyperelastic model

The method is only briefly described here, since a detailed report has been published elsewhere (Qi et al., 2006). A polynomial hyperelastic constitutive law was applied, which allows us to simulate nearly incompressible biological materials with large deformations. The strain energy is given by

$$W = C_{10}(I_1 - 3) + C_{01}(I_2 - 3) + \frac{\kappa}{2}(J - 1)^2 \quad [\text{Equation 1}]$$

where I_1 and I_2 are the first and second strain invariants; J is the volume-change ratio; and κ is the bulk modulus. C_{10} and C_{01} are material constants. Under small strains the Young's modulus of the material, E , may be written as

$$E = 6(C_{10} + C_{01}) \quad [\text{Equation 2}]$$

and the bulk modulus may be written as

$$\kappa = \frac{E}{3(1-2\nu)} \quad [\text{Equation 3}]$$

where ν is Poisson's ratio. We assume that the Poisson's ratios of the TM and ligaments are 0.48, which is a typical value used for nearly incompressible soft tissue (e.g., Qi et al., 2006); and that the Poisson's ratio of the ossicles is 0.3, a widely used value for bone (e.g. Funnell and Laszlo, 1982). The ratio $C_{10}:C_{01}$ is taken to be 1:1, which has been widely used for biological soft tissue (e.g., Mendis et al., 1995; Samani and Plewes, 2004; Qi et al., 2006); from Equation 2, therefore, $C_{10}=C_{01}=E/12$.

The TM volume displacement was calculated by the integration of the nodal displacements over the entire TM surface using COMSOL.

5. Boundary conditions

The boundary of the TM and the ends of the anterior malleolar and posterior incudal ligaments are taken to be fixed. The positive and negative static pressures are uniformly applied to the lateral surface of the TM.

C. Middle-ear cavity

The middle-ear cavity is an irregular, air-filled space within the temporal bone, and is mainly comprised of four parts: tympanic cavity, aditus ad antrum, mastoid antrum and mastoid air cells (e.g. Anson & Donaldson, 1981). In the human adult, the middle-ear cavity volume is between 2 000 and 22 000 mm³ (e.g., Molvaer et al., 1978). The air enclosed in the middle-ear cavity has a compliance that is proportional to its volume, so the larger the volume of the trapped air, the larger the compliance. Studies have shown that the middle-ear cavity may exert significant effects on middle-ear admittance (e.g., Zwislocki, 1962; Guinan & Peake, 1967; Funnell and Laszlo, 1982; Ravicz and Rosowski, 1997; Stepp and Voss, 2005). Ravicz et al. (1992), for example, estimated that reducing the air volume of the gerbil middle-ear cavity by 75% would approximately triple the effective middle-ear input impedance.

The compliance at the TM (C_{TM}) can be written as

$$1/C_{TM} = 1/C_{TOC} + 1/C_{CAV} \quad [Equation 4]$$

where C_{TOC} is the compliance of the TM, ossicles and cochlea; and C_{CAV} is the compliance of the middle-ear air cavity (cf. Stepp and Voss, 2005, equation 2). In our case C_{TOC} represents the compliance of the TM, malleus and incus, since the stapes and cochlea are not included in our model. (Note that the compliances C_{TM} , C_{TOC} and C_{CAV} are not related to the material constants C_{10} and C_{01} in equation 1.)

Previous studies have shown that the mastoid grows in all three dimensions, length, width and depth, from birth to adulthood (Eby and Nadol, 1986). However, the volume of the mastoid in infants has not been quantitatively measured so far. To the best of our knowledge, only the tympanic cavity has been quantitatively measured in infants. Ikui et al. (2000) reconstructed 14 normal human temporal bones aged from 3 months old to adulthood. They reported that the tympanic cavity is about 1.5 times as large in adults (about 640 mm³) as in infants (about 450 mm³).

One factor affecting the volume of the middle-ear cavity in newborns and infants is the presence of residual mesenchyme (embryonic tissue of mesodermal origin). It has been reported that most of the mesenchyme is found in the aditus ad antrum, the round-window niche and the oval-window niche (Takahara et al., 1986; Northrop et al., 1986). Northrop et al. (1986) found that the volume of mesenchyme remained constant at approximately 72 mm³ in newborns from 20 to 36 days old. They estimated that mesenchyme probably occupies less than one-tenth of the entire middle-ear cavity.

In this study, the middle-ear cavity volume was estimated based on our CT-scan reconstruction. The mesenchyme was excluded from the calculation. The tympanic cavity alone is approximately 330 mm³, which is smaller than the reports from Ikui et al. (2000). This is consistent with the fact that our subject was a 22-day-old while their subjects were about 3 months old. It is very difficult to accurately estimate the entire middle-ear cavity volume because the mastoid antrum and some air-cell spaces have very complicated shapes that are difficult to delineate accurately in the CT images. Based on an approximate segmentation of all but the smallest spaces, the combined volume of the aditus ad antrum, the

mastoid antrum and the mastoid air cells in our scan was estimated to be between 400 and 600 mm³. The total middle-ear cavity volume is thus between 730 and 930 mm³. For the model we have thus used minimum and maximum middle-ear cavity-volume parameter values of 700 mm³ and 1000 mm³, respectively.

D. Tympanometry measurements

The multi-frequency tympanometry data for well babies presented here are based on measurements from Shahnaz et al. (2007). Sixteen full-term healthy 3-week-olds participated in the study. All infants passed a hearing screening at birth and again at 3 weeks of age. Multi-frequency tympanometry was done in both ears of fifteen out of sixteen subjects, and in the right ear of the remaining subject. Tympanograms were recorded in the 31 ears using the Virtual 310 system with the extended high-frequency option. The admittance magnitude and phase were recorded at 9 frequencies (226, 355, 450, 560, 630, 710, 800, 900 and 1000 Hz). The susceptance and conductance were derived from the measured magnitude and phase. The pump rate was 125 daPa/sec and the pressure was varied from +250 to -300 daPa (1 daPa = 10 Pa). For a more detailed description see Shahnaz et al. (2007).

We use the following equations to calculate equivalent volumes (Shanks et al., 1993) from the susceptance tails (Equation 5) and from the admittance tails (Equation 6), respectively:

$$V_{ea}^{B\pm} = B^\pm \frac{1000}{f/226} \quad [\text{Equation 5}]$$

$$V_{ea}^{Y\pm} = Y^\pm \frac{1000}{f/226} \quad [\text{Equation 6}]$$

where $V_{ea}^{B\pm}$ and $V_{ea}^{Y\pm}$ represent the equivalent volume (mm³) calculated from the positive or negative susceptance or admittance tail; B^\pm and Y^\pm are the susceptance and the admittance magnitude at the positive (+) or negative (-) tail, respectively; and f is frequency (Hz). It should be noted that equation 6 is valid only when the conductance (the real part of the admittance) is zero. For newborns, the equivalent volume calculated from equation 6 may include

significant errors due to non-zero conductance at the tails. In this study, however, the model results are compared with the difference between the equivalent volumes at the two tails (ΔV_{ea}^B , ΔV_{ea}^Y), calculated as

$$\Delta V_{ea}^B = V_{ea}^{B+} - V_{ea}^{B-} \quad [\text{Equation 7}]$$

$$\Delta V_{ea}^Y = V_{ea}^{Y+} - V_{ea}^{Y-} \quad [\text{Equation 8}]$$

As discussed in Section IV below, in newborns the conductances at the two tails are almost equal and therefore almost cancel each other.

5.3. RESULTS

A. Model displacements

Convergence tests were conducted to investigate how many elements should be used in the model. A non-uniform mesh was created. Four different resolutions were compared. The TM has nominal numbers of elements per diameter of 80, 120, 160 and 200, respectively. The ossicles and ligaments have nominal numbers of elements per diameter of 20, 40, 60 and 90, respectively. We found that the difference in TM volume displacement is less than 1.7% between the model with 160 elements/diameter for the TM and 40 elements/diameter for the ossicles and ligaments and the model with 200 elements/diameter for the TM and 90 elements/diameter for the ossicles and ligaments. Thus, the former model (160 and 40 elements/diameter) was selected for further simulations. The model has a total of 12 815 elements, 9 250 of which belong to the TM.

Our simulations show that varying the Young's modulus of the ossicles and ligaments has little effect on the TM volume displacements. The changes of the TM volume displacements are less than 3% when the Young's modulus of the ossicles increases from 1 to 6 GPa. The changes of the TM volume displacements are less than 6% when the Young's modulus of the ligaments increases from 0.6 to 6 MPa.

Figure 2 shows the model displacement patterns corresponding to different static pressures under open-cavity conditions. The location of the maximum displacement moves when the pressures are changed, which agrees with

observations in human adult middle-ear measurements (Dirckx and Decraemer, 1991). At low pressures (± 100 Pa), the negative and positive displacement patterns are similar, with the maximum displacements in the antero-superior quadrant. When pressures are increased, the negative and positive displacement patterns become significantly different from each other. At the extreme positive pressure, the maximum displacement occurs inferiorly. At the extreme negative pressure, however, the maximum displacements occur anteriorly and posteriorly.

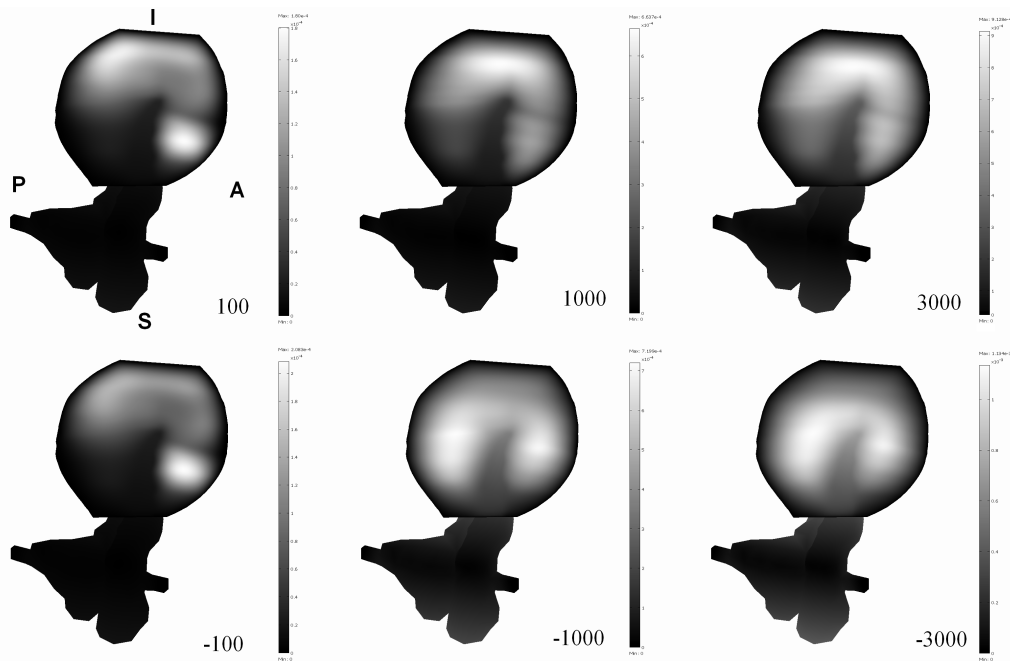


FIG. 2. Simulated displacement patterns for static pressures of ± 100 , ± 1000 and ± 3000 Pa. Lighter colors represent larger values.

B. Middle-ear cavity effects on TM volume displacement

Our finite-element model does not explicitly include the middle-ear cavity. We use Boyle's Law to estimate the effects of the cavity volume on TM volume displacements. Details are given in the Appendix.

Figure 3 compares the model TM volume displacements corresponding to different Young's moduli of the TM under open and closed-cavity conditions (700 mm^3), and the TM volume displacement measured in adults (Elner, 1971; Dirckx and Decraemer, 1991). The TM volume-displacement curves are non-linear, with larger slopes for low pressures than for high pressures; and asymmetrical, with larger displacements for negative pressures, which agrees with adult TM measurements (Dirckx and Decraemer, 1991; Elner, 1971). The form of the observed non-linearity is determined by a combination of the material non-linearity (expressed by equation 1) and geometric non-linearities resulting from the large deformations.

Our simulation results indicate that, from -3 to $+3 \text{ kPa}$, the TM volume displacements are approximately 27 , 32 and 35 mm^3 when the middle-ear cavity volume is 700 mm^3 ; and approximately 46 , 60 and 75 mm^3 under open-cavity conditions, corresponding to Young's moduli of the TM of 2.4 , 1.2 and 0.6 MPa . The closed middle-ear cavity significantly reduces the TM volume displacements, and also reduces the degree of non-linearity and asymmetry of the TM volume displacement. The TM volume displacements under open-cavity conditions are about 1.7 to 2.2 times as large as those under closed-cavity conditions with a volume of 700 mm^3 . The simulated TM volume displacements under open-cavity conditions show an asymmetry similar to that of the volume displacements measured in adults, with larger volume displacements at negative pressures.

Figure 4 compares the TM volume displacements between -3 and $+3 \text{ kPa}$ when the middle-ear cavity is 700 mm^3 , 1000 mm^3 and open. When the middle-ear cavity volume increases, the TM volume displacement increases, and the non-linearity and asymmetry of the TM volume displacement increase as well. When the cavity volume increases from 700 to 1000 mm^3 (an increase of about 43%),

the TM volume displacements increase by approximately 16%, 20% and 22% for TM Young's moduli of 2.4, 1.2 and 0.6 MPa, respectively. When the cavity volume increases from 1000 mm³ to the open situation (infinitely large), the TM volume displacements increase by 50%, 81% and 88% for TM Young's moduli of 2.4, 1.2 and 0.6 MPa, respectively.

C. Comparisons with tympanometric data

To date, no direct measurements of newborn TM displacements have been made. Thus, in this section we shall compare our simulation results with two sets of tympanometric equivalent-volume differences, one calculated from 3-week-olds (Shahnaz et al., 2007) and the other calculated from healthy infants and NICU infants aged from 1 day to 2 months old (Margolis et al., 2003).

1. Equivalent-volume differences from Shahnaz et al.

The equivalent-volume difference (ΔV_{ea}^B) between the positive tail (+2.5 kPa) and the negative tail (-2.75 kPa) was derived from susceptances using equation 7 in sixteen 3-week-olds (Shahnaz et al., 2007). Figure 5 shows the ΔV_{ea}^B (median and 25th and 75th percentiles) for left and right ears combined. As shown in the figure, the medians of ΔV_{ea}^B in newborns stay almost constant over the entire frequency range. The median ΔV_{ea}^B across frequencies is about 132 mm³.

Our simulation results indicate that from -2.75 to +2.5 kPa the TM volume displacements, corresponding to a Young's modulus of the TM of 2.4, 1.2 or 0.6 MPa, were approximately 24, 28 and 31 mm³ for a middle-ear cavity volume of 700 mm³, and 28, 34 and 38 mm³ for a cavity volume of 1000 mm³.

2. Equivalent-volume differences from Margolis et al.

Margolis et al. (2003) investigated the 1-kHz admittance both in 46 ears of 30 full-term healthy newborns (aged 2 to 4 weeks) and in 105 ears of 65 NICU newborns (aged 3.9±3.8 weeks, mean±SD). The equivalent-volume difference (ΔV_{ea}^Y) between the positive tail (+2 kPa) and the negative tail (-4 kPa) was derived from the admittance using equation 8. The median ΔV_{ea}^Y at 1000 Hz is

158 and 136 mm³ for NICU newborns and healthy full-term newborns, respectively.

Our simulation results indicate that from -4 to +2 kPa the TM volume displacements, corresponding to a Young's modulus of the TM of 2.4, 1.2 or 0.6 MPa, were approximately 28, 33 and 36 mm³ for a middle-ear cavity volume of 700 mm³, and 33, 39 and 44 mm³ for a cavity volume of 1000 mm³.

The predicted TM volume displacements calculated for the NICU newborns are larger than those calculated for the healthy newborns. This may be caused by the age difference between the two groups. The healthy-newborn ages were from 2 to 4 weeks, while the NICU-newborn age distribution was 3.9±3.8 weeks (mean±SD). A larger number of very young infants in the NICU group might account for the larger median ΔV_{ea} in that group.

3. Comparison

In both cases the simulation results are lower than the median equivalent-volume differences calculated from tympanometric measurements. This is consistent with the fact that the experimental equivalent-volume changes include contributions from the movements of the ear-canal wall, probe tip and tympanic ring as well as the TM. This will be further discussed below.

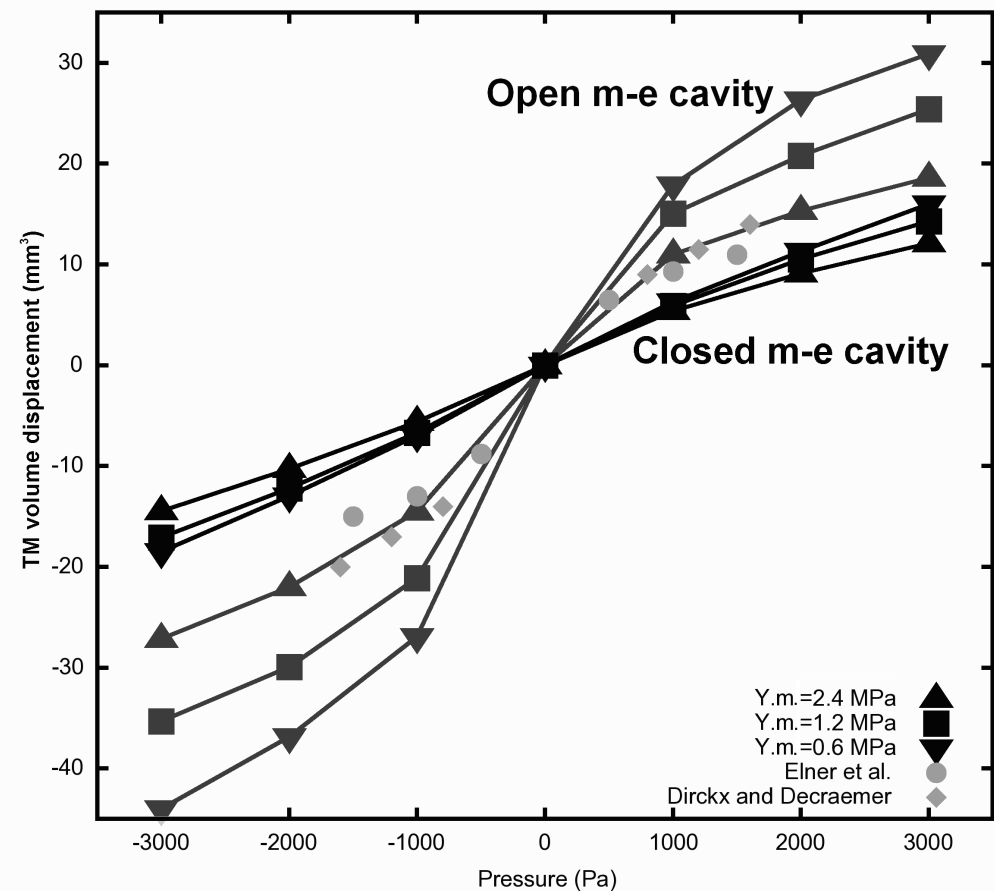


FIG. 3. Simulated TM volume displacements as functions of pressure, for different TM Young's moduli, for both open middle-ear cavity and closed middle-ear cavity 700 mm³, and experimental volume displacements measured in human adults from Dirckx and Decraemer 1992, Table VI and Elner et al. 1971, Table III, respectively. Dirckx and Decraemer 1992 gave middle-ear cavity pressures rather than canal pressures, so their curve has been reversed.

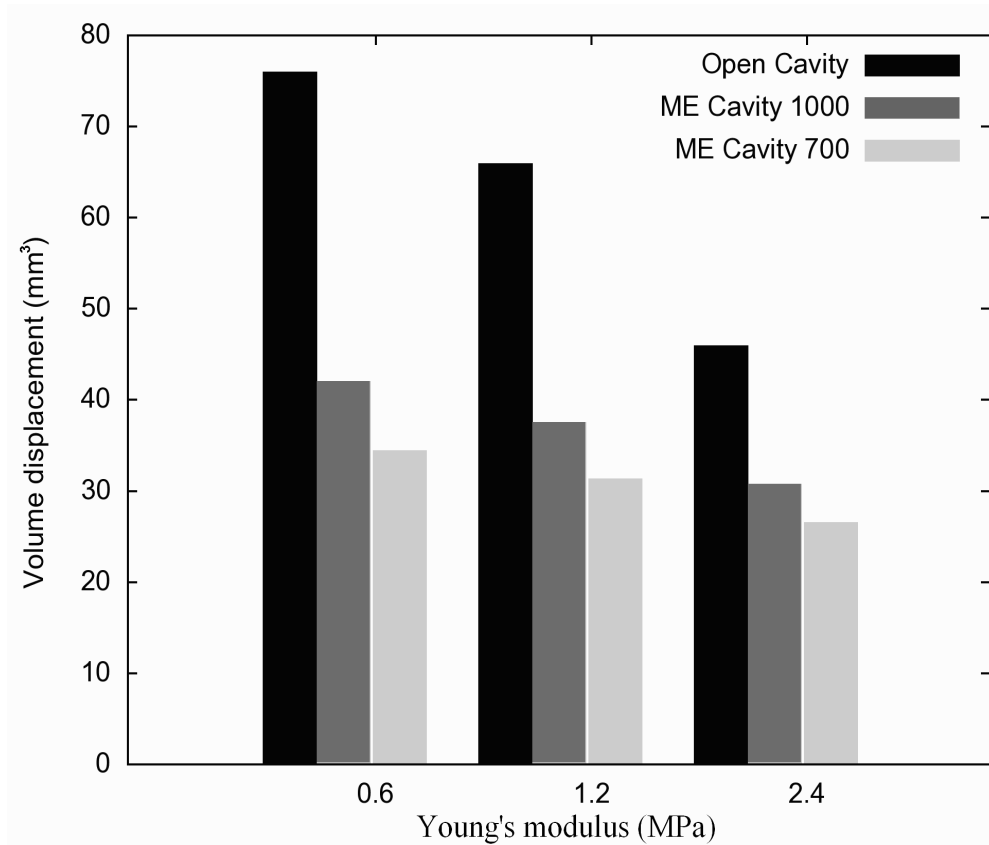


FIG. 4. Simulated TM volume displacements between -3 and +3 kPa, for different middle-ear cavity volumes 700, 1000 mm³ and open cavity.

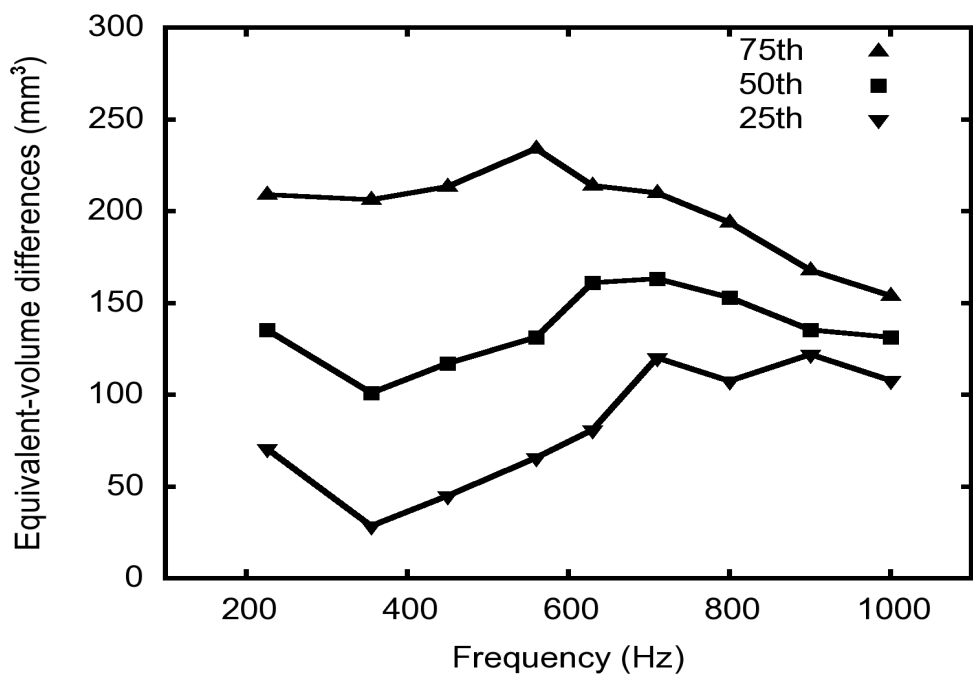


FIG. 5. Equivalent-volume differences median and 25th and 75th percentiles between susceptance tails from study of Shahnaz et al. 2008.

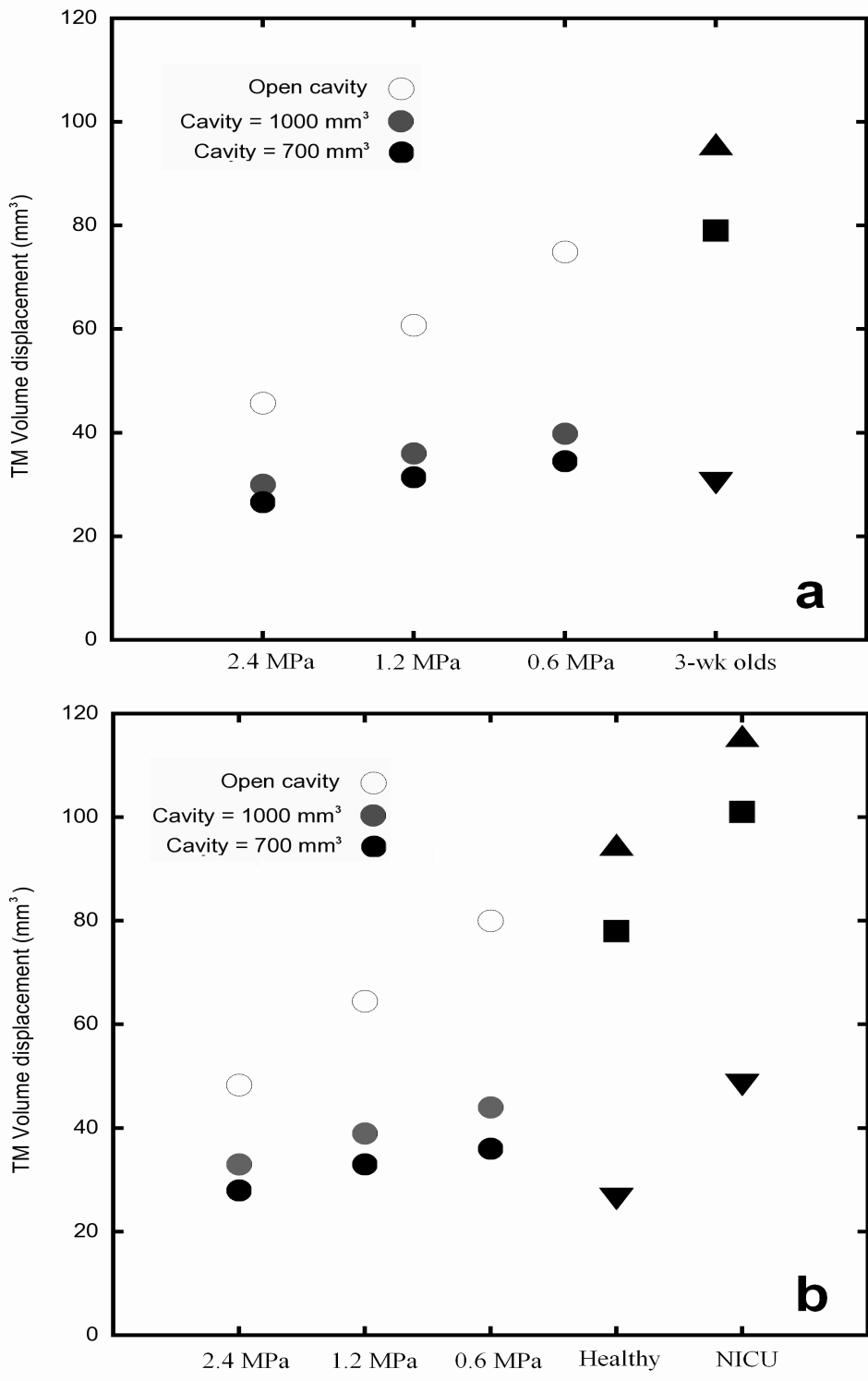


FIG. 6. Comparison of simulated TM volume displacements, for different cavity volumes, with the equivalent-volume differences in 3-week-old newborns (a), and with the equivalent-volume differences in NICU and healthy newborns (b).

5.4. DISCUSSION AND CONCLUSIONS

A non-linear hyperelastic model of the newborn middle ear is presented and compared with tympanometric data. For static pressures from -3 kPa to $+3$ kPa, the simulated TM displacements and volume displacements are non-linear.

In our simulations, the TM volume displacements show considerable asymmetry under open-cavity conditions, with larger displacements for negative pressures. Adult human TM volume displacements also displayed asymmetry in the measurements of Dirckx and Decraemer (1992), which were conducted under open-cavity conditions, and in the measurements of Elner et al., (1971), which were conducted under closed-cavity conditions. The similarity between the measurements of Dirckx and Decraemer and those of Elner et al. suggests that in adults the middle-ear cavity volume generally has little effect on the TM volume displacement. This does not appear to be true for newborns.

Our simulated TM volume displacements are nearly symmetrical under closed-cavity conditions, as shown in Figure 3. The reason for the near symmetry under closed-cavity conditions is that the newborn cavity is relatively small, so C_{CAV} is relatively low, which leads to smaller displacements. This means that the TM is not driven into its non-linear range. This is similar to the way that the nonlinearities decrease when Young's modulus increases: the system is still intrinsically non-linear but it is not pushed so far into the non-linear range.

The effects of cavity volume on TM volume displacements increase as the Young's modulus of the TM decreases. As shown in Figure 4, when the volume of the middle-ear cavity increases from 700 to 1000 mm 3 , the TM volume displacements increase by 16%, 20% and 22% when the Young's modulus of the TM is 2.4, 1.2 and 0.6 MPa, respectively. Similarly, when the volume of the middle-ear cavity increases from 700 mm 3 to infinitely large (the open-cavity condition), the TM volume displacements increase by 70%, 91% and 117% when the Young's modulus of the TM is 2.4, 1.2 and 0.6 MPa, respectively. This is to be expected because when the Young's modulus of the TM decreases, $1/C_{TOC}$ decreases and the ratio of $1/C_{CAV}$ to $1/C_{TOC}$ increases.

Our simulations show that the Young's modulus of the TM has a significant effect on the TM volume displacement, as shown in Figures 3, 4 and 5. The effect is more pronounced for a larger middle-ear cavity. As the Young's modulus of the TM decreases from 2.4 MPa to 1.2 MPa and then to 0.6 MPa, the TM volume displacements increase by approximately 19% and 10% when the middle-ear cavity is 700 mm³; by approximately 23% and 12% when the middle-ear cavity is 1000 mm³; and by approximately 44% and 15% when the middle-ear cavity is open.

The simulated TM volume changes do not reach a plateau when the pressure is varied to either -3 kPa or +3 kPa, which is consistent with the non-flat tails often found in susceptance tympanograms in newborns (e.g., Paradise et al., 1976; Holte et al., 1990). The failure of the model to reach a plateau is also consistent with the report by Shanks and Lilly (1981) that even at pressures of +2 and -4 kPa the adult middle ear is not rigid.

The tail-to-tail equivalent-volume differences shown in Figure 5 consist of two components: (1) the actual air-volume change in response to the static pressure, corresponding to the static displacement of the ear-canal wall, the TM and the probe tip; and (2) a component due to the vibration of the canal wall and TM in response to the probe tone. The actual air-volume change should be independent of frequency, while the vibration-related component is presumably dependent on frequency. Both our previous newborn ear-canal model (Qi et al., 2006) and the current middle-ear model under closed-cavity conditions predict nearly symmetrical non-linear responses, which suggests that the vibrations at the extreme positive and negative pressures are similar. In that case, their effects will tend to cancel when subtracting either admittances or susceptances and the ΔV_{ea} will be mainly determined by the actual volume change (Qi et al., 2006). In our analysis of the data of Shahnaz et al. (2007), shown in Figure 5, the median ΔV_{ea} varies little across the entire frequency range, which is consistent with interpreting the equivalent-volume difference as the actual volume change. (It should be mentioned, however, that tail-to-tail equivalent-volume differences

calculated for human adults may have a significant vibration-related component, given the asymmetrical TM volume displacement in adults.)

Based on our previous ear-canal model (Qi et al., 2006), when the Young's modulus of the ear-canal wall is 30, 60 and 90 kPa, the simulated canal-wall volume displacement is 101, 53 and 37 mm³, respectively, from -2.75 kPa to +2.5 kPa. Subtracting these canal-wall volume displacements from the median equivalent-volume change of 132 mm³ obtained from the tympanometric data of Shahnaz et al. (Section III C 1) yields predicted TM volume displacements of about 31, 79 and 95 mm³, respectively.

For use with the data of Margolis et al. (2003), the pressure response of our canal model has been extended from -3 to -4 kPa. The resulting simulated canal-wall volume displacements, for Young's modulus of 30, 60 and 90 kPa, are 109, 56 and 42 mm³, respectively. Again subtracting the simulated canal-wall volume displacements from the median tympanometric equivalent-volume differences (Section III C 2), we obtain predicted TM volume displacements of 48, 101 and 115 mm³ for NICU newborns and 27, 77 and 94 mm³ for healthy full-term babies.

In Figure 6, parts *a* and *b* compare the TM-model volume displacements under closed-cavity (700 and 1000 mm³) and open-cavity conditions with the TM volume displacements predicted by combining our canal-model results with the measurements of Shahnaz et al. (2007) and Margolis et al. (2003), respectively.

In an attempt to obtain an estimate of canal-wall displacement separate from that of the TM, we note that Margolis et al. (2003) recommended using the peak-to-negative-tail difference of admittance at the 5th percentile as a pass-fail criterion for conductive hearing loss. Since middle-ear effusion (MEE) is the most common cause of conductive hearing loss in newborns, we suppose that the pass-fail criterion can be used as a criterion for MEE. For newborns with MEE, the TM cannot move as freely as usual and the admittance of the middle ear may be nearly zero. As a result, the equivalent-volume difference (ΔV_{ea}) between the two tails would be mainly due to the canal-wall, tympanic-ring and probe-tip movement. The ΔV_{ea} at the 5th percentile of Margolis et al. is 113 mm³. This is close to the maximum canal-wall volume displacement of 109 mm³ predicted by

our canal model, when the Young's modulus of the ear-canal wall is 30 MPa. In that case, the closed-cavity TM-model volume displacements are close to the minimum TM volume displacements predicted from the canal model. Note that the TM volume displacement predicted from our canal model actually also includes any volume displacements due to tympanic-ring and probe-tip movement. Thus, on the one hand, if we adopt the lowest Young's modulus (30 MPa) for the canal-wall model then the predicted canal-wall and TM volume displacements match the total volume displacements obtained from the tympanometric data. On the other hand, if the canal wall is stiffer, then we would predict some additional volume displacement due to the tympanic ring and probe tip. The fact that 113 mm³ is a large fraction of their median ΔV_{ea}^Y values of 136 mm³ and 158 mm³ is consistent with our model-based prediction that the canal-wall volume displacement makes a major contribution to the total canal volume change. The relative contributions of these different components clearly depend strongly on the corresponding material properties, especially stiffnesses and TM thicknesses. Further work is required in order to further constrain estimates of the Young's moduli, and the effects of current simplifications such as the rigidity of the incudomallear joint and the uniform TM thickness in each quadrant should be explored.

As a first step in modelling the newborn middle ear, our results show that the volume of the middle-ear cavity and the Young's modulus of the TM have significant effects on the TM volume displacement. It is not clear whether the volume displacement of the probe tip and tympanic ring make significant contributions to the total volume change. It will be necessary to combine the ear-canal and middle-ear models and to incorporate the tympanic ring and the probe tip. Modelling the small-amplitude dynamic response of the ear canal and middle ear to the probe tone, and then combining that with the non-linear static response modelled here, will permit a complete model of tympanometry in newborns.

ACKNOWLEDGEMENTS

This work was supported by the Canadian Institutes of Health Research and the Natural Sciences and Engineering Research Council (Canada), the Fonds de recherche en santé du Québec, the Montréal Children's Hospital Research Institute, the McGill University Health Centre Research Institute, and the Hearing Foundation of Canada. We thank C. Northrop (Temporal Bone Foundation, Boston) for the histological images used to supplement and help interpret our CT scan, C. B. Ruah for helpful discussion of his TM thickness data, and J. Lufty for his work on the initial segmentation of the CT scan.

APPENDIX: Calculation of effects of middle-ear cavity on TM volume displacement

1. Setting up equations

Our finite-element model does not include the effects of the middle-ear cavity. In order to estimate the effects of the cavity on TM volume displacement, we start with Boyle's law, assuming that temperature is constant because the pressure changes are slow (cf. Elner, 1971):

$$P_0 V_0 = P_1 V_1 \quad [\text{Equation 1}]$$

where P_0 (in Pa) is the initial pressure in the middle ear (atmospheric pressure, 10^5 Pa); V_0 (in mm^3) is the initial middle-ear cavity volume, before the TM is displaced; and P_1 and V_1 are the final pressure and volume in the middle ear. Suppose that overpressure p is applied in the ear canal. The pressure difference across the TM is then

$$\Delta P = P_0 + p - P_1 \quad [\text{Equation 2}]$$

and the TM volume displacement is

$$\Delta V = V_0 - V_1 \quad [\text{Equation 3}]$$

The relationship between ΔP and ΔV is defined by our finite-element model, as shown in Figure 3. The relationship is strongly asymmetrical, but on each side of the origin it can be approximated by using a second-order polynomial equation. Therefore, for the purpose of calculating the effect of the closed middle-ear cavity, we represent the relationship by

$$\Delta P = a \Delta V^2 + b \Delta V \quad [\text{Equation 4}]$$

where a and b are fitted coefficients. The coefficients a and b in Equation 4 were estimated using the least-squares method (Gnuplot version 4.0, <http://www.gnuplot.info>). The coefficients were estimated separately for the positive-pressure and negative-pressure parts and for each of the three TM Young's modulus values. Therefore, six sets of a and b were estimated.

Given P_0 , V_0 , p , a and b , we have four simultaneous equations (1, 2, 3 and 4) and four unknowns (P_1 , V_1 , ΔP and ΔV). The computer-algebra system Axiom (<http://axiom-wiki.newsynthesis.org>) is used to solve the system of equations either symbolically or numerically.

2. Numerical solutions

If we adopt some specific values for the given parameters, e.g., $P_0=10^5$, $V_0=700$, $p=1000$, $a=8.89$ and $b=-4.71$, then we can solve the set of equations 1–4 numerically using the Axiom *solve* command. Since the solution to the set of equations involves a cubic equation, we obtain three sets of answers, as shown in Table A1. Since we know that $\Delta V>0$ and $\Delta V<V_0$, only one answer is physically reasonable. Thus we see that, for these particular values for P_0 , V_0 , a and b , the TM volume displacement is approximately 5.35 mm^3 when the canal pressure p is 1 kPa.

3. Results

The results for two different initial middle-ear volumes (700 and 1000 mm^3) are given in Tables A2 and A3 for six different pressures (± 1000 , ± 2000 and ± 3000 Pa) and three different values of TM Young's modulus (0.6, 1.2 and 2.4 MPa). Only the physically reasonable solutions are shown in Tables A2 and A3.

Table A1. Three sets of answers for initial cavity volume = 700 mm³ and canal pressure = 1 kPa

	V_1	P_1	ΔP	ΔV
Answer 1	720.554	97147.5	3852.52	20.5539
Answer 2	15.7314	0.444972	0.455072 E7	715.731
Answer 3	694.647	100771.0	229.475	5.35243

Table A2. TM volume displacements for initial cavity volume = 700 mm³

Young's modulus (MPa)	Pressure (Pa)					
	-3000	-2000	-1000	1000	2000	3000
2.4	-14.44	-10.26	-5.55	5.35	9.07	12.09
1.2	-17.04	-12.16	-6.61	5.93	10.46	14.26
0.6	-18.86	-12.97	-6.90	6.23	11.26	15.60

Table A3. TM volume displacements for initial cavity volume = 1000 mm³

Young's modulus (MPa)	Pressure (Pa)					
	-3000	-2000	-1000	1000	2000	3000
2.4	-17.14	-12.49	-7.01	6.50	10.53	13.72
1.2	-20.81	-15.31	-8.74	7.52	12.65	16.81
0.6	-23.40	-16.82	-9.37	8.11	14.02	18.90

CHAPTER 6: CONCLUSIONS AND FUTURE WORK

In this chapter, a summary of this work is reviewed in Section 6.1, and the major original contributions are presented in Section 6.2. Clinical implications of this work are introduced in Section 6.3. Finally, future work is suggested in Section 6.4.

6.1. SUMMARY

Early hearing screening and diagnosis in newborns are important in order to avoid problems with language acquisition and psychosocial development, but the available tests result in too many screening false positives and in delayed diagnoses. Understanding the mechanics of the newborn ear canal and middle ear is essential for reducing the number of false positives and for differentiating conductive hearing loss from sensorineural hearing loss in newborn hearing screening.

The objective of this work is to obtain better techniques for diagnosis of conductive hearing loss in newborns. Our approach is to quantitatively analyse tympanogram tails recorded in newborns and to use the non-linear finite-element method (FEM) to model behaviour of the newborn ear canal and middle ear in response to high static pressures. The models' behaviours are compared with analyses of tympanogram tails. .

6.2. MAJOR ORIGINAL CONTRIBUTIONS

Major original contributions include:

- I. Provided preliminary normative data for equivalent volumes in newborns.
- II. Presented the variations of admittance, susceptance, and conductance across different tympanometric indices and probe frequencies in newborns.
- III. Developed the first non-linear finite-element models of a human ear, and the first models of the newborn ear.
- IV. Developed a method for estimating the effects of the middle-ear air cavity in a non-linear model.

Specific new findings are listed below.

1. The analysis of tympanogram tails in newborns indicates that both positive and negative tails of both the susceptance and conductance increase with frequency and the phase angles of the admittance decrease from 226 to 660 Hz and then stay almost constant from 660 to 1000 Hz.
2. The analysis of tympanogram tails in newborns indicates that the equivalent volumes calculated from both the positive and negative tails of both admittance and susceptance decrease as frequency increases. The volumes derived from susceptance decrease faster than do those derived from admittance.
3. The analysis of tympanogram tails in newborns indicates that the differences between the equivalent volumes calculated from the susceptance and admittance are much larger at high frequencies than at low frequencies, and are much larger than in adults.
4. The analysis of tympanogram tails in newborns indicates that both the equivalent volumes and the energy reflectances tend to be lower than previous measurements in older children and adults.
5. Our models indicate that tails recorded in newborn tympanometry are not flat because neither the ear canal wall nor the TM is driven to be rigid enough under high static pressures as used in tympanometry.
6. Our models indicate that the middle-ear cavity has significant effects on TM volume displacements in the newborn. The small middle-ear cavity volume in newborns results in reduced non-linearity and asymmetry of TM volume displacement.
7. Our models indicate the relative contributions of different parameters, e.g. Young's modulus, Poisson's ratio etc., on the behaviour of the canal wall and middle ear.

8. Our model results suggest that in tympanometry measurements the canal-wall volume displacement is a relatively large fraction of the total ear-canal volume change.

6.3. CLINICAL IMPLICATIONS OF THIS WORK

The analysis of tympanometry tails recorded in healthy newborns has provided preliminary normative data for equivalent volumes in newborns. The analysis results suggest that a significant error will be introduced if the equivalent volume is calculated from the admittance tails at 1000 Hz, as most tympanometers do for newborn hearing screening. As a result, the admittance of the middle ear will be significantly underestimated or overestimated depending on whether the positive or negative tympanogram tail is used.

Our ear-canal model indicates that the volume displacements of the newborn canal wall do not reach a plateau at high pressures as generally assumed in tympanometry, which implies that the compensated admittance of the middle ear will be compromised. Our middle-ear model indicates that volume displacements of the newborn TM in response to high static pressures are much less than those of adult TMs, which implies that the compliance of the newborn TM is much lower than that of the adult TM. Taken together, our ear-canal and middle-ear models indicate that the canal-wall volume displacement may be larger than the TM volume displacement which is the real clinical interest in tympanometry. This emphasizes the importance of developing better methods for correcting for the effects of the canal.

The ear-canal and middle-ear models presented here may allow us to use a smaller static pressure range in tympanometry for newborns by providing model-based extrapolation to larger pressures. A reduced pressure range could decrease the test time, and also reduce the sensation that often causes newborns to become upset. It might also decrease the complexity of the instrumentation and make it possible to combine tympanometry with OAE measurements.

The present studies investigated the variations of the equivalent volume across different tympanometric indices and probe frequencies and the volume

displacements of newborn canal wall and middle ear in response to high static pressures. We found that the variabilities of equivalent volumes derived from both admittance and susceptance are noticeably less at the higher frequencies. This may suggest an advantage to using the high-frequency volume estimates when compensating for the ear canal. However, the high-frequency estimates are presumably more contaminated by mass and resistive effects, which may make the volume estimates less accurate. In any case, measurements from a larger number of newborns are required to pursue this issue.

These studies brings us a step closer to a clear understanding of the acoustical and mechanical properties of the newborn outer and middle ear, which will ultimately allow us to refine the application of tympanometry in infants.

6.4. FUTURE WORK

In order to achieve the overall objective of this work, a large amount of important future work needs to be done, including clinical tests, fundamental measurements, modelling and simulation, etc. Here, only a few major aspects are discussed.

6.4.1 Experimental work

Three types of experimental work are desired. The first is to measure multi-frequency tympanometry or single high-frequency tympanometry in infants of different ages and with confirmed abnormal hearing. Such measurements can be used to establish population-specific susceptance, conductance and admittance normative data, as well as assess the sensitivity and specificity of high-frequency tympanometry for newborns. The second is to directly measure the behaviour of the canal wall and TM. Such experiments may measure the vibrations of the canal wall and TM at ambient pressures, and the static displacements or volume displacements of the canal wall and TM in response to high static pressures. Experimental results from such studies will help us better validate our models and better understand tympanograms in newborns. Techniques such as laser Doppler vibrometry (e.g., Whittemore et al., 2000) or phase-shift moiré topography (e.g.,

Dirckx and Decraemer, 1989) might be used in such experiments. The third is to directly measure the material properties of the newborn ear canal wall and middle ear. Direct measurements of the material properties of the middle ear in adult have been conducted (e.g. Békésy, 1960; Decraemer et al., 1980; Cheng and Gan, 2007) but such work has not been reported yet for newborns. In this work, we made *a priori* estimates of parameters based on measurements from other parts of the body. Further modelling work will require better measurements of material properties.

6.4.2 Three-dimensional reconstruction of newborn outer and middle ear

Due to limitations of clinical X-ray data, future reconstructions of newborn outer and middle ear need to be supplemented by data obtained from other imaging modalities such as ultrasound, magnetic resonance imaging, histology, X-ray microCT, magnetic resonance microscopy, etc. By combining these imaging modalities together, we can obtain more accurate and specific anatomical and physiological information about the newborn outer and middle ear. Quantitative measurements of postnatal development of the outer and middle ear and measurements of individual variability are also important for understanding of the mechanics of the newborn ear.

6.4.3 Finite-element modelling

Further modelling work is required to model the small-amplitude dynamic response of the ear canal and middle ear to the tympanometric probe tone, and to then combine that with the non-linear static response. Modelling of the response to the probe tone will require inclusion of inertial, damping and viscoelastic effects. In order to obtain a complete model of tympanometry in newborns, the tympanic ring and probe tip should also be incorporated into the current models.

REFERENCES

- Agache PG, Monneur C, Leveque JL, De Rigal J (1980) Mechanical properties and Young's modulus of human skin in vivo. *Arch Dermatol Res.* 269: 221-232
- Alaerts J, Lutz H, Woulters J (2007) Evaluation of middle ear function in young children: clinical guidelines for the use of 226- and 1,000-Hz tympanometry. *Otol Neurotol.* 28: 727-732
- Allen JB, Jeng PS, Levitt H (2005) Evaluation of human middle ear function via an acoustic power assessment. *J Rehabil Res Dev.* 42(4 Suppl 2):63-78
- Anson BJ, Donaldson JA (1981) *The temporal bone: surgical anatomy of the temporal bone.* Philadelphia, Pennsylvania
- Ballachanda B, Staab WJ, Miyamoto RT, Oliveira RJ (1995) *Human Ear Canal: Theoretical Implications and Clinical Considerations.* Barnes & Noble, New York
- Békésy G v (1960) *Experiments in Hearing.* AIP Press, New York
- Calandruccio L, Fitzgerald TS, Prieve BA (2006) Normative Multifrequency Tympanometry in infants and Toddlers. *J Am Acad Audiol.* 17: 470–480
- Crelin ES (1973) *Functional anatomy of the newborn.* Yale University Press
- Cheng T, Dai C, Gan RZ (2007) Viscoelastic properties of human tympanic membrane. *Ann Biomed Eng* 35: 305-314
- Cheung JTM, Zhang M, Leung AKL, Fan YB (2004) Three-dimensional finite element analysis of the foot during standing A material sensitivity study *J Biomech* 38: 1045-1054
- Chui C, Kobayashi E, Chen X, Hisada T, Sakuma I (2004) Combined compression and elongation experiments and non-linear modelling of liver tissue for surgical simulation. *Med Biol Eng Comput* 42: 787-798
- Clemens CJ, Davis SA, Bailey AR. (2000) The false-positive in universal

newborn hearing screening. *Pediatrics*. 106: E7

Colletti V (1975) Methodological observations on tympanometry with regard to the probe tone frequency. *Acta Otolaryngol* 80 : 54-60

Colletti V (1976) Tympanometry from 200 to 2000 Hz probe tone. *Audiology* 15: 106-119

Colletti V (1977) Multifrequency tympanometry. *Audiology* 16: 278-287

Cull P (1989) *The sourcebook of medical illustration*. Parthenon Publ., Carnforth (UK)

Decraemer WF, Khanna SM (1995) Malleus vibration modelled as rigid body motion. *Acta Otorhinolaryngol Belg.* 49: 139-145

Decraemer WF, Maes MA, Vanhuyse VJ (1980) An elastic stress-strain relation for soft biological tissues based on a structural model. *J Biomech* 13: 463-468

Dirckx JJJ, Buytaert JA, Decraemer WF (2006) Quasi-static transfer function of the rabbit middle ear" measured with a heterodyne interferometer with high-resolution position decoder. *J Assoc Res Otolaryngol.* 7: 339-351

Dirckx, JJJ, Decraemer, WF (1991) Human tympanic membrane deformation under static pressure. *Hear Res.* 51: 93-105

Dirckx JJJ, Decraemer WF (1992) Area change and volume displacement of the human tympanic membrane under static pressure. *Hear Res* 51: 93-105

Dirckx JJJ, Decraemer WF, von Unge M, Larsson C (1997) Measurement and modeling of boundary shape and surface deformation of the Mongolian gerbil pars flaccida. *Hear Res.* 111: 153-164

Dirckx JJJ, Decraemer WF, von Unge M, Larsson C (1998) Volume displacement of the gerbil eardrum pars flaccida as a function of middle ear pressure. *Hear Res.* 118: 35-46

Dirckx JJJ, Decraemer WF (2001) Effect of middle ear components on eardrum quasi-static deformation. *Hear Res* 157: 124-137

Early Hearing Detection and Intervention Program Guidance Manual (2003)
<http://www.cdc.gov/ncbddd/ehdi/nationalgoals.htm>.

Eavey RD (1993) Abnormalities of the neonatal ear: otoscopic observations, histologic observations, and a model for contamination of the middle ear by cellular contents of amniotic fluid. *Laryngoscope* 103: 1-31

Eby TL, Nadol JB Jr (1986) Postnatal growth of the human temporal bone Implications for cochlear implants in children. *Ann Otol Rhinol Laryngol* 95: 356-364

Elkhouri N, Liu H, Funnell WRJ (2006) Low-frequency finite-element modelling of the gerbil middle ear. *J Assoc Res Otolaryngol* 7: 399-411

Elner A, Ingelstedt S, Ivarson A (1971) The elastic properties of the tympanic membrane system. *Acta Otolaryng* 72: 397-403

Fay J, Puria S, Decraemer WF, Steele C (2005) Three approaches for estimating the elastic modulus of the tympanic membrane. *J Biomech* 38: 1807-1815

Feldman AS (1976) Tympanometry – Procedures, interpretations and variables. Pp. 103-155 in *Acoustic impedance & admittance – The measurement of middle ear function*, Feldman AS & Wilber LA (eds.), Williams & Wilkins, Baltimore

Fung YC (1993) *Biomechanics: Mechanical Properties of Living Tissues*. second. Springer-Verlag, New York

Funnell WRJ, Laszlo CA (1978) Modeling of the cat eardrum as a thin shell using the finite-element method. *J Acoust Soc Am* 63: 1461-1467

Funnell WRJ, Laszlo CA (1982) A critical review of experimental observations on ear-drum structure and function. *ORL* 44: 181-205

Funnell WRJ (1996) On the low-frequency coupling between eardrum and manubrium in a finite-element model. *J Acoust Soc Am* 99: 3036-3043

Funnell WRJ, Decraemer WF (1996) On the incorporation of moiré shape

measurements in finite-element models of the cat eardrum. *J Acoust Soc Am* 100: 925-932

Gaihede M (1999) Mechanics of the middle ear system: computerized measurements of its pressure-volume relationship. *Auris Nasus Larynx* 26: 383-399

Gan RZ, Sun Q, Dyer RK Jr, Chang KH, Dormer KJ (2002) Three-dimensional modeling of middle ear biomechanics and its applications. *Otol Neurotol* 23: 271-280

Gan RZ, Feng B, Sun Q (2004) 3-Dimensional finite element modeling of human ear for sound transmission. *Ann Biomed Eng* 32 : 847-856

Grahame R, Holt PJ (1969) The influence of ageing on the in vivo elasticity of human skin. *Gerontologia*. 15: 121-319

Guinan JJJ, Peake WT (1967) Middle-ear characteristics of anesthetized cats. *J Acoust Soc Am* 41: 1237-1261

Gulya AJ, Schuknecht HF (1995) *Gulya and Schuknecht's Anatomy of the Temporal Bone with Surgical Implications*. Barnes & Noble, New York

Gundersen T, Hogmoen K (1976) Holographic vibration analysis of the ossicular chain. *Acta Otolaryngol* 82: 16-25

Gyo K, Goode RL, Miller C (1986) Effect of middle-ear modification on umbo vibration—human temporal bone experiments with a new vibration measuring system. *Arch. Otolaryngol. Head Neck Surg.* 112: 1262–1268

Hall DA (1976) *The aging of connective tissue*. Academic Press, London and New York

Hartley JG. (1986) *Fundamentals of the Finite Element Method*. Macmillan. New York

Himelfarb MZ, Popelka GR, Shanon E (1979) Tympanometry in normal neonates. *J Speech Hear Res* 22: 179–191

Holte L, Cavanova RMJ, Margolis RH (1990) Ear canal wall mobility and

tympanometric shape in young infants. *J Pediatr* 117: 77–80

Holte L, Margolis RH, Cavanaugh RM Jr (1991) Developmental changes in multifrequency tympanograms. *Audio* 30: 1–24

Holzapfe GA (2000) *Nonlinear Solid Mechanics: A Continuum Approach for Engineering*. Chichester , New York

Hsu GS, Margolis RH, Schachern PA (2000) Development of the middle ear in neonatal chinchillas. I. Birth to 14 days. *Acta Otolaryngol* 120: 922-932

Hunter LL, Margolis RH (1992) Multifrequency tympanometry: Current clinical application. *Am J Audiol* 1: 33–43

Ikui A, Sando I, Haginomori S, Sudo M (2000) Postnatal development of the tympanic cavity: a computer-aided reconstruction and measurement study. *Acta Otolaryngol* 120: 375-379

Ikui A, Sando I, Sudo M, Fujita S (1997) Postnatal change in angle between the tympanic annulus and surrounding structures. Computer-aided three-dimensional reconstruction study. *Ann Otol Rhinol Laryngol* 106: 33-36

Joint Committee on Infant Hearing (2000) Year 2000 Position Statement: Principles and Guidelines for early hearing detection and intervention programs. *Am J Audio* 9: 9-29

Jerger J (1970) Clinical expereince with impedance audiometry. *Arch Otolaryngol* 92: 311-324

Katz J (2002) *Handbook of clinical audiology*, Lippincott Willams & Wikins

Keefe DH, Bulen JC, Arehart KH, Burns EM (1993) Ear-canal impedance and reflectance coefficient in human infants and adults. *J Acoust Soc Am* 94: 2617–2637

Keefe DH, Folsom RC, Gorga MP, Vohr BR, Bulen JC, Norton SJ. (2000) Identification of neonatal hearing impairment: ear-canal measurements of acoustic admittance and reflectance in neonates. *Ear Hear* 21: 443–461

Keefe DH, Gorga MP, Jesteadt W, Smith LM. (2008) Ear asymmetries in

middle-ear, cochlear, and brainstem responses in human infants. *J Acoust Soc Am.* 123:1504–1512

Keefe DH, Levi E (1996) Maturation of the middle and external ears: Acoustic power-based responses and reflectance tympanometry. *Ear Hear* 17: 361–372

Keefe DH, Simmons JL (2003) Energy transmittance predicts conductive hearing loss in older children and adults. *J Acoust Soc Am.* 114: 3217-3238

Kei J, Allison-Levick J, Dockray J (2003) High-frequency (1000 Hz) tympanometry in normal neonates. *J Am Acad Audiol.* 14: 20–28

Kirikae I (1960) *The Structure and Function of the Middle Ear*. University of Tokyo, Tokyo

Koç A, Ekinci G, Bilgili AM, Akpinar IN, Yakut H, Han T (2003) Evaluation of the mastoid air cell system by high resolution computed tomography: Three-dimensional multiplanar volume rendering technique. *J Laryngol Otol* 117: 595–598

Koike T, Wada H, Kobayashi T (2002) Modeling of the human middle ear using the finite-element method. *J Acoust Soc Am* 111:1306-1317

Kuypers LC, Decraemer WF, Dirckx JJJ (2006) Thickness distribution of fresh and preserved human eardrums measured with confocal microscopy. *Otol Neurotol.* 27: 256-264

Ladak HM, Decraemer WF, Dirckx JJJ, Funnell WRJ (2004) Response of the cat eardrum to static pressures: mobile versus immobile malleus. *J Acoust Soc Am* 116: 3008-3021

Ladak HM, Funnell WRJ, Decraemer WF, Dirckx JJJ (2006) A geometrically nonlinear finite-element model of the cat eardrum. *J Acoust Soc Am* 119: 2859-2868

Larsson C, Dirckx JJJ, Bagger-Sjöbäck D, von Unge M (2005) Pars flaccida displacement pattern in otitis media with effusion in the gerbil. *Otol Neurotol.* 26: 337-343

Larsson C, von Unge M, Dirckx JJJ, Decraemer WF, Bagger-Sjöbäck D (2001) Displacement pattern of the normal pars flaccida in the gerbil. *Otol Neurotol.* 22: 558-566

Lee CY, Rosowski JJ (2001) Effects of middle-ear static pressure on pars tensa and pars flaccida of gerbil ears. *Hear Res* 153: 146-163

Li G, Lopez O, Rubash H (2001) Variability of a three-dimensional finite element model constructed using magnetic resonance images of a knee for joint contact stress analysis. *J Biomech Eng* 123: 341-346

Liden G (1969) Tests for stapes fixation. *Arch Otolaryngol* 89: 215-219

Lilly D (1984) Multiple frequency, multiple component tympanometry: New approaches to an old diagnostic problem. *Ear Hear* 5: 300-308

Lim DJ (1970) Human tympanic membrane. An ultrastructural observation. *Acta Otolaryngol* 70 : 176-186

Liu Y, Kerdok AE, Howe RD (2004) A nonlinear finite element model of soft tissue indentation. Proceedings of Medical Simulation: International Symposium, Cambridge, MA, 67-76

Marchant CD, McMillan PM, Shurin PA (1986) Objective diagnosis of otitis media in early infancy by tympanometry and ipsilateral acoustic reflex thresholds. *J Pediatr* 109: 590-595

Margolis RH, Bass-Ringdahl S, Hanks WD, Holte L, Zapala DA (2003) Tympanometry in newborn infants 1 kHz norms. *J Am Acad Audiol* 14: 383-392

Margolis RH, Goycoolea HG (1993) Multifrequency tympanometry in normal adults. *Ear Hear* 1993 14: 408-413

Margolis RH, Heller JW (1987) Screening tympanometry: criteria for medical referral. *Audiology*. 26: 197-208

Margolis RH and Hunter LL (1999) Tympanometry-basic principles and clinical applications in Contemporary perspective on hearing assessment, edited by Rintelmann WF and Musiek F (Allyn and Bacon, Boston)

Margolis RH, Paul S, Saly GL, Schachern PA, Keefe DH (2001) Wideband reflectance tympanometry in chinchillas and human. *J Acoust Soc Am*. 110: 1453-1464

Margolis RH, Popelka GR (1975) Static and dynamic acoustic impedance measurements in infant ears. *J Speech Hear Res*. 18: 435–443

Margolis RH, Saly GL, Keefe DH (1999) Wideband reflectance tympanometry in normal adults. *J Acoust Soc Am* 106: 265-280

Margolis RH, Shanks JE (1991) Tympanometry: Principles and procedures In W. F. Rintelmann (Ed.), *Hearing assessment* (pp. 179-246). Texas: Pro-Ed

Matthews PC (2000) *Vector calculus*. Springer, New York

McKinley AM, Grose JH, Roush J (1997) Multifrequency tympanometry and evoked otoacoustic emissions in neonates during the first 24 hours of life. *J Am Acad Audiol*. 3: 218–223

McLellan, M.S., Webb. C.H. (1957) Ear studies in the newborn infant. *J Pediatr* 51: 672–677

Mendis KK, Stalnaker RL, Advani SH. (1995) A constitutive relationship for large deformation finite element modeling of brain tissue. *J Biomech Eng* 117: 279-285

Metz O (1946) The acoustic impedance measured on normal and pathological ears. *Acta Otolaryngol (Suppl 63)*: 1-245

Meyer SE, Jardine CA, Deverson W (1997) Developmental changes in tympanometry: A case study. *Brit J Audiol* 31: 189-195

Molvaer O, Vallersnes F, Kringlebotn M (1978) The size of the middle ear and the mastoid air cell. *Acta Oto-Laryngol*. 85: 24–32

Nakajima HH, Ravicz ME, Merchant SN, Peake WT, Rosowski JJ (2005) Experimental ossicular fixations and the middle ear's response to sound: evidence for a flexible ossicular chain. *Hear Res*. 204: 60-77

National Institute on Deafness and Other Communication Disorders (1993)

National Institutes of Health Consensus Statement: Early identification of hearing-impairment in infants and young children. Bethesda, MD

Nigg BM, Herzog W (1999) *Biomechanics of the musculo-skeletal system*. 2nd edition, John Wiley & Sons

Northrop C, Piza J, Eavey R.D. (1986) Histological observations of amniotic fluid cellular content in the ear of neonates and infants. *Int J Pediatr Otorhinolaryngol.* 11: 113-127

Olsewski J (1990) The morphometry of the ear ossicles in humans during development. *Anat. Anz* 171: 187-191

Osguthorpe JD, Lam C (1981) Methodologic aspects of tympanometry in cats. *Otolaryngol Head Neck Surg* 89: 1037-1040

Paradise JL, Smith CG, Bluestone CD (1976) Tympanometric detection of middle ear effusion in infants and young children. *Pediatrics* 58: 198-210

Polka L, Shahnaz N, Zeitouni A (2002) A comparison of middle ear acoustic admittance in adults and 3-week-old infants based on multifrequency tympanometry. *J Acoust Soc Am* 112: 2272 (abstract)

Qi L, Liu H, Lutfy J, Funnell WRJ, Daniel SJ (2006) A non-linear finite-element model of the newborn ear canal, *J Acoust Soc Am* 120: 3789-3798

Qi L, Funnell WRJ, Daniel SJ (2008) A non-linear finite-element model of the newborn middle ear, *J Acoust Soc Am* (2008) 124: 337-347

Qi L, Funnell WRJ, Shahnaz N, Polka L, Daniel SJ (2007) "Analysis of multi-frequency tympanogram tails in three-week-old newborns." *Ear and hearing (submitted)*

Qi L, Mikhael CS, Funnell WRJ (2004) Application of the Taguchi method to sensitivity analysis of a middle-ear finite-element model. *Proc 28th Ann Conf Can Med Biol Eng Soc*: 153-156

Ravicz ME, Rosowski JJ (1997) Sound-power collection by the auditory periphery of the Mongolian gerbil *Meriones unguiculatus*: III. Effect of variations

in middle-ear volume. *J Acoust Soc Am.* 101: 2135-2147

Ravicz ME, Rosowski JJ, Voigt HF (1992) Sound-power collection by the auditory periphery of the Mongolian gerbil *Meriones unguiculatus*. I: Middle-ear input impedance. *J Acoust Soc Am.* 92: 157-177

Roberts DG, Johnson CE, Carlin SA, Turczyk V, Karnuta MA, Yaffee K (1995) Resolution of middle ear effusion in newborns, *Arch Pediatr Adolesc Med* 149: 873-877

Rollhauser H (1950) Die Zungfestigkeit der Menslichen Haut. *Gegenbaurs Morphol Jahrb* 90: 249-261

Rosowski JJ, Lee CY (2002) The effect of immobilizing the gerbil's pars flaccida on the middle-ear's response to static pressure. *Hear Res* 174: 183-195

Ruah CB, Schachern PA, Zelterman D, Paparella MM, Yoon TH (1991) Age-related morphologic changes in the human tympanic membrane. A light and electron microscopic study. *Arch Otolaryngol Head Neck Surg.* 117: 627-634

Samani A, Plewes D (2004) A method to measure the hyperelastic parameters of ex vivo breast tissue sample. *Phys Med Bio* 49: 4395-4405

Sanford CA, Feeney MP (2008) Effects of maturation on tympanometric wideband acoustic transfer functions in human infants. *J Acoust Soc Am* (conditionally accepted for publication)

Saunders JC, Kaltenbach JA, Relkin, EM (1983) The structural and functional development of the outer and middle ear. In R. Romand (Ed). *Development of Auditory and Vestibular Systems*. New York: Academic

Schmidt SH, Hellstrom S (1991) Tympanic-membrane structure new views. A comparative study. *J Otorhinolaryngol Relat Spec.* 53: 32-36

Schwarz W (1957) Connective tissue. Oxford: Blackwells.

Shahnaz N (2002) Multifrequency, multicomponent tympanometry in 3-weeks old infants. 2nd Internat Conf Newborn Hearing Screening, Diagnosis & Intervention. Villa Erba (Como), Italy (abstract)

Shahnaz N, Miranda T, Polka L (2008) Multi-frequency tympanometry in neonatal intensive care unit and well babies. *J Am Acad Audiol.* In press

Shahnaz N, Polka L (1997) Standard and multifrequency tympanometry in normal and otosclerotic ears. *Ear Hear 18:* 268–280

Shahnaz N, Polka L (2002) Distinguishing healthy from otosclerotic ears: Effect of probe-tone frequency on static admittance. *J Am Acad Audiol. 13:* 345–355

Shahnaz N, Miranda T, Polka L (2007) Multi-frequency tympanometry in neonatal intensive care unit and well babies. *J Am Acad Audiol.* Accepted

Shanks JE (1984) Tympanometry. *Ear Hear 5:* 268-280

Shanks JE, Lilly DJ (1981) An evaluation of tympanometric estimates of ear canal volume. *J Speech Hear Res 24:* 557–566

Shanks JE, Stelmachowicz PG, Beauchaine KL, Schulte L (1992) Equivalent ear canal volumes in children pre- and post-tympanostomy tube insertion. *J Speech Hear Res 35:* 936-941

Shanks JE, Wilson RH, Cambron NK (1993) Multiple frequency tympanometry: effects of ear canal volume compensation on static acoustic admittance and estimates of middle ear resonance. *J Speech Hear Res 36:* 178–185

Stepp CE, Voss SE (2005) Acoustics of the human middle-ear air space. *J Acoust Soc Am. 118(2):* 861-871

Stoltz JF (2006) *Mechanobiology : cartilage and chondrocyte.* Vol (4) IOS Press Washington DC

Stinson MR, Shaw, EA, Lawton BW (1982) Estimation of acoustical energy reflectance at the eardrum from measurements of pressure distribution in the human ear canal. *J Acoust Soc Am. 72:* 766–773

Stinson MR, Lawton BW (1989) Specification of the geometry of the human ear canal for the prediction of sound-pressure level distribution. *J Acoust Soc Am*

Stuart A, Yang EY, Green WB (1994) Neonatal auditory brainstem response thresholds to air- and bone-conducted clicks: 0 to 96 hours postpartum. *J Am Acad Audiol* 5:163-172

Takahara T, Sando I, Hashida Y, Shibahara Y (1986) Mesenchyme remaining in human temporal bones. *Otolaryngol Head Neck Surg.* 95: 349-357

Terkildsen K, Thomsen KA (1959) The influence of pressure variations on the impedance measuring bridge for clinical use. *J. Laryngol. Otol.* 73: 409–418

Torres-Moreno R, Derek J, Stephan E, Hamish M (1999) Magnetic resonance imaging to develop a first-generation 3-D generic finite element model in producing an improved socket fit is analyzed in this case study. *J Pros Orth* 11: 6-11

Van Camp KJ, Margolis RH, Wilson RH, Creten WL, Shanks JE (1986) Principles of tympanometry. Monograph no. 24. Rockville MD: ASHA

Vanhuyse VJ, Creten WL, Van Camp KJ (1975) On the W-notching of tympanograms. *Scan Audiol* 4 : 45-50

von Unge M, Decraemer WF, Bagger-Sjöback D, Dirckx JJJ (1993) Displacement of the gerbil tympanic membrane under static pressure variations measured with a real-time differential moire interferometer. *Hear Res* 70: 229-242

Vorwerk U, Steinicke G, Begall K (1999) Observation of eardrum movements during quasi-static pressure changes by high-speed digital imaging. *Audiol Neurootol* 4: 150-155

Voss SE, Allen JB (1994) Measurement of acoustic impedance and reflectance in the human ear canal. *J Acoust Soc Am.* 95: 372–384

Unur E, Ülger H, Ekinci N (2002) Morphometrical and morphological variations of middle ear ossicles in the newborn. *Erciyes Med. J.* 24: 57-63. (<http://tipdergisi.erciyes.edu.tr/project6/112.pdf>, last viewed 2007 Dec 22)

Wada H, Metoki T, Kobayashi T (1992) Analysis of dynamic behavior of

human middle ear using a finite-element method. *J Acoust Soc Am* 92:3157-3168

Wang X, Cheng T, Gan RZ. (2007) Finite-element analysis of middle-ear pressure effects on static and dynamic behavior of human ear. *J Acoust Soc Am.* 122: 906-917

Wellman P, Howe RH, Dalton E, and Kern KA (1999) Breast tissue stiffness in compression is correlated to histological diagnosis. Technical report, Harvard Biorobotics Laboratory, <http://biorobotics.harvard.edu/pubs/mechprops.pdf>

Whittemore KR, Merchant SN, Rosowski JJ (1998) Acoustic mechanisms. Canal wall-up versus canal wall-down mastoidectomy. *Otolaryngol.-Head Neck Surg* 118: 751-761

Wiley TL and Stoppenbach DT (2002) Basic principles of acoustic immitance measures in Katz J (Ed) *Handbook of clinical audiology*, Lippincott Williams & Wikins

Williamson AK, Chen AC, Sah RL (2001) Compressive properties and function-composition relationships of developing bovine articular cartilage. *J Orthop Res* 19: 1113-1121

Yamada H (1970) *Strength of biological materials*. Baltimore, Williams and Wilkins

Yokoyama T, Iino Y, Kakizaki K, Murakami Y (1999) Human temporal bone study on the postnatal ossification process of auditory ossicles. *Laryngoscope* 109: 927-930

Yoshinaga-Itano C, Sedey A, Coulter DK, Mehl AL (1998) Language of early and later identified children with hearing loss. *Pediatrics* 102: 1161-1171

Zhang M, Zheng YP, Mak AF (1997) Estimating the Effective Young's Modulus of Soft Tissues from Indentation Tests - Nonlinear Finite Element Analysis of Effects of Friction and Large Deformation. *Med Eng Phys* 19: 512-517

Zwislocki J (1962) Analysis of the middle-ear function. 1. Input impedance. *J Acoust. Soc. Am.* 34: 1514-1523